

StruSoft



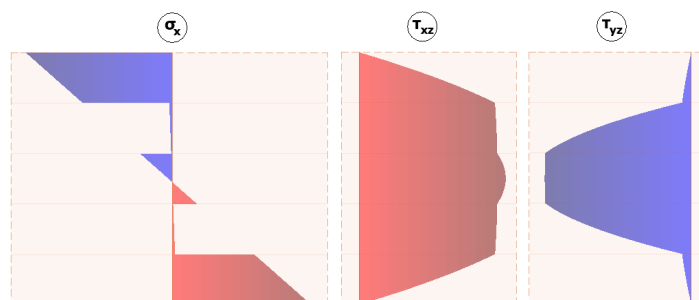
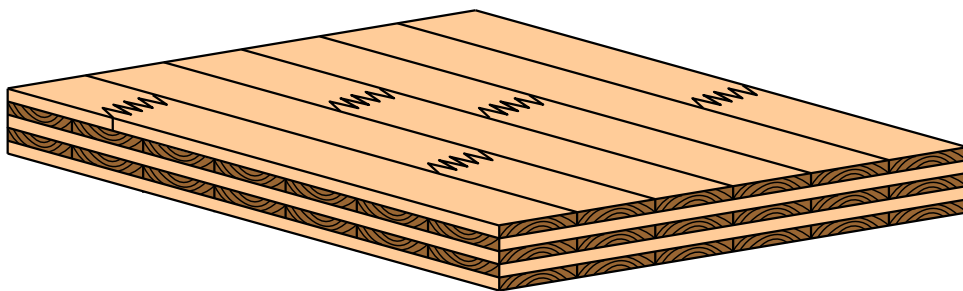
FEM-Design

FEM-Design

Theory of Laminated Composite Shells Cross Laminated Timber Application

version 1.0
2019

$$\begin{bmatrix} m_x \\ m_y \\ m_{xy} \\ n_x \\ n_y \\ n_{xy} \\ q_x \\ q_y \end{bmatrix} = \begin{bmatrix} D_{11} & D_{12} & D_{16} & B_{11} & B_{12} & B_{16} & 0 & 0 \\ D_{12} & D_{22} & D_{26} & B_{12} & B_{22} & B_{26} & 0 & 0 \\ D_{16} & D_{26} & D_{66} & B_{16} & B_{26} & B_{66} & 0 & 0 \\ B_{11} & B_{12} & B_{16} & A_{11} & A_{12} & A_{16} & 0 & 0 \\ B_{12} & B_{22} & B_{26} & A_{12} & A_{22} & A_{26} & 0 & 0 \\ B_{16} & B_{26} & B_{66} & A_{16} & A_{26} & A_{66} & 0 & 0 \\ 0 & 0 & 0 & 0 & 0 & 0 & S_{55} & S_{45} \\ 0 & 0 & 0 & 0 & 0 & 0 & S_{45} & S_{44} \end{bmatrix} \begin{bmatrix} \kappa_x \\ \kappa_y \\ \kappa_{xy} \\ \varepsilon_{0x} \\ \varepsilon_{0y} \\ \gamma_{0xy} \\ \gamma_{xz} \\ \gamma_{yz} \end{bmatrix}$$





StruSoft AB

Visit the StruSoft website for company and FEM-Design information at
www.strusoft.com

Theory of Laminated Composite Shells

Copyright © 2019 by StruSoft, all rights reserved.

Trademarks

FEM-Design is a registered trademark of StruSoft.

Edited by

Zoltán I. Bockai, Ph.D.
Strusoft Ltd., Hungary

Contents

List of symbols.....	5
Preface.....	10
Basic definitions.....	11
1 Few words about linear elasticity.....	12
1.1 Material model.....	12
1.2 The Voight notation of the general Hooke's law.....	14
2 The approximations due to the Reissner-Mindlin shell model in the constitutive law.....	16
2.1 The independent material constants in a general case.....	16
2.2 The independent material constants in orthotropic case.....	16
3 Homogenization method by a laminated composite shell.....	18
3.1 General layer properties to the ABD matrix and the transverse shear part.....	19
3.2 Calculation of the stiffness matrix with shear coupling behaviour.....	21
3.2.1 Bending stiffness part.....	21
3.2.2 Membrane stiffness part.....	22
3.2.3 Eccentricity stiffness part.....	22
3.2.4 The transverse shear stiffness part.....	22
3.2.4.1 Main stiffness direction	24
3.2.4.2 Energy equivalency method.....	25
3.3 Calculation of the stiffness matrix without shear coupling behaviour.....	27
3.3.1 Bending stiffness part.....	27
3.3.2 Membrane stiffness part.....	27
3.3.3 Eccentricity stiffness part.....	27
3.3.4 The transverse shear stiffness part.....	27
4 Stress calculation in composite laminated shells.....	28
4.1 In-plane stresses.....	28
4.1.1 With shear coupling behaviour between layers.....	28
4.1.2 Without shear coupling behaviour between layers.....	29
4.2 Transverse shear stresses.....	29
4.2.1 With shear coupling behaviour between layers.....	29
4.2.2 Without shear coupling behaviour between layers.....	30
5 Cross Laminated Timber application of the laminated composite shell theory.....	32
5.1 Additional settings to CLT application of laminated composite shells.....	33
5.1.1 Shear coupling or no shear coupling settings between layers.....	33
5.1.2 No glue at narrow side option.....	34
5.1.3 Additional reduction factors on the constitutive shell stiffness matrix.....	34
5.2 Load duration classes.....	35
5.3 Service classes.....	36
5.4 Modification factors on strength and stiffness.....	36
5.4.1 Effect of load-duration and moisture content on strength.....	36
5.4.2 Effect of moisture content on deformation.....	36
5.4.3 System strength.....	37
5.4.4 Effect of cracks.....	38
5.4.5 Effect of shape and size of cross section on strength.....	38
5.4.6 Partial factor for material properties.....	38
5.5 Design value of a material properties.....	38
5.6 Strength resistance properties of CLT panels.....	40

5.7 Design values of strength resistance properties of CLT panels.....	42
5.8 Design checks in ultimate limit state.....	42
5.8.1 Normal stresses from compression, tension and bending.....	42
5.8.1.1 Tension and bending parallel to grain direction.....	43
5.8.1.2 Tension and bending perpendicular to grain direction.....	43
5.8.1.3 Compression and bending parallel to grain direction.....	43
5.8.1.4 Compression and bending perpendicular to grain direction.....	44
5.8.2 Shear stresses from in-plane shear, torsion and transverse shear force.....	44
5.8.2.1 Shear stresses from in-plane shear and torsion.....	44
5.8.2.2 Shear stresses from transverse shear force parallel to grain direction.....	45
5.8.2.3 Shear stresses from transverse shear force (rolling shear).....	45
5.8.3 Shear interaction formulas.....	45
5.8.3.1 Summarized shear stresses parallel to grain direction.....	45
5.8.3.2 Perpendicular tensile normal stresses and rolling shear.....	45
5.8.3.3 Perpendicular compressive normal stresses and rolling shear.....	46
5.8.4 Shear check at glued contact surface from rolling shear and torsion between layers....	46
5.8.5 Buckling check	49
5.8.5.1 The generalized relative slenderness.....	50
5.8.5.2 The calculation of the elastic critical force with shear deformation.....	51
5.8.5.3 Calculation of the reduction factor.....	52
5.8.5.4 The compressive stress separation by the buckling check in one specific layer.....	53
5.9 Deflection design check in serviceability limit state.....	54
5.10 Remarks on data of manufacturers and some recommendations.....	55
6 Verification examples	56
6.1 Calculation of the homogenized shell material stiffness matrix.....	56
6.1.1 Calculation with shear coupling.....	56
6.1.1.1 Glue at narrow side.....	57
6.1.1.2 No glue at narrow side.....	62
6.1.2 Calculation without shear coupling.....	67
6.1.2.1 Glue at narrow side.....	67
6.1.2.2 No glue at narrow side.....	70
6.2 Deflection and stresses of a CLT panel supported on two opposite edges.....	73
6.3 Deflection and stresses of a CLT simply supported two-way slab.....	77
6.4 In-plane loaded CLT design check to shear failure at glued contact surface.....	83
6.5 Buckling check of a CLT wall.....	87
References.....	101
Notes.....	104

List of symbols

Scalars

Latin upper case letters

A	cross-sectional area
A_{max}	A_{11} element of the membrane stiffness part in the main stiffness direction
E	elastic modulus in isotropic case
$E_{0,mean}; E_{90,mean}$	mean values of elastic moduli in grain and perpendicular to grain
$E_1; E_2$	elastic moduli in the orthotropy directions
$E_x; E_y$	elastic moduli in grain and perpendicular to grain directions
$E_{x,05}; E_{y,05}$	characteristic value of elastic moduli in grain and perpendicular to grain
G	shear modulus in isotropic case
$G_{12}; G_{13}; G_{23}$	shear moduli in the symmetry planes of the orthotropy
G_{mean}	mean value of shear modulus
$G_{xy}; G_{xz}; G_{yz}$	in-plane, transverse and rolling shear moduli of a plank
$G_{xy,05}; G_{xz,05}; G_{yz,05}$	characteristic in-plane, transverse and rolling shear moduli of a plank
I_p	polar moment of inertia
L	span length
L_{cr}	effective buckling length
$M_{tor,d}$	design value of torque between planks in the RVSE
N	total number of the layers
N_{cr}	elastic critical force
$R_1; R_2$	weighted inertia-like quantity by transverse shear stress calculation
X_d	design value of strength parameter
X_k	characteristic value of strength parameter

Latin lower case letters

a	individual plank (board) width
$d_1; d_2$	weighted shear stiffness by transverse shear stress calculation
f	general letter to strength parameter
$f_{c,0,d}$	design value of compressive strength along the grain
$f_{c,0,k}$	characteristic value of compressive strength along the grain
$f_{c,90,d}$	design value of compressive strength perpendicular to the grain

$f_{c,90,k}$	characteristic value of compressive strength perpendicular to the grain
$f_{c,\alpha,k,i}$	characteristic value of compressive strength in α_i angle from the i^{th} layer grain dir.
$f_{m,0,d}$	design value of bending strength along the grain
$f_{m,0,k}$	characteristic value of bending strength along the grain
$f_{m,90,d}$	design value of bending strength perpendicular to the grain
$f_{m,90,k}$	characteristic value of bending strength perpendicular to the grain
$f_{R,d}$	design value of shear strength from rolling shear
$f_{R,k}$	characteristic value of shear strength from rolling shear
$f_{t,0,d}$	design value of tensile strength along the grain
$f_{t,0,k}$	characteristic value of tensile strength along the grain
$f_{t,90,d}$	design value of tensile strength perpendicular to the grain
$f_{t,90,k}$	characteristic value of tensile strength perpendicular to the grain
$f_{tor,d}$	design value of torsional strength at glued contact surface
$f_{tor,k}$	characteristic value of torsional strength at glued contact surface
$f_{v,d}$	design value of shear strength from transverse effects along the grain
$f_{v,k}$	characteristic value of shear strength from transverse effects along the grain
$f_{xy,d}$	design value of shear strength from in-plane effects
$f_{xy,k}$	characteristic value of shear strength from in-plane effects
$g_1(z) ; g_2(z)$	weighted first moment of area by transverse shear stress calculation
k_c	strength reduction factor due to buckling, instability factor
k_{cr}	crack factor for shear resistance
k_{def}	deformation factor
k_{defU}	deformation factor in ULS load combination
k_{defSq}	deformation factor in SLS quasi-permanent load combination
k_{defSf}	deformation factor in SLS frequented load combination
k_{defSc}	deformation factor in SLS characteristic load combination
k_h	depth factor
k_{mod}	strength modification factor
k_{shape}	factor depending on the shape of the cross-section
k_{sys}	system strength factor
$m_x ; m_y ; m_{xy}$	specific bending moments
n_{cr}	specific elastic critical force
$n_x ; n_y ; n_{xy}$	specific normal forces
$q_1 ; q_2$	specific transverse shear forces in the main stiffness direction

$q_x ; q_y$	specific transverse shear forces
r	reduction factor on elasticity parameters by buckling calculation
$r_{33} ; r_{66} ; r_{77} ; r_{88}$	reduction factors to the shell material stiffness matrix
t	total thickness of the shell/plate
t_i	thickness of the i^{th} layer or thickness of the RVSE
w_{creep}	additional deflection from creep effect
w_{fin}	final deflection
w_{inst}	instantaneous deflection
z_i	coordinates of the top and bottom edge of the layers
$z_{n1} ; z_{n2}$	weighted centroid co-ordinates by transverse shear stress calculation

Greek upper case letters

$\Gamma_{13}(z) ; \Gamma_{23}(z)$ transverse shear strain along thickness of the shell in main stiffness direction

Greek lower case letters

α	angle between the main stiffness direction and the shell local system
α_i	angle between the grain direction and buckling length direction at the i^{th} layer
β_c	straightness factor
$\gamma_{13} ; \gamma_{23}$	shear strain in the main stiffness direction from the FSDT shell theory
γ_M	partial factor for timber material
$\gamma_{yz} ; \gamma_{xz} ; \gamma_{xy}$	engineering shear strains
$\varepsilon_{0x} ; \varepsilon_{0y} ; \gamma_{0xy}$	mid-plane strains
$\varepsilon_x ; \varepsilon_y ; \varepsilon_z$	normal strains
$\varepsilon_{yz} ; \varepsilon_{xz} ; \varepsilon_{xy}$	tensorial shear strains
θ_i	angles between the local system of the shell and the layers orthotropy directions
$\kappa_x ; \kappa_y ; \kappa_{xy}$	curvatures
λ_{rel}	relative slenderness
ν_{12}	Poisson's ratio in the 1-2 plane of the layer
ν_{xy}	Poisson's ratio in the x-y plane of the board (plank)
$\rho_{13} ; \rho_{23}$	shear correction factors
$\sigma_{c,0,d}$	design compressive stress along the grain
$\sigma_{c,0,d}^{buckling}$	design compressive stress along the grain in case of buckling check
$\sigma_{c,0,d}^{total}$	design total compressive stress along the grain in case of buckling check
$\sigma_{c,90,d}$	design compressive stress perpendicular to grain

$\sigma_{m,0,d}$	design bending stress along the grain
$\sigma_{m,0,d}^{buckling}$	design bending stress along the grain in case of buckling check
$\sigma_{m,90,d}$	design bending stress perpendicular to grain
$\sigma_{t,0,d}$	design tensile stress along the grain
$\sigma_{t,90,d}$	design tensile stress perpendicular to grain
$\sigma_x; \sigma_y; \sigma_z$	normal stresses
$\tau_{0,d}$	design value of nominal shear stress from in-plane effect
$\tau_{13}; \tau_{23}$	transverse shear stresses in the main stiffness direction
$\tau_{yz}; \tau_{xz}; \tau_{xy}$	shear stresses
$\tau_{net,d}$	design value of net shear stress from in-plane effect
$\tau_{tor,d}$	design value of torsional stress at glued contact surface
$\tau_{xy,d}$	design value of shear stress from in-plane effects of the plank
$\tau_{xz,d}$	design value of shear stress from transverse effects along the grain
$\tau_{yz,d}$	design value of shear stress from rolling shear
$\tau_{yz,d}^{inplane}$	design value of rolling shear stress from additional in-plane effects
ψ_0	factor for combination value of a variable action
ψ_2	factor for quasi-permanent value of a variable action

Matrices, tensors

$\sigma_{ij}; \underline{\sigma}; \boldsymbol{\sigma}$	stress tensor with different notations
$\varepsilon_{ij}; \underline{\varepsilon}; \boldsymbol{\varepsilon}$	strain tensor with different notations
$C_{ijkl}; \underline{\underline{C}}; \mathbf{C}$	fourth order material stiffness tensor by the general Hooke's law
$Q_{ij}; \underline{Q}$	general material stiffness matrix
$\overline{Q}_{ij}; \overline{\underline{Q}}$	material stiffness matrix in the shell local system
$\overline{\overline{Q}}_{ij}; \overline{\overline{\underline{Q}}}$	material stiffness matrix in the main stiffness direction
$D_{ij}; \underline{D}; \mathbf{D}$	bending stiffness matrix in the shell local system
$B_{ij}; \underline{B}; \mathbf{B}$	eccentricity (coupling) stiffness matrix in the shell local system
$A_{ij}; \underline{A}; \mathbf{A}$	membrane stiffness matrix in the shell local system
$S_{ij}; \underline{S}; \mathbf{S}$	shear stiffness matrix in the shell local system
$\overline{S}_{ij}; \overline{\underline{S}}; \mathbf{S}$	shear stiffness matrix in the main stiffness direction
$\underline{T}_{(3 \times 3)}$	transformation matrix to the in-plane stiffnesses
$\underline{T}_{(2 \times 2)}$	transformation matrix to the out-of-plane material stiffnesses
$\underline{T}_{(2 \times 2)}^*$	transformation matrix to the out-of-plane structural stiffnesses

Abbreviations

<i>CLT</i>	cross laminated timber
<i>EP</i>	elastic parameters
<i>ESLM</i>	equivalent single layer method
<i>FE</i>	finite element
<i>FSDT</i>	first-order shear deformation theory
<i>GMNIA</i>	geometric and material non-linear analysis with imperfections
<i>RVE</i>	representative volume element
<i>RVSE</i>	representative volume sub-element

Preface

In the first part of this description we will show the theoretical background of the implemented laminated composite shell method in FEM-Design and in the second one the cross laminated timber (CLT) application of this theory will be shown.

In the literature the authors refer this applied mechanical model as “the equivalent single layer method” (ESLM, see Ref. [1-3]). In FEM-Design we implemented this laminated composite shell model into our 3D Structure program module. The main advantage of this method is that with a bit more calculation time by the element stiffness matrix using a homogenization procedure the same equation number remains by the final structural equation system regardless of the number of the layers. Another advantage is that the ESLM is applicable in a general commercial structural finite element (FE) software with arbitrary geometry of shell regions and boundary conditions with additional solid, shell and bar elements because this way the degrees of freedom are compatible to each other. In addition to solve the problem we used new FE formulation techniques (see Ref. [4-5]) which fit into the FEM-Design 3D Structure program module, namely into the linear (standard) and the quadratic (fine) FE groups. The tricky part by the FE formulation of the laminated composite shell is the coupling effect between the bending and the membrane behaviour (see more detailed explanation later).

By the laminated composite shells FEM-Design uses the first-order shear deformation shell theory (FSDT, Reissner-Mindlin theory, see Ref. [6]) such as by the former regular orthotropic shells in FEM-Design. This is very important because by the deflections of a moderately thick shells the shear deformations are not negligible especially in case of laminated composite shells. In that case the shear correction factors by the transverse shear stiffnesses have an even greater role in the calculation procedure to get the appropriate displacements and stresses (by a CLT panel this means e.g. the rolling shear effect).

As a general structural analysis tool by the calculation results of the composite laminated shells not only the displacements and internal forces will be available but also the in-plane (σ_x , σ_y , τ_{xy}) and out-of-plane (τ_{xz} , τ_{yz}) stresses layer-by-layer which provide an appropriate result to design check by general laminated composites.

One application of the laminated composite shells is the calculation and design of CLT panels. Therefore by the timber design tab of FEM-Design 3D Structure module the user can confirm the CLT panels to certain interaction formulas of stresses layer-by-layer, the buckling of a CLT panel and by the analysis tab the adequate deflections can be verified.

The proposed calculation method is mainly valid in the following range: $0.01 < t/L < 0.1$, where t is the thickness of the laminated composite shell and L is the average span length.

The precondition to using this new laminated shell calculation is a deep knowledge of

mechanical shell theory [3][6].

Basic definitions

A **beam** is a structural element, its geometric configuration is a prismatic three-dimensional solid whose **cross-section is small when compared with its length**.

A **plate/shell** is a structural element, its geometric configuration is a three-dimensional solid whose **thickness is small when compared with other dimensions of it**.

These basic assumptions by the mechanical model of a plate/shell results that when somebody would like to calculate a plate/shell (such as a CLT panel which is a surface structure) the appropriate mechanical model is a plate/shell model instead of a beam model. Thus during the modelling of a surface structure we should use a mechanical model which applicable by a surface structure namely e.g. plate/shell theory. It means that (ignoring some special cases) the beam model is not applicable to calculate a surface structure. If someone using a beam model to design a surface structure the results can be misleading and the solution could be very uneconomical.

1 Few words about linear elasticity

1.1 Material model

In solid mechanical point of view the material model is a mathematical characterisation of the connection between the stress and strain field. In solid mechanics the stress field and strain field are **second order tensors**.

The stress tensor of one point in a solid with different notations:

$$\sigma_{ij} = \boldsymbol{\sigma} = \underline{\underline{\boldsymbol{\sigma}}} = \begin{bmatrix} \sigma_{11} & \sigma_{12} & \sigma_{13} \\ \sigma_{21} & \sigma_{22} & \sigma_{23} \\ \sigma_{31} & \sigma_{32} & \sigma_{33} \end{bmatrix} \quad (\text{Eq. 1})$$

The infinitesimal strain tensor of one point in a solid with different notations:

$$\varepsilon_{ij} = \boldsymbol{\varepsilon} = \underline{\underline{\boldsymbol{\varepsilon}}} = \begin{bmatrix} \varepsilon_{11} & \varepsilon_{12} & \varepsilon_{13} \\ \varepsilon_{21} & \varepsilon_{22} & \varepsilon_{23} \\ \varepsilon_{31} & \varepsilon_{32} & \varepsilon_{33} \end{bmatrix} \quad (\text{Eq. 2})$$

The most known material model in solid mechanics is the linear elastic material model (Hooke's law). In general the following equation describes this material model. With index notation system and with matrix notation system:

$$\sigma_{ij} = C_{ijkl} : \varepsilon_{kl} \quad \text{or} \quad \underline{\underline{\boldsymbol{\sigma}}} = \underline{\underline{\boldsymbol{C}}} : \underline{\underline{\boldsymbol{\varepsilon}}} \quad (\text{Eq. 3})$$

In general linear elastic behaviour the connection between the stress and strain tensors is a **fourth-order material stiffness tensor**.

The double dot product of a fourth-order tensor and a second-order tensor is a second-order tensor (see Eq. 3).

With index notation Eq. 3 means the following:

$$\begin{bmatrix} \sigma_{11} & \sigma_{12} & \sigma_{13} \\ \sigma_{21} & \sigma_{22} & \sigma_{23} \\ \sigma_{31} & \sigma_{32} & \sigma_{33} \end{bmatrix} = \begin{bmatrix} C_{1111} & C_{1211} & C_{1311} \\ C_{2111} & C_{2211} & C_{2311} \\ C_{3111} & C_{3211} & C_{3311} \end{bmatrix} \begin{bmatrix} \varepsilon_{11} & \varepsilon_{12} & \varepsilon_{13} \\ \varepsilon_{21} & \varepsilon_{22} & \varepsilon_{23} \\ \varepsilon_{31} & \varepsilon_{32} & \varepsilon_{33} \end{bmatrix} \quad (\text{Eq. 4})$$

It can be represented with matrix notation with the same meaning as well:

$$\begin{bmatrix} \sigma_{11} \\ \sigma_{12} \\ \sigma_{13} \\ \sigma_{21} \\ \sigma_{22} \\ \sigma_{23} \\ \sigma_{31} \\ \sigma_{32} \\ \sigma_{33} \end{bmatrix} = \begin{bmatrix} C_{1111} & C_{1112} & C_{1113} & C_{1121} & C_{1122} & C_{1123} & C_{1131} & C_{1132} & C_{1133} \\ C_{1211} & C_{1212} & C_{1213} & C_{1221} & C_{1222} & C_{1223} & C_{1231} & C_{1232} & C_{1233} \\ C_{1311} & C_{1312} & C_{1313} & C_{1321} & C_{1322} & C_{1323} & C_{1331} & C_{1332} & C_{1333} \\ C_{2111} & C_{2112} & C_{2113} & C_{2121} & C_{2122} & C_{2123} & C_{2131} & C_{2132} & C_{2133} \\ C_{2211} & C_{2212} & C_{2213} & C_{2221} & C_{2222} & C_{2223} & C_{2231} & C_{2232} & C_{2233} \\ C_{2311} & C_{2312} & C_{2313} & C_{2321} & C_{2322} & C_{2323} & C_{2331} & C_{2332} & C_{2333} \\ C_{3111} & C_{3112} & C_{3113} & C_{3121} & C_{3122} & C_{3123} & C_{3131} & C_{3132} & C_{3133} \\ C_{3211} & C_{3212} & C_{3213} & C_{3221} & C_{3222} & C_{3223} & C_{3231} & C_{3232} & C_{3233} \\ C_{3311} & C_{3312} & C_{3313} & C_{3321} & C_{3322} & C_{3323} & C_{3331} & C_{3332} & C_{3333} \end{bmatrix} \begin{bmatrix} \varepsilon_{11} \\ \varepsilon_{12} \\ \varepsilon_{13} \\ \varepsilon_{21} \\ \varepsilon_{22} \\ \varepsilon_{23} \\ \varepsilon_{31} \\ \varepsilon_{32} \\ \varepsilon_{33} \end{bmatrix} \quad (\text{Eq. 5})$$

In this relationship (Eq. 4 or 5) the material stiffness fourth-order tensor contains **81 independent parameters**.

Considering that the Cauchy stress tensor and the infinitesimal strain tensor are symmetrical this 81 independent parameters reduce to **36 independent parameters**. This means that:

$$C_{ijkl} = C_{jikl} = C_{ijlk} = C_{jilk} \quad (\text{Eq. 6})$$

Considering a fully linear elastic stress-strain relationship (without plastic deformation and without any failure) and according to the the positive strain energy it can be proved that:

$$C_{(ij)(kl)} = C_{(kl)(ij)} \quad (\text{Eq. 7})$$

This induces that the 36 parameters reduce to 21 material parameters, see Ref. [3]. This means that **by a general linear elastic anisotropic material 21 independent stiffness parameters are necessary**.

1.2 The Voight notation of the general Hooke's law

Instead of the tensorial notation system the wide spreaded Voight notation system (see Ref. [7]) is popular in engineering practice. With the Voight notation system the second order stress and the strain tensors will be vectors considering the mentioned symmetrical conditions of Eq. 1-2. According to Eq. 6-7 the fourth order material stiffness tensor can rewrite as a 6×6 matrix \underline{Q} .

With Voight notation system if the orthogonal Cartesian co-ordinate system is 1≡x; 2≡y; 3≡z :

$$\begin{bmatrix} \sigma_{xx} \\ \sigma_{yy} \\ \sigma_{zz} \\ \sigma_{yz} \\ \sigma_{xz} \\ \sigma_{xy} \end{bmatrix} = \begin{bmatrix} Q_{11} & Q_{12} & Q_{13} & Q_{14} & Q_{15} & Q_{16} \\ Q_{12} & Q_{22} & Q_{23} & Q_{24} & Q_{25} & Q_{26} \\ Q_{13} & Q_{23} & Q_{33} & Q_{34} & Q_{35} & Q_{36} \\ Q_{14} & Q_{24} & Q_{34} & Q_{44} & Q_{45} & Q_{46} \\ Q_{15} & Q_{25} & Q_{35} & Q_{45} & Q_{55} & Q_{56} \\ Q_{16} & Q_{26} & Q_{36} & Q_{46} & Q_{56} & Q_{66} \end{bmatrix} \cdot \begin{bmatrix} \varepsilon_{xx} \\ \varepsilon_{yy} \\ \varepsilon_{zz} \\ 2\varepsilon_{yz} \\ 2\varepsilon_{xz} \\ 2\varepsilon_{xy} \end{bmatrix} \quad (\text{Eq. 8})$$

In Eq. 8 by the mixed index elements of the strain vector a multiplier 2 is appering due to the original Eq. 5 connection between the stresses and strains. You can also see here the 21 independent element of the material stiffness matrix by a general anisotropic material what was indicated by Eq. 7.

This strain vector in Eq. 8 is the so-called engineering strain vector. Rewrite Eq. 8 with the most common engineering notation for stress and strain we get:

$$\begin{bmatrix} \sigma_x \\ \sigma_y \\ \sigma_z \\ \tau_{yz} \\ \tau_{xz} \\ \tau_{xy} \end{bmatrix} = \begin{bmatrix} Q_{11} & Q_{12} & Q_{13} & Q_{14} & Q_{15} & Q_{16} \\ Q_{12} & Q_{22} & Q_{23} & Q_{24} & Q_{25} & Q_{26} \\ Q_{13} & Q_{23} & Q_{33} & Q_{34} & Q_{35} & Q_{36} \\ Q_{14} & Q_{24} & Q_{34} & Q_{44} & Q_{45} & Q_{46} \\ Q_{15} & Q_{25} & Q_{35} & Q_{45} & Q_{55} & Q_{56} \\ Q_{16} & Q_{26} & Q_{36} & Q_{46} & Q_{56} & Q_{66} \end{bmatrix} \cdot \begin{bmatrix} \varepsilon_x \\ \varepsilon_y \\ \varepsilon_z \\ \gamma_{yz} \\ \gamma_{xz} \\ \gamma_{xy} \end{bmatrix} \quad (\text{Eq. 9})$$

In Eq. 8-9 we used a different letter by the material stiffness matrix part than by the fourth order material stiffness tensor because we would like to emphasize the rearrangements and the mentioned simplification from Eq. 6 and 7.

If we have a composite laminated material (e.g. CLT, etc.) we can say that the behaviour of the layers one-by-one will be the so-called **monoclinic material**, see Ref. [3]. By a monoclinic material Eq. 9 reduces to the following equation if the x-y is the plane of the symmetry in the material (z is perpendicular to this plane):

$$\begin{bmatrix} \sigma_x \\ \sigma_y \\ \sigma_z \\ \tau_{yz} \\ \tau_{xz} \\ \tau_{xy} \end{bmatrix} = \begin{bmatrix} Q_{11} & Q_{12} & Q_{13} & 0 & 0 & Q_{16} \\ Q_{12} & Q_{22} & Q_{23} & 0 & 0 & Q_{26} \\ Q_{13} & Q_{23} & Q_{33} & 0 & 0 & Q_{36} \\ 0 & 0 & 0 & Q_{44} & Q_{45} & 0 \\ 0 & 0 & 0 & Q_{45} & Q_{55} & 0 \\ Q_{16} & Q_{26} & Q_{36} & 0 & 0 & Q_{66} \end{bmatrix} \begin{bmatrix} \varepsilon_x \\ \varepsilon_y \\ \varepsilon_z \\ \gamma_{yz} \\ \gamma_{xz} \\ \gamma_{xy} \end{bmatrix} \quad (\text{Eq. 10})$$

When there are three mutually perpendicular symmetry planes the material is referred to as **orthotropic material**. By an orthotropic material we specify the stiffness matrix in the following way if and only if the coordinate system defined in such a way that the axes (x, y and z) are perpendicular to the three planes of symmetry:

$$\begin{bmatrix} \sigma_x \\ \sigma_y \\ \sigma_z \\ \tau_{yz} \\ \tau_{xz} \\ \tau_{xy} \end{bmatrix} = \begin{bmatrix} Q_{11} & Q_{12} & Q_{13} & 0 & 0 & 0 \\ Q_{12} & Q_{22} & Q_{23} & 0 & 0 & 0 \\ Q_{13} & Q_{23} & Q_{33} & 0 & 0 & 0 \\ 0 & 0 & 0 & Q_{44} & 0 & 0 \\ 0 & 0 & 0 & 0 & Q_{55} & 0 \\ 0 & 0 & 0 & 0 & 0 & Q_{66} \end{bmatrix} \begin{bmatrix} \varepsilon_x \\ \varepsilon_y \\ \varepsilon_z \\ \gamma_{yz} \\ \gamma_{xz} \\ \gamma_{xy} \end{bmatrix} \quad (\text{Eq. 11})$$

It means that by an **orthotropic material 9 independent stiffness parameters are necessary**.

REMARK: Note that in case of different coordinate system than the three planes of symmetry the orthotropic stiffness matrix will be similar than in Eq. 10 but only 9 parameters will be independent.

2 The approximations due to the Reissner-Mindlin shell model in the constitutive law

2.1 The independent material constants in a general case

Considering the **plane stress state** (in x - y plane, which is the plane of the shell) neglecting the normal stresses perpendicular to the plane of the shell, the material model in Eq. 10 (layer-by-layer) reduces:

$$\begin{bmatrix} \sigma_x \\ \sigma_y \\ \tau_{yz} \\ \tau_{xz} \\ \tau_{xy} \end{bmatrix} = \begin{bmatrix} Q_{11} & Q_{12} & 0 & 0 & Q_{16} \\ Q_{12} & Q_{22} & 0 & 0 & Q_{26} \\ 0 & 0 & Q_{44} & Q_{45} & 0 \\ 0 & 0 & Q_{45} & Q_{55} & 0 \\ Q_{16} & Q_{26} & 0 & 0 & Q_{66} \end{bmatrix} \cdot \begin{bmatrix} \varepsilon_x \\ \varepsilon_y \\ \gamma_{yz} \\ \gamma_{xz} \\ \gamma_{xy} \end{bmatrix} \quad (\text{Eq. 12})$$

2.2 The independent material constants in orthotropic case

Considering the relevant mechanical behaviour by shells one layer material stiffness matrix (Eq. 12) can be separated into two parts, namely the in-plane strain part and the transverse shear strain part (see Eq. 13a-b). The Reissner-Mindlin theory is the so-called first-order shear deformation plate theory (FSDT), that is why the second transverse shear strain part will have a great role in the calculations, see Ref. [6].

Due to this the following separation (and sequences) are wide-spread in the literature, see Ref. [3]:

In-plane behaviour:

$$\begin{bmatrix} \sigma_x \\ \sigma_y \\ \tau_{xy} \end{bmatrix} = \begin{bmatrix} Q_{11} & Q_{12} & Q_{16} \\ Q_{12} & Q_{22} & Q_{26} \\ Q_{16} & Q_{26} & Q_{66} \end{bmatrix} \cdot \begin{bmatrix} \varepsilon_x \\ \varepsilon_y \\ \gamma_{xy} \end{bmatrix} \quad (\text{Eq. 13a})$$

Out-of-plane behaviour:

$$\begin{bmatrix} \tau_{xz} \\ \tau_{yz} \end{bmatrix} = \begin{bmatrix} Q_{55} & Q_{45} \\ Q_{45} & Q_{44} \end{bmatrix} \cdot \begin{bmatrix} \gamma_{xz} \\ \gamma_{yz} \end{bmatrix} \quad (\text{Eq. 13b})$$

Eq. 12 and Eq. 13 are equivalent to each other.

In the laminated composite shells the laminates one-by-one typically show orthotropic behaviour. Eq. 13 in case of **the coordinate system defined in such a way that the axes are**

perpendicular to the three planes of symmetry (orthotropy directions) reduces to:

$$\begin{bmatrix} \sigma_x \\ \sigma_y \\ \tau_{xy} \end{bmatrix} = \begin{bmatrix} Q_{11} & Q_{12} & 0 \\ Q_{12} & Q_{22} & 0 \\ 0 & 0 & Q_{66} \end{bmatrix} \cdot \begin{bmatrix} \varepsilon_x \\ \varepsilon_y \\ \gamma_{xy} \end{bmatrix} ; \quad \begin{bmatrix} \tau_{xz} \\ \tau_{yz} \end{bmatrix} = \begin{bmatrix} Q_{55} & 0 \\ 0 & Q_{44} \end{bmatrix} \cdot \begin{bmatrix} \gamma_{xz} \\ \gamma_{yz} \end{bmatrix} \quad (\text{Eq. 14})$$

It can be seen that **by one layer - considering Reissner-Mindlin shell theory - 6 independent stiffness parameters are necessary** (see Eq. 14).

This stiffness matrix in the mentioned co-ordinate system (in orthotropy directions) can be expressed with the engineering material constants (see Eq. 15).

In-plane stiffness:

$$\begin{bmatrix} Q_{11} & Q_{12} & 0 \\ Q_{12} & Q_{22} & 0 \\ 0 & 0 & Q_{66} \end{bmatrix} = \begin{bmatrix} \frac{E_1}{1-\nu_{12}^2 \frac{E_2}{E_1}} & \nu_{12} \frac{E_2}{1-\nu_{12}^2 \frac{E_2}{E_1}} & 0 \\ \nu_{12} \frac{E_2}{1-\nu_{12}^2 \frac{E_2}{E_1}} & \frac{E_2}{1-\nu_{12}^2 \frac{E_2}{E_1}} & 0 \\ 0 & 0 & G_{12} \end{bmatrix} \quad (\text{Eq. 15a})$$

Out-of-plane stiffness:

$$\begin{bmatrix} Q_{55} & 0 \\ 0 & Q_{44} \end{bmatrix} = \begin{bmatrix} G_{13} & 0 \\ 0 & G_{23} \end{bmatrix} \quad (\text{Eq. 15b})$$

In Eq. 15 the mentioned 6 independent engineering material constants appear, namely:

E_1 - The elastic modulus in orthotropy direction 1 in the plane of the layer.

E_2 - The elastic modulus in orthotropy direction 2 in the plane of the layer.

ν_{12} - The Poisson's ratio in the 1-2 plane, ($-\varepsilon_2/\varepsilon_1$).

G_{12} - The shear modulus in the 1-2 plane.

G_{13} - The shear modulus in the 1-3 plane.

G_{23} - The shear modulus in the 2-3 plane.

Here 1-2-3 are the directions of the orthotropy and 1-2 plane is the plane of one layer.

3 Homogenization method by a laminated composite shell

If we make a step from the material behaviour (Eq. 14) to the structural behaviour of a Reissner-Mindlin shell model then the connection between the shell strains and shell internal forces in case of homogeneous isotropy is the following well-known connection (see Eq. 16).

$$\begin{bmatrix} m_x \\ m_y \\ m_{xy} \\ n_x \\ n_y \\ n_{xy} \\ q_x \\ q_y \end{bmatrix} = \begin{bmatrix} \frac{Et^3}{12(1-\nu^2)} & \frac{\nu Et^3}{12(1-\nu^2)} & 0 & 0 & 0 & 0 & 0 & 0 \\ \frac{\nu Et^3}{12(1-\nu^2)} & \frac{Et^3}{12(1-\nu^2)} & 0 & 0 & 0 & 0 & 0 & 0 \\ 0 & 0 & \frac{Gt^3}{12} & 0 & 0 & 0 & 0 & 0 \\ 0 & 0 & 0 & \frac{Et}{1-\nu^2} & \frac{\nu Et}{1-\nu^2} & 0 & 0 & 0 \\ 0 & 0 & 0 & \frac{\nu Et}{1-\nu^2} & \frac{Et}{1-\nu^2} & 0 & 0 & 0 \\ 0 & 0 & 0 & 0 & 0 & Gt & 0 & 0 \\ 0 & 0 & 0 & 0 & 0 & 0 & \frac{5}{6}Gt & 0 \\ 0 & 0 & 0 & 0 & 0 & 0 & 0 & \frac{5}{6}Gt \end{bmatrix} \begin{bmatrix} \kappa_x \\ \kappa_y \\ \kappa_{xy} \\ \varepsilon_{0x} \\ \varepsilon_{0y} \\ \gamma_{0xy} \\ \gamma_{xz} \\ \gamma_{yz} \end{bmatrix}, \quad (\text{Eq. 16})$$

where E , G and ν are the elastic modulus, shear modulus and Poisson's ratio in case of isotropy and t is the thickness of the shell.

On the left side of Eq. 16 those values are the internal forces of a shell, namely:

m_x, m_y, m_{xy} – specific bending moments [kNm/m],

n_x, n_y, n_{xy} – specific normal forces [kN/m],

q_x, q_y – specific transverse shear forces [kN/m].

On the right side in the vector the values are the shell strains, namely:

$\kappa_x, \kappa_y, \kappa_{xy}$ – curvatures [rad/m],

$\varepsilon_{0x}, \varepsilon_{0y}, \gamma_{0xy}$ – mid-plane strains [-],

γ_{xz}, γ_{yz} – transverse shear strains [-].

The matrix in Eq. 16 contains an integration along the thickness of the shell taken into account the isotropic material model and the equilibrium equations. This so-called constitutive shell stiffness matrix to Reissner-Mindlin shells is not that simple if the material model is not isotropic.

If the shell contains different parallel layers with different directions of orthotropy layer-by-layer this matrix which gives the relation between the shell internal forces and shell strains will

be much more complicated. To calculate this kind of shells a homogenization method along the thickness of the shell is necessary. The name of the mechanical theory in the literature which contains this laminated composite shell homogenization method is **the equivalent single layer method** (ESLM). In the next chapter we will show the shell constitutive stiffness matrix in case of general laminated composite shells.

3.1 General layer properties to the ABD matrix and the transverse shear part

Before the details of the calculation of the ABD matrix with shear parts (see Eq. 17) which will gives the connection between the shell internal forces and shell strains according to the equivalent single layer method we need to define a sequence of the layers and the directions of the orthotropy layer-by-layer.

Fig. 1 shows the layer sequence and thicknesses in FEM-Design. This figure also indicate the direction of the orthotropy layer-by-layer.

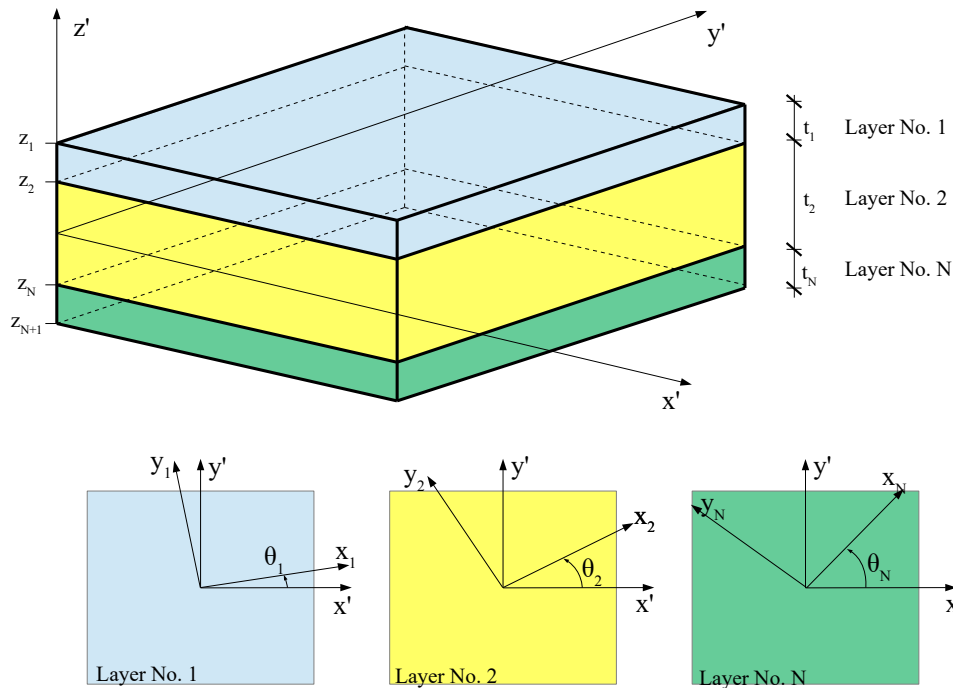


Figure 1 – A general laminated composite in FEM-Design with the local system of the shell (x' - y') and with the orthotropy directions of the individual layers (x_i - y_i)

$[x'-y'-z']$ is the local Cartesian coordinate system of the defined shell region (see Fig. 1).

$[x_i-y_i-z_i]$ is the orthotropy directions of the i^{th} layer (see Fig. 1).

t_1, t_2, \dots, t_N are the thicknesses of the layers (see Fig. 1).

$\theta_1, \theta_2, \dots, \theta_N$ are the angles between the local system of the shell and the own orthotropy direction of the i^{th} layer (see Fig. 1).

$z_1, z_2, \dots, z_N, z_{N+1}$ are the coordinates of the top and bottom edge of the layers (perpendicular to the plane of the shell) based on the mid-surface and the thickness of the layers (see, Fig. 2).

N is the total number of the layers (see Fig. 1-2).

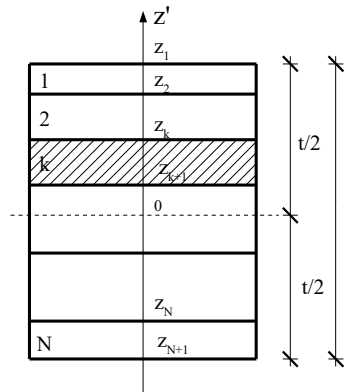


Figure 2 – The perpendicular coordinates of a laminate

According to Chapter 2.2 to every layer the following engineering material constants should be defined regarding the own orthotropy directions of the specific layer (see Fig. 1):

E_x - The elastic modulus in orthotropy direction x_i in the plane of the i^{th} layer.

E_y - The elastic modulus in orthotropy direction y_i in the plane of the i^{th} layer.

ν_{xy} - The Poisson's ratio in the x_i - y_i plane of the i^{th} layer, ($-\varepsilon_y/\varepsilon_x$).

G_{xy} - The shear modulus in the x_i - y_i plane of the i^{th} layer.

G_{xz} - The shear modulus in the x_i - z_i plane of the i^{th} layer.

G_{yz} - The shear modulus in the y_i - z_i plane of the i^{th} layer.

In case of general laminated composite shells which was introduced in the beginning of this chapter the constitutive shell stiffness matrix (see Eq. 17) will be much more complicated than in isotropic case (see Eq. 16). This comes from the fact that in this case the layers have own orthotropy directions separately as we saw in Fig. 1.

$$\begin{bmatrix} m_x \\ m_y \\ m_{xy} \\ n_x \\ n_y \\ n_{xy} \\ q_x \\ q_y \end{bmatrix} = \begin{bmatrix} D_{11} & D_{12} & D_{16} & B_{11} & B_{12} & B_{16} & 0 & 0 \\ D_{12} & D_{22} & D_{26} & B_{12} & B_{22} & B_{26} & 0 & 0 \\ D_{16} & D_{26} & D_{66} & B_{16} & B_{26} & B_{66} & 0 & 0 \\ B_{11} & B_{12} & B_{16} & A_{11} & A_{12} & A_{16} & 0 & 0 \\ B_{12} & B_{22} & B_{26} & A_{12} & A_{22} & A_{26} & 0 & 0 \\ B_{16} & B_{26} & B_{66} & A_{16} & A_{26} & A_{66} & 0 & 0 \\ 0 & 0 & 0 & 0 & 0 & 0 & S_{55} & S_{45} \\ 0 & 0 & 0 & 0 & 0 & 0 & S_{45} & S_{44} \end{bmatrix} \begin{bmatrix} \kappa_x \\ \kappa_y \\ \kappa_{xy} \\ \varepsilon_{0x} \\ \varepsilon_{0y} \\ \gamma_{0xy} \\ \gamma_{xz} \\ \gamma_{yz} \end{bmatrix} \quad (\text{Eq. 17a})$$

Or shortly:

$$\begin{bmatrix} m \\ n \\ q \end{bmatrix} = \begin{bmatrix} D & B & 0 \\ B & A & 0 \\ 0 & 0 & S \end{bmatrix} \begin{bmatrix} \kappa \\ \varepsilon_0 \\ \gamma \end{bmatrix} \quad (\text{Eq. 17b})$$

Before we show the calculation method of the elements of the matrix in Eq. 17 we need to make a transformation on the orthotropic material stiffness matrix of the layers individually because those matrices in Eq. 15 based on the engineering material constants are relevant in their own orthotropy directions but we would like to write the final shell material stiffness matrix in the local co-ordinate system ($x'-y'$) of the shell. Because the matrices in Eq. 15 are tensor quantities we need to use the following transformations.

The necessary transformation matrix for the in-plane stiffnesses of one layer from the orthotropy direction into the local $x'-y'$ system of the shell:

$$\underline{T}_{(3 \times 3)} = \begin{bmatrix} \cos^2 \theta & \sin^2 \theta & \cos \theta \sin \theta \\ \sin^2 \theta & \cos^2 \theta & -\cos \theta \sin \theta \\ -2\cos \theta \sin \theta & 2\cos \theta \sin \theta & \cos^2 \theta - \sin^2 \theta \end{bmatrix}, \quad (\text{Eq. 18})$$

where θ is the angle between the local system of the shell and the layer own orthotropy direction (see Fig. 1).

Based on this transformation matrix the in-plane stiffness matrix layer-by-layer will be the following in the shell local system $x'-y'$:

$$\begin{bmatrix} \bar{Q}_{11} & \bar{Q}_{12} & \bar{Q}_{16} \\ \bar{Q}_{12} & \bar{Q}_{22} & \bar{Q}_{26} \\ \bar{Q}_{16} & \bar{Q}_{26} & \bar{Q}_{66} \end{bmatrix} = \underline{T}_{(3 \times 3)}^T \begin{bmatrix} Q_{11} & Q_{12} & 0 \\ Q_{12} & Q_{22} & 0 \\ 0 & 0 & Q_{66} \end{bmatrix} \underline{T}_{(3 \times 3)} \quad (\text{Eq. 19})$$

Using these matrices we can assemble the different parts of the laminated shell constitutive stiffness matrix in the shell local system $x'-y'$ as you can see in the following chapters.

Here we should emphasize that during the calculation of the shell constitutive stiffness matrix we need to decide first that is there any longitudinal shear coupling (e.g. glue between layers) or not. If the shear coupling between layers is the case what we want to consider then we will get stress distribution what you can see in Fig. 4 and 6 and if the case what we would like to consider is the stiffnesses without shear coupling behaviour finally we will get stress distribution what you can see in Fig. 5 and 7.

3.2 Calculation of the stiffness matrix with shear coupling behaviour

3.2.1 Bending stiffness part

In Eq. 17 matrix the D_{ij} part is the so-called **bending stiffness** part of a mechanical shell. In case of isotropy Eq. 16 shows how this part looks like but in case of a general laminated composite shell the calculation is much more complicated when shear coupling is considered between layers. In a general case with the aim of Eq. 19 the bending stiffness part can be calculated with the following equation (see Eq. 20):

$$D_{ij} = \frac{1}{3} \sum_{k=1}^N (\bar{Q}_{ij})_k (z_k^3 - z_{k+1}^3) \quad (i, j = 1, 2, 6) \quad \text{unit: [kNm}^2/\text{m]} \quad (\text{Eq. 20})$$

3.2.2 Membrane stiffness part

In Eq. 17 matrix the A_{ij} part is the so-called **membrane stiffness** part of a mechanical shell. In case of isotropy Eq. 16 shows how this part looks like but in case of a general laminated composite shell the calculation is much more complicated when shear coupling is considered between layers. In a general case with the aim of Eq. 19 the membrane stiffness part can be calculated with the following equation (see Eq. 21):

$$A_{ij} = \sum_{k=1}^N (\bar{Q}_{ij})_k (z_k - z_{k+1}) \quad (i, j = 1, 2, 6) \quad \text{unit: [kN/m]} \quad (\text{Eq. 21})$$

3.2.3 Eccentricity stiffness part

In Eq. 17 matrix the B_{ij} part is the so-called **eccentricity (coupling) stiffness** part of a mechanical shell. In case of isotropy Eq. 16 shows that this part is equal to zero but in case of a general laminated composite shell the calculation is much more complicated when shear coupling is considered between layers. This part of the shell constitutive stiffness matrix indicates that the membrane strains and bending strains can have interaction on each other. **It means that by a general laminated composite if only membrane strains are in the shell then not only in-plane internal forces arise but also bending moments and vice versa if only bending strains are in the shell then not only bending internal forces arise but also in-plane internal forces.**

In a general case with the aim of Eq. 19 the eccentricity stiffness part can be calculated with the following equation (see Eq. 22):

$$B_{ij} = \frac{1}{2} \sum_{k=1}^N (\bar{Q}_{ij})_k (z_k^2 - z_{k+1}^2) \quad (i, j = 1, 2, 6) \quad \text{unit: [kNm/m]} \quad (\text{Eq. 22})$$

The quantities in the former three equations are based on Eq. 19 and Fig. 2.

3.2.4 The transverse shear stiffness part

The transverse shear part calculation is also complicated according to the effect of the shear correction factors which are necessary when we are talking about FSDT shells. The detailed description of the calculation of the shear correction factors will be shown in Chapter 3.2.4.1-2 when shear coupling is considered between layers.

First of all the orthotropic transverse shear stiffness (see Eq. 15b) should be transformed into the so-called main stiffness direction of the laminated shell (see the reasons and details of the main stiffness direction in Chapter 3.2.4.1).

The necessary transformation matrix for the out-of-plane stiffnesses of one layer from the orthotropy direction into the main stiffness direction:

$$\underline{T}_{(2 \times 2)} = \begin{bmatrix} \cos(\alpha - \theta) & \sin(\alpha - \theta) \\ -\sin(\alpha - \theta) & \cos(\alpha - \theta) \end{bmatrix}, \quad (\text{Eq. 23})$$

where α is the angle between the main stiffness direction and the shell local system x' (see Chapter 3.2.4.1 and Fig. 3) and θ is the angle between the local system of the shell and the own orthotropy direction of one layer (see Fig. 1).

Based on this transformation matrix the out-of-plane stiffness matrix layer-by-layer will be the following in the main stiffness direction:

$$\begin{bmatrix} \bar{\bar{Q}}_{55} & \bar{\bar{Q}}_{45} \\ \bar{\bar{Q}}_{45} & \bar{\bar{Q}}_{44} \end{bmatrix} = \underline{T}_{(2 \times 2)} \begin{bmatrix} G_{13} & 0 \\ 0 & G_{23} \end{bmatrix} \underline{T}_{(2 \times 2)}^T \quad (\text{Eq. 24})$$

With these matrix in Eq. 24 layer-by-layer the transverse shear stiffness part $\bar{\bar{S}}_{55}$ and $\bar{\bar{S}}_{44}$ can be calculated with the following ways:

$$\bar{\bar{S}}_{55} = \rho_{13} \sum_{k=1}^N (\bar{\bar{Q}}_{55})_k (z_k - z_{k+1}) \quad \text{unit: [kN/m]} \quad (\text{Eq. 25})$$

$$\bar{\bar{S}}_{44} = \rho_{23} \sum_{k=1}^N (\bar{\bar{Q}}_{44})_k (z_k - z_{k+1}) \quad \text{unit: [kN/m]} \quad (\text{Eq. 26})$$

where ρ_{13} and ρ_{23} are the shear correction factors. These shear correction factors should be calculated in the main stiffness direction and perpendicular to it according to Chapter 3.2.4.2.

The shear correction factors are necessary here because the Reissner-Mindlin shell theory assumes only constant transverse shear strain along the thickness (FSDT) of the shell and without these corrections by the shear stiffnesses the theory underestimate the shear deformations. We emphasize here that the shear correction factors by a laminated shell are not equal to the well-known 5/6 value (see Eq. 16). The 5/6 value for the shear correction factor is only valid by homogeneous plates. By a general laminated shell these values are typically smaller (e.g.: by a typical CLT panel these values are closer to 1/4). The calculation method of the shear correction factors by a laminated shell will be discussed in Chapter 3.2.4.2.

When we have the transverse shear stiffness of the laminated shell in the main stiffness direction (see Eq. 25-26) it should be transformed back to the local $x'-y'$ system of the shell to get the final constitutive shell stiffness matrix (Eq. 17) which can be use to get the structural stiffness matrix of the shell finite element. To get this back transformation another transformation matrix is necessary:

$$\underline{T}_{(2 \times 2)}^* = \begin{bmatrix} \cos \alpha & -\sin \alpha \\ \sin \alpha & \cos \alpha \end{bmatrix}, \quad (\text{Eq. 27})$$

where α is the angle between the main stiffness direction and the shell local system x' of the shell (see Fig. 3). Based on this transformation matrix the shear stiffness part in the local co-ordinate system of the shell will be:

$$\begin{bmatrix} S_{55} & S_{45} \\ S_{45} & S_{44} \end{bmatrix} = \underline{T}_{(2 \times 2)}^* \begin{bmatrix} \bar{S}_{55} & 0 \\ 0 & \bar{S}_{44} \end{bmatrix} \underline{T}_{(2 \times 2)}^{*T} \quad (\text{Eq. 28})$$

This was the last missing block in Eq. 17 matrix to get the constitutive stiffness matrix of a general laminated shell.

3.2.4.1 Main stiffness direction

The shear correction factors should be calculated in the so-called main stiffness direction (and perpendicular to it) because otherwise the problem of the shear correction factors for a laminated shell using FSDT would be stress (internal force) dependent, therefore the whole calculation would be nonlinear, see Ref. [8].

To calculate this main stiffness direction we need to find the global maximum of the following equation (Eq. 29, the equation comes from tensor transformation, see Ref. [3]) regarding α . It means that we need to find this α direction in the local Cartesian co-ordinate system of the shell (see Fig. 3) where the A_{11} element of the former mentioned membrane stiffness (Eq. 21) of the laminated shell has maximum extreme value.

$$A_{\max} = \cos^4 \alpha A_{11} + \sin^4 \alpha A_{22} + \cos^2 \alpha \sin^2 \alpha (2 A_{12} + 4 A_{66}) + \cos^3 \alpha \sin \alpha 4 A_{16} + \cos \alpha \sin^3 \alpha 4 A_{26} \quad (\text{Eq. 29})$$

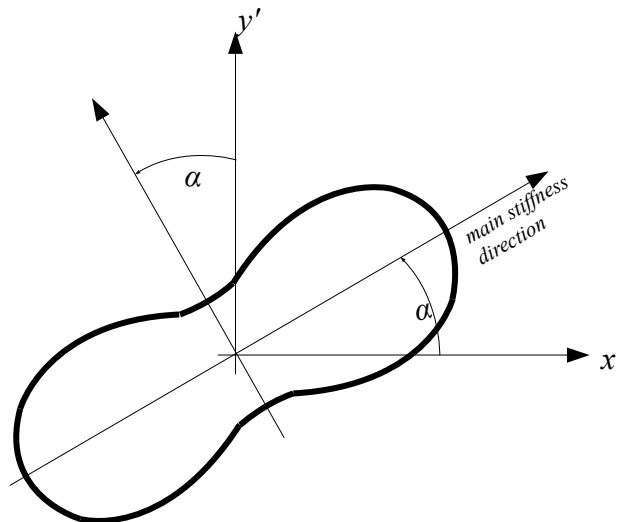


Figure 3 – The interpretation of the main stiffness direction on a polar curve, the thick curve shows the amount of the A_{11} value in the different directions

The α angle which satisfies the previous equation and give the maximum extremum of A_{II} will be the angle of the main stiffness direction what was used in Eq. 23 and 27. Fig. 3 shows the interpretation of the main stiffness direction on a polar curve.

3.2.4.2 Energy equivalency method

In this chapter we will show the calculation method of the shear correction factor in the main stiffness direction (and perpendicular to it) what was mentioned in the previous chapter. The transverse shear strain energy from shear forces and from the transverse shear stresses must be equal to each other to ensure the correct shear deformation behaviour of the laminated shell due to the simplification of the Reissner-Mindlin theory what was mentioned at the beginning of this Chapter. In this sub-chapter the indices 1,3 show the main stiffness direction and the normal direction of the flat shell element. The 2,3 indices show the direction perpendicular to the main stiffness direction and the normal direction of the flat shell element.

According to the energy equivalency we can write the transverse shear energy from the assumed shear stress distribution along the thickness and from the shear force (see Eq. 30). These two energy must be equal to each other (see Ref. [9-10] for further information).

$$\int_{-\frac{t}{2}}^{\frac{t}{2}} \tau_{13}(z) \Gamma_{13}(z) dz = \frac{q_1 \gamma_{13}}{\rho_{13}} \quad , \quad (\text{Eq. 30})$$

where $\tau_{13}(z)$ and $\Gamma_{13}(z)$ are the relevant shear stress and the shear strain along the thickness of the shell. q_1 and γ_{13} are the relevant shear force and the constant transverse shear strain along the thickness which comes from the Reissner-Mindlin shell theory (FSDT) and finally ρ_{13} is the shear correction factor.

The assumed $\tau_{13}(z)$ transverse shear stress along the thickness can be written with the following formula (similarly as transverse shear stresses by Zhuravskii):

$$\tau_{13}(z) = \frac{q_1}{R_1} g_1(z) \quad , \quad (\text{Eq. 31})$$

where:

$$g_1(z) = - \int_{-\frac{t}{2}}^z \bar{\bar{Q}}_{11}(z)(z - z_{n1}) dz \quad (\text{Eq. 32})$$

and

$$R_I = \int_{-\frac{t}{2}}^{\frac{t}{2}} \bar{\bar{Q}}_{II}(z) (z - z_{nI})^2 dz \quad (\text{Eq. 33})$$

In Eq. 32 and 33 z_{nI} is the following:

$$z_{nI} = \frac{\int_{-\frac{t}{2}}^{\frac{t}{2}} \bar{\bar{Q}}_{II}(z) z dz}{\int_{-\frac{t}{2}}^{\frac{t}{2}} \bar{\bar{Q}}_{II}(z) dz} \quad (\text{Eq. 34})$$

$\bar{\bar{Q}}_{II}(z)$ is the first element of the in-plane material stiffness matrix (see Eq. 15a) transformed into the main stiffness direction layer-by-layer.

Based on these equations we can rewrite Eq. 30:

$$\int_{-\frac{t}{2}}^{\frac{t}{2}} \frac{q_I g_I(z)}{R_I} \frac{q_I g_I(z)}{R_I \bar{\bar{Q}}_{55}(z)} dz = \frac{q_I q_I}{\rho_{I3} \int_{-\frac{t}{2}}^{\frac{t}{2}} \bar{\bar{Q}}_{55}(z) dz} \quad (\text{Eq. 35})$$

If we define the following:

$$d_I = \int_{-\frac{t}{2}}^{\frac{t}{2}} \bar{\bar{Q}}_{55}(z) dz, \quad (\text{Eq. 36})$$

where $\bar{\bar{Q}}_{55}(z)$ is the transverse shear stiffness of the layers in the main stiffness direction according to Eq. 24, then the shear correction factor in the main stiffness direction can be expressed as:

$$\rho_{I3} = \frac{R_I^2}{d_I \int_{-\frac{t}{2}}^{\frac{t}{2}} \frac{g_I^2(z)}{\bar{\bar{Q}}_{55}(z)} dz} \quad (\text{Eq. 37})$$

Perpendicular to the main stiffness direction the shear correction factor can be calculated in a similar way.

$$\rho_{23} = \frac{R_2^2}{d_2 \int_{-\frac{t}{2}}^{\frac{t}{2}} \frac{g_2^2(z)}{\bar{Q}_{44}(z)} dz}, \quad (\text{Eq. 38})$$

where above the already mentioned variables the values comes from the index changing in Eq. 30-37, namely $1 \rightarrow 2$; $5 \rightarrow 4$.

3.3 Calculation of the stiffness matrix without shear coupling behaviour

3.3.1 Bending stiffness part

In case of without shear coupling between layers the calculation of the bending stiffness is only a summation of the bending stiffnesses of the layers such as individual layers which are not working together.

$$D_{ij} = \sum_{k=1}^N (\bar{Q}_{ij})_k \frac{(z_k - z_{k+1})^3}{12} \quad (i, j = 1, 2, 6) \quad \text{unit: [kNm}^2/\text{m]} \quad (\text{Eq. 39})$$

3.3.2 Membrane stiffness part

The calculation of the membrane stiffness part is the same as in Eq. 21 independendly from the shear coupling behaviour.

$$A_{ij} = \sum_{k=1}^N (\bar{Q}_{ij})_k (z_k - z_{k+1}) \quad (i, j = 1, 2, 6) \quad \text{unit: [kN/m]} \quad (\text{Eq. 21})$$

3.3.3 Eccentricity stiffness part

Without shear coupling between the layers the eccentricity (coupling) behaviour between bending and membrane part is missing, therefore this part always equal to zero in this case.

$$B_{ij} = 0 \quad (i, j = 1, 2, 6) \quad \text{unit: [kNm/m]} \quad (\text{Eq. 40})$$

3.3.4 The transverse shear stiffness part

Without shear coupling between the layers the shear correction factor is the very well-know 5/6 (see Ref. [6]) therefore the calculation of this part has much simple form.

$$S_{ij} = \frac{5}{6} \sum_{k=1}^N (\bar{Q}_{ij})_k (z_k - z_{k+1}) \quad (i, j = 4, 5) \quad \text{unit: [kN/m]} \quad (\text{Eq. 41})$$

4 Stress calculation in composite laminated shells

4.1 In-plane stresses

4.1.1 With shear coupling behaviour between layers

The in-plane stresses are calculated with the following formulas. First of all we need to calculate the in-plane strains at that height (z' coordinate) where we would like to know the in-plane stresses. After this we need to use Eq. 13a to calculate the in-plane stresses.

$$\begin{bmatrix} \varepsilon_x \\ \varepsilon_y \\ \gamma_{xy} \end{bmatrix} = \begin{bmatrix} \varepsilon_{0x} \\ \varepsilon_{0y} \\ \gamma_{0xy} \end{bmatrix} + z' \begin{bmatrix} K_x \\ K_y \\ K_{xy} \end{bmatrix} \quad (\text{Eq. 42})$$

Recall again Eq. 13a:

$$\begin{bmatrix} \sigma_x \\ \sigma_y \\ \tau_{xy} \end{bmatrix} = \begin{bmatrix} Q_{11} & Q_{12} & Q_{16} \\ Q_{12} & Q_{22} & Q_{26} \\ Q_{16} & Q_{26} & Q_{66} \end{bmatrix} \begin{bmatrix} \varepsilon_x \\ \varepsilon_y \\ \gamma_{xy} \end{bmatrix} \quad (\text{Eq. 13a})$$

Here the x - y co-ordinate system can be interpreted in any Cartesian directions of the specific layer but the Q in-plane stiffness matrix of one layer should be also interpreted in the same system as well the stresses and strains. Usually due to the strength check of one point of the layer these directions should be in the direction of the orthotropy of the layer one-by-one. Thus it means that usually the necessary direction can be in different directions layer-by-layer by a general laminated shell.

For example Fig. 4 shows typical normal stress distributions in a general laminated shell in case of shear coupling between layers.

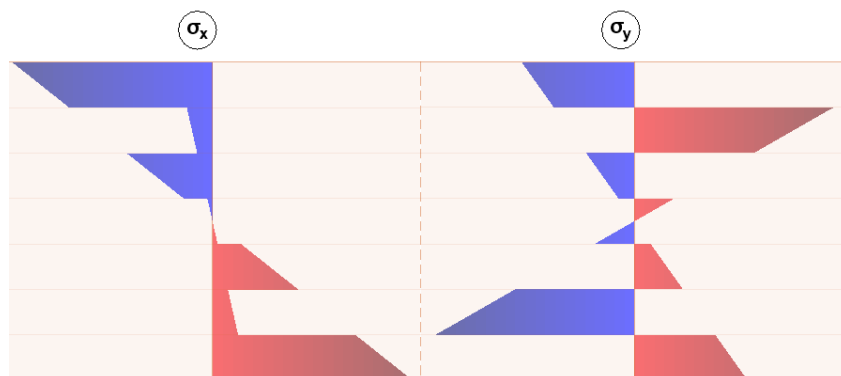


Figure 4 – Typical normal stress distributions in a general laminated shell with shear coupling between layers

4.1.2 Without shear coupling behaviour between layers

This calculation can be done with the consideration of the layers as individual shells:

$$\begin{bmatrix} \sigma_x \\ \sigma_y \\ \tau_{xy} \end{bmatrix} = \begin{bmatrix} Q_{11} & Q_{12} & Q_{16} \\ Q_{12} & Q_{22} & Q_{26} \\ Q_{16} & Q_{26} & Q_{66} \end{bmatrix} \begin{bmatrix} \varepsilon_x \\ \varepsilon_y \\ \gamma_{xy} \end{bmatrix} + z' \begin{bmatrix} Q_{11} & Q_{12} & Q_{16} \\ Q_{12} & Q_{22} & Q_{26} \\ Q_{16} & Q_{26} & Q_{66} \end{bmatrix} \begin{bmatrix} \kappa_x \\ \kappa_y \\ \kappa_{xy} \end{bmatrix} , \quad (\text{Eq. 43})$$

where z' should satisfy the following equation by the analyzed (specific) layer where we would like to get the stresses:

$$-\frac{(z_k - z_{k+1})}{2} \leq z' \leq \frac{(z_k - z_{k+1})}{2} \quad (\text{Eq. 44})$$

Here the x - y co-ordinate system can be interpreted in any Cartesian directions of the specific layer but the \underline{Q} in-plane stiffness matrix of one layer should be also interpreted in the same system as well the stresses and strains. Usually due to the strength check of one point of the layer these directions should be in the direction of the orthotropy of the layer one-by-one. Thus it means that the necessary direction can be in different directions layer-by-layer by a general laminated shell.

For example Fig. 5 shows typical normal stress distributions in a general laminated shell in case of without shear coupling between layers.

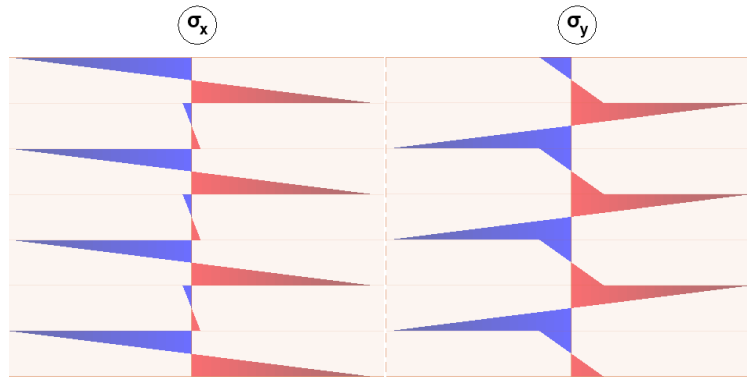


Figure 5 – Typical normal stress distributions in a general laminated shell without shear coupling between layers

4.2 Transverse shear stresses

4.2.1 With shear coupling behaviour between layers

The transverse shear stresses along the thickness should be calculated in the main stiffness direction (and perpendicular to it) with the following formulas from Chapter 3.2.4.2:

$$\tau_{13}(z) = \frac{q_1}{R_1} g_1(z) , \quad (\text{Eq. 45})$$

$$\tau_{23}(z) = \frac{q_2}{R_2} g_2(z) \quad , \quad (\text{Eq. 46})$$

As you can see the transverse shear stresses are calculated from the transverse shear forces using the equilibrium condition between the normal stress increments and transverse shear with reciprocal theorem (as by transverse shear stresses by Zhuravskii).

For example Fig. 6 shows a typical transverse shear stress distribution in a general laminated shell in case of shear coupling between layers.

After we get these shear stresses in the main stiffness direction they can be transformed into arbitrary directions (e.g. shell local or layer local systems).

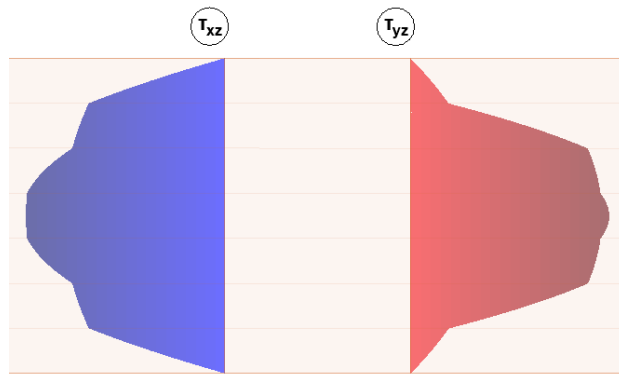


Figure 6 – A typical transverse shear stress distribution in a general laminated shell with shear coupling between layers

4.2.2 Without shear coupling behaviour between layers

Without shear coupling between layers the transverse shear stresses at the top and the bottom of each individual layers will be zero. The maximum value of the transverse shear stresses layer-by-layer will be at the center (mid-surface) of each individual layers and calculated with the following formula (see Ref. [6]):

$$\begin{bmatrix} \tau_{xz} \\ \tau_{yz} \end{bmatrix}_{\max} = 1.5 \frac{5}{6} \begin{bmatrix} Q_{55} & Q_{45} \\ Q_{45} & Q_{44} \end{bmatrix} \begin{bmatrix} \gamma_{xz} \\ \gamma_{yz} \end{bmatrix} \quad (\text{Eq. 47})$$

Here the x - y co-ordinate system can be interpreted in any Cartesian directions of the specific layer but the \underline{Q} out-of-plane stiffness matrix of one layer should be also interpreted in the same system as well the stresses and strains.

In the rest part of the layers the transverse shear stresses show a parabolic distribution which are clear according to the mentioned information above.

For example Fig. 7 shows a typical transverse shear stress distribution in a general laminated shell in case of without shear coupling between layers.

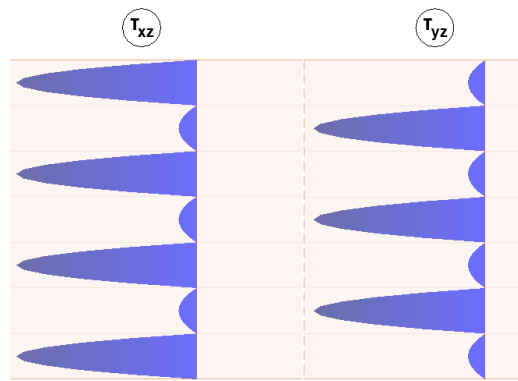


Figure 7 – A typical transverse shear stress distribution in a general laminated shell without shear coupling between layers

5 Cross Laminated Timber application of the laminated composite shell theory

The laminated composite shell theory (ESLM) - what was introduced in the previous chapters - was implemented in FEM-Design 3D Structure and in general it is usable to check the correct deformations and stress distribution (layer-by-layer) of a composite shell.

Here in this chapter the cross laminated timber (CLT) application of the composite shell theory will be discussed with the aim of some part of the Eurocode 5 and other recommendations as well. We will show the design calculations related to CLT products with ESLM what was implemented in FEM-Design program.

In Europe there are several methods which have been adopted to calculate the basic mechanical properties (displacements and stresses) of CLT panels. Some of these methods are experimental and others are analytical/numerical. In the former chapters we indicated how the calculations are performed in FEM-Design, but here we summarize in few sentences including but not limited to, mechanically jointed beams theory (γ method), composite theory (k method), shear analogy method and Timoshenko beam theory based on [11-12].

Mechanically Jointed Beams Theory (γ method) [13]

In the past years in Europe a common analytical approach has been adopted for CLT design the Mechanically Jointed Beams Theory (so-called Gamma Method) that is available in Eurocode 5. This rudimentary method was developed for beams connected together with mechanical fasteners with stiffness k uniformly spaced at distance s . In this theory the effective stiffness and the connection efficiency factor are used to take into account the effect of shear deformation of crossing layers. Only layers acting in the direction of loading are used and the shear deformation of longitudinal layers is neglected. This concept gives a good solution for the differential equation but the main limitation is that it is only valid for simply supported beams with sinusoidal load distribution.

Composite theory (k method) [14-15]

This method is predict some design properties of CLT, but this method does not account the shear deformation at all, thus it is only accurate for high span-to-depth ratios. Other disadvantage of this method is that the necessary composition factors (k_i) are determined for certain loading configurations and impossible to use in a general case.

Shear analogy method [12][16]

With this procedure the different modulus of elasticity and shear modulus of single layers considered into a compound virtual beam model with two separated virtual beams. There is a limitation by this model also, namely the load should be perpendicular to the panel and by the final deflection calculation some parameters are derived only for certain load situations.

Timoshenko beam theory [17-18]

Recently this is the most common and practically used beam theory if the shear deformation is considered. It is also applicable to design CLT panel considering beam behaviour. By this method the precise shear correction factor calculation is necessary, which is the most critical part of this model to get the correct deflections.

Remarks on the previously mentioned methods

Obviously all of the mentioned beam theoretical approaches - or we can say here the beam theories at all - are not able to account surface structure load transfer and basically not able to provide such mechanical behaviour like plate/shell. It is more clear that the CLT panels are unable to treat as a beam because the width of one individual panel can reach 3 meters. With this width a CLT panel goes beyond the definition of a beam! It means that the mentioned four different calculation methods regarding CLT panels are inapplicable if we would like to model an arbitrary shaped plate or wall with arbitrary boundary (support) conditions.

In addition it is also a requirement in FEM-Design 3D Structure module that the applied external loads on the panels need to be arbitrary. Therefore the previously introduced laminated composite shell theory (ESLM with FSDT) is much better calculation method which provides more realistic results in all aspects than the mentioned beam theories and last but not least it is suitable for integration into FEM-Design 3D Structure module.

Laminated composite shell theory (ESLM) as CLT application

Structural elements made of CLT material with different mechanical plate theories were modeled and calculated in Ref. [19]. In this reference compared with experimental studies they stated that with ESLM theory the deflections are very close to the experimental results. Based on Ref. [19] displacements from the calculations and from measured values were almost the same, thus it means that the stiffness representation of the laminated composite shells are very adequate to model a CLT structure. In Ref. [20] it is also concluded that the stiffnesses of the laminated composite shell theory is more than appropriate to CLT structural design compared to analytical plate solution in Ref. [21]. Although in Ref. [20] it is also stated that more advanced plate theories are capable of producing more accurate shear stress results directly, however the ESLM provides corresponding shear stress results in engineering point of view based on Eq. 45-46.

5.1 Additional settings to CLT application of laminated composite shells

5.1.1 Shear coupling or no shear coupling settings between layers

In Chapter 3.2, 4.1.1 and 4.2.1 the stiffness and stress calculation of a laminated composite shell with shear coupling between layers have been derived. In Chapter 3.3, 4.1.2 and 4.2.2 the stiffness and stress calculation of a laminated composite shell without shear coupling between layers have been stated. Fig. 8 shows the position of the glue what is necessary to provide the shear coupling behaviour between layers. These glue between the layers what was indicated in Fig. 8 mostly provided by the manufacturers. By default FEM-Design considers the shear coupling between layers.

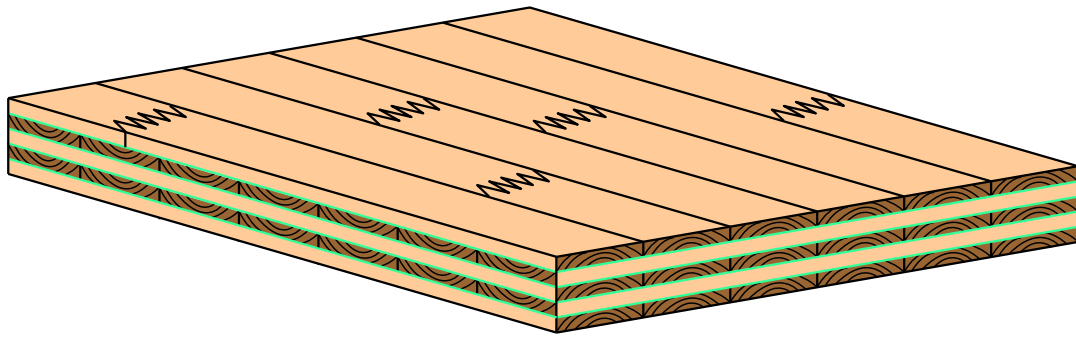


Figure 8 – The necessary positions of the glued surfaces to ensure shear coupling between layers (green lines)

5.1.2 No glue at narrow side option

If our laminated composite shell modelled with CLT material then there is an additional option in the program namely: “no glue at narrow sides” option. Fig. 9 shows the positions of these narrow sides gluing area. Some of the manufacturers provides the glue at these narrow sides between the planks but some of the manufacturers don't. By default FEM-Design considers glue at narrow sides. If there is glue between the narrow sides of the planks the stiffness matrix calculation is according to Chapter 3.2 and 3.3.

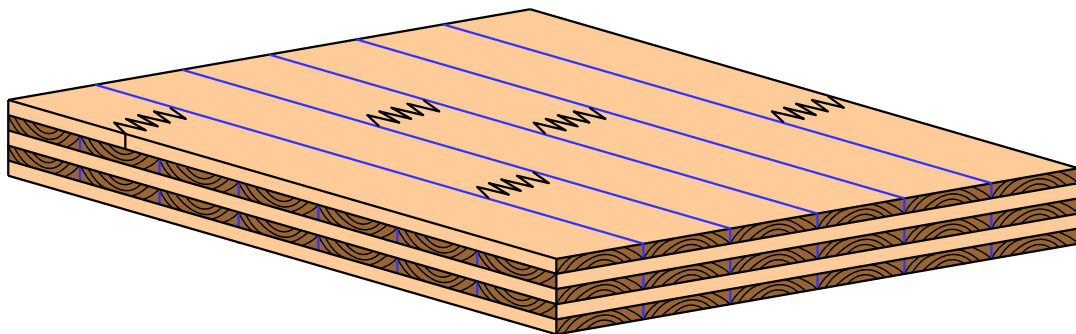


Figure 9 – The positions of the glued surfaces to ensure glue at narrow sides behaviour option (blue lines)

If the no glue at narrow sides is the adjusted case then the following modification by the stiffness matrix calculation will be made:

- One of the layers elastic constants properties will be modified. According to Chapter 3.1 notation system for every layers the value of $E_y = 0$ during the homogenization method to the stiffness matrix. It means that the Young's modulus perpendicular to the grain direction will be zero during the stiffness and stress calculation.

5.1.3 Additional reduction factors on the constitutive shell stiffness matrix

There could be made some other stiffness reduction with r_{33} , r_{66} , r_{77} and r_{88} on the stiffness matrix namely on the elements which are indicated in Eq. 48. These reduction factors could be useful if the manufacturer or the handbook of the CLT provider give these reduction factors to the homogenization considering measurements and experimental formulas.

$$\begin{bmatrix}
 D_{11} & D_{12} & D_{16} & B_{11} & B_{12} & B_{16} & 0 & 0 \\
 D_{12} & D_{22} & D_{26} & B_{12} & B_{22} & B_{26} & 0 & 0 \\
 D_{16} & D_{26} & r_{33} D_{66} & B_{16} & B_{26} & B_{66} & 0 & 0 \\
 B_{11} & B_{12} & B_{16} & A_{11} & A_{12} & A_{16} & 0 & 0 \\
 B_{12} & B_{22} & B_{26} & A_{12} & A_{22} & A_{26} & 0 & 0 \\
 B_{16} & B_{26} & B_{66} & A_{16} & A_{26} & r_{66} A_{66} & 0 & 0 \\
 0 & 0 & 0 & 0 & 0 & 0 & r_{77} S_{55} & S_{45} \\
 0 & 0 & 0 & 0 & 0 & 0 & S_{45} & r_{88} S_{44}
 \end{bmatrix} \quad (\text{Eq. 48})$$

REMARK 1: Regarding the consequent stress calculation and the physical causes of these modifications on the stiffness matrix (Eq. 48) these options only applicable by a CLT panel if the laminated composite has symmetrical layers or with other words the eccentricity stiffness part is zero ($B_{ij}=0$; ($i, j = 1, 2, 6$)).

REMARK 2: There is additional recommendations in the literature if the no glue at narrow sides option adjusted, namely e.g. in Ref. [22] instead of Eq. 21 the A_{66} element of the stiffness matrix should be calculated with the following formula, see Eq. 49:

$$A_{66} = 0.25 \sum_{k=1}^N (\bar{Q}_{66})_k (z_k - z_{k+1}) \quad (\text{Eq. 49})$$

If the user would like to apply this specific recommendation in FEM-Design by the stiffness reduction factors (see Eq. 48) the r_{66} value should be adjust to 0.25.

5.2 Load duration classes

According to Eurocode 5 (see Ref. [23]) the actions shall be assigned to one of the load-duration classes given in the following table:

Load Duration Class	Accumulated Duration of load
Permanent	> 10 years
Long term	6 months – 10 years
Medium term	1 week – 6 months
Short term	< 1 week
Instantaneous	N/A

Table 1 – Load duration classes

5.3 Service classes

According to Eurocode 5 structures shall be assigned to one of the service classes given below:

- Service class 1: characterised by a moisture content in the materials corresponding to a temperature of 20°C and the relative humidity of the surrounding air only exceeding 65 % for a few weeks per year. The average moisture content in most softwoods will not exceed 12 %.
- Service class 2: characterised by a moisture content in the materials corresponding to a temperature of 20°C and the relative humidity of the surrounding air only exceeding 85 % for a few weeks per year. The average moisture content in most softwoods will not exceed 20 %.
- Service class 3: characterised by climatic conditions leading to higher moisture contents than in service class 2.

5.4 Modification factors on strength and stiffness

5.4.1 Effect of load-duration and moisture content on strength

The load-duration classes and service classes have effect on the design strength properties of the timber structures. The general calculation formula of the design strength parameters in Eurocode 5:

$$X_d = k_{mod} \frac{X_k}{\gamma_M}, \quad (\text{Eq. 50})$$

where X_d is the design value of a strength parameter, X_k is the characteristic value of a strength parameter, γ_M is the partial factor for a strength parameter and k_{mod} is the modification factor according to the following table to CLT members (see Ref. [23-24]):

Service class	Load duration class – k_{mod} values				
	Permanent	Long term	Medium term	Short term	Instantaneous
1	0.60	0.70	0.80	0.90	1.10
2	0.60	0.70	0.80	0.90	1.10
3	0.50	0.55	0.65	0.70	0.90

Table 2 – Strength modification factors in different service and load duration classes

5.4.2 Effect of moisture content on deformation

For the different limit states (ultimate or serviceability) the service classes have effect on the used deformation properties of the timber structures. The general calculation formula of the used deformation parameters in Eurocode 5:

$$\frac{EP}{1 + k_{def}}, \quad (\text{Eq. 51})$$

where EP is an elastic parameter (Young's or shear modulus) and k_{def} is the deformation modification factor. We will talk about this used deformation properties in Chapter 5.5 that how it is applied in FEM-Design by the different load combinations.

According to Ref. [24] the recommended values of k_{def} for CLT members:

Service class	CLT – k_{def}
1	0.60
2	0.80
3	N/A

Table 3 – The recommended deformation factors by CLT panels according to Ref. [24]

According to Ref. [25-26] the recommended values of k_{def} for CLT members:

Service class	CLT – k_{def}
1	0.90
2	1.10
3	N/A

Table 4 – The recommended deformation factors by CLT panels according to Ref. [25-26]

5.4.3 System strength

According to Eurocode 5 when several equally spaced similar members, components or assemblies are laterally connected by continuous load distribution system, the member strength properties may be multiplied by a system strength factor k_{sys} . For glued laminated timber decks or floors the k_{sys} value according to the Eurocode 5 is the following:

$$k_{sys} = \min [1.2; 0.9714 + 0.02857 N] \quad , \quad (\text{Eq. 52})$$

where N is the loaded laminations.

REMARK: Although this value is given in Eurocode 5 the application of k_{sys} is not necessary because EC5 design methodology is based on beam mechanical model, which neglects many effects (e.g. Poisson's ratio etc.) if the analyzed structure is a plate such as CLT floor decks, walls. In FEM-Design the new mechanical model for the CLT panel is the mentioned laminated composite shell theory, therefore the recommended value for system strength factor:

$$k_{sys} = 1.0 \quad .$$

5.4.4 Effect of cracks

In Eurocode 5 for the verification of shear resistance of members in bending the influence of cracks should be taken into account using a crack factor k_{cr} . However in Ref. [27] it is noted that it is not necessary, because CLT is a plane element with connected glued layers and potential cracks are assumed to be considered in the product confirmations, therefore we neglect this effect in the new CLT calculation method in FEM-Design.

5.4.5 Effect of shape and size of cross section on strength

In Eurocode 5 the modification on strength parameters due to cross-sectional size and shape of a beam and other members is taken into account by applying a factor k_{shape} and k_h to the design strength. The theory behind k_{shape} parameter presumes the consumption a beam model thus in FEM-Design the $k_{shape} = 1.0$. The size effect on strength parameters has not standardized yet by a CLT panel so the size effect also neglected, $k_h = 1.0$.

5.4.6 Partial factor for material properties

The relevant partial factor to CLT members should be stated in the National Annex, but according to Ref. [23] the recommended value by CLT members is $\gamma_M = 1.25$ by ultimate limit state load combinations.

5.5 Design value of a material properties

Usually if the material of the different layers in the laminated shell is made by timber material the following elastic properties should be considered layer-by-layer but of course these values are adjustable by the users. Here you can see the specific material values which are related to C24 timber which is mostly the main component of CLT members. These values are only informative and mainly according to EN 338 and other recommendations (e.g. Ref. [28]). Additional information can be found in the documentations of manufacturers as well.

The Young's modulus in the direction of the grain:

$$E_x = E_{0, mean} = 11000 \text{ MPa}$$

The Young's modulus perpendicular to the grain direction:

$$E_y = E_{90, mean} = 370 \text{ MPa}$$

The shear modulus parallel with grain direction:

$$G_{xy} = G_{xz} = G_{mean} = 690 \text{ MPa}$$

The rolling shear modulus:

$$G_{yz} \approx \frac{G_{mean}}{10} = 69 \text{ MPa}$$

The Poisson's ratio in the relevant direction of the planks (see Chapter 2.2, Ref. [28]):

$$0.2 \leq \nu_{xy} \leq 0.45$$

By the stiffness matrix calculation the considered elastic properties are calculated based on the deformation factor (k_{def} , see Eq. 51). In FEM-Design the users are able to define different deformation factors for the different type of load combinations:

- k_{defU} in ultimate limit state combinations,
- k_{defSc} characteristic serviceability limit state combinations,
- k_{defSf} frequented serviceability limit state combinations,
- k_{defSq} quasi-permanent serviceability limit state combinations.

The elastic parameters which will be used by the finite element calculation are derived with the following formulas. All of the elastic properties (except Poisson's ratio) will be reduced according to the following table.

The elastic properties EP can be the Young's modulus (elastic modulus) or shear modulus as well:

Elastic properties (Young's or shear modulus)		
Load case calculation Load group calculation 1 st order load combination Construction stage	ULS	$\frac{EP}{1+k_{defU}}$
	SLS characteristic	$\frac{EP}{1+k_{defSc}}$
	SLS frequented	$\frac{EP}{1+k_{defSf}}$
	SLS quasi-permanent	$\frac{EP}{1+k_{defSq}}$
2 nd order load combination Imperfection calculation	ULS	$\frac{EP}{\gamma_M}$
	SLS characteristic	$\frac{EP}{\gamma_M}$
	SLS frequented	$\frac{EP}{\gamma_M}$
	SLS quasi-permanent	$\frac{EP}{\gamma_M}$
Stability analysis		EP
Eigenfrequency calculation Seismic analysis All dynamic analysis		EP

Table 5 – The used elastic parameters to the homogenization procedure by the different types of calculations in FEM-Design

In Table 5 γ_M is the partial factor for timber material in ULS, see Chapter 5.4.6.

5.6 Strength resistance properties of CLT panels

Due to the fact that a CLT panel in mechanical point of view is a plate and not a beam additional strength parameters appears than by a beam. In FEM-Design program we use the following strength parameters. The meanings of them can be seen in Fig. 10.

- $f_{m,0,k}$ – the characteristic value of bending strength along the grain
- $f_{m,90,k}$ – the characteristic value of bending strength perpendicular to the grain
- $f_{t,0,k}$ – the characteristic value of tensile strength along the grain
- $f_{t,90,k}$ – the characteristic value of tensile strength perpendicular to the grain
- $f_{c,0,k}$ – the characteristic value of compressive strength along the grain
- $f_{c,90,k}$ – the characteristic value of compressive strength perpendicular to the grain
- $f_{xy,k}$ – the characteristic value of shear strength from in-plane effects
- $f_{v,k}$ – the characteristic value of shear strength from transverse effects along the grain
- $f_{R,k}$ – the characteristic value of rolling shear strength
- $f_{tor,k}$ – the characteristic value of torsional strength at glued contact surface

By a regular C24 timber the recommended characteristic strength parameters are as follows (considering EN338 and Ref. [22-29]):

- $f_{m,0,k} = 24.0 \text{ MPa}$
- $f_{m,90,k} = 1.0 \text{ MPa}$
- $f_{t,0,k} = 14.5 \text{ MPa}$
- $f_{t,90,k} = 0.5 \text{ MPa}$
- $f_{c,0,k} = 21.0 \text{ MPa}$
- $f_{c,90,k} = 2.5 \text{ MPa}$
- $f_{xy,k} = 4.0 \text{ MPa}$
- $f_{v,k} = 4.0 \text{ MPa}$
- $f_{R,k} = 1.5 \text{ MPa}$
- $f_{tor,k} = 3.5 \text{ MPa}$

Naturally more precise values can be found in the brochures of the manufacturers.

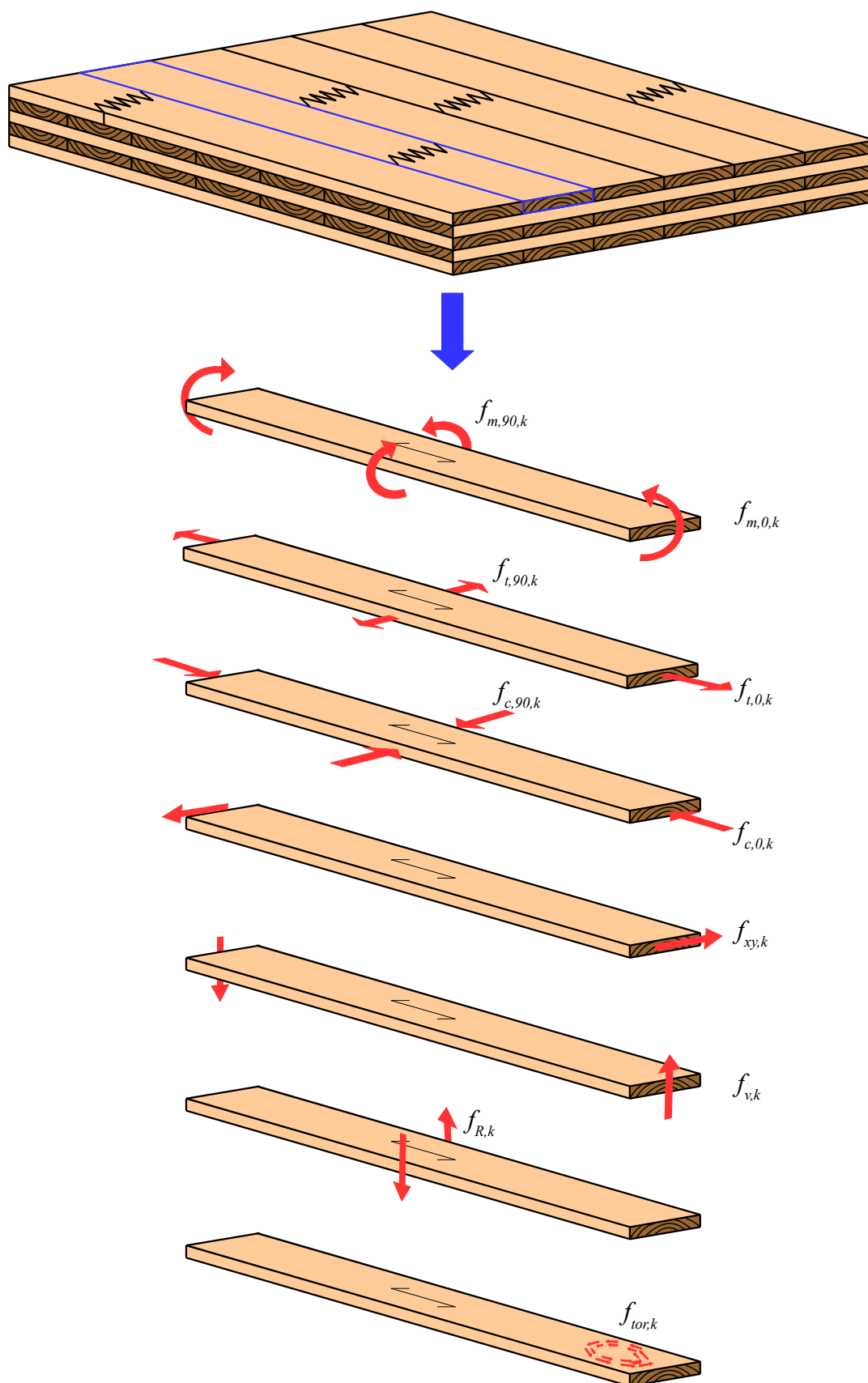


Figure 10 – Representation of the causes of the different strength values

5.7 Design values of strength resistance properties of CLT panels

The design values of the CLT strength parameters considering the mentioned load duration classes, system modification factor and partial factor are as follows:

$$\begin{pmatrix} f_{m,0,d} \\ f_{m,90,d} \\ f_{t,0,d} \\ f_{t,90,d} \\ f_{c,0,d} \\ f_{c,90,d} \\ f_{xy,d} \\ f_{v,d} \\ f_{R,d} \\ f_{tor,d} \end{pmatrix} = k_{sys} \frac{k_{mod}}{\gamma_M} \begin{pmatrix} f_{m,0,k} \\ f_{m,90,k} \\ f_{t,0,k} \\ f_{t,90,k} \\ f_{c,0,k} \\ f_{c,90,k} \\ f_{xy,k} \\ f_{v,k} \\ f_{R,k} \\ f_{tor,k} \end{pmatrix}, \quad (\text{Eq. 53})$$

where on the left side the values are the design strength values of the mentioned characteristic properties in Chapter 5.6. The recommended value k_{sys} is 1.0 for CLT members according to the explanation in Chapter 5.4.3, but of course it is adjustable by the user.

5.8 Design checks in ultimate limit state

In Chapter 5.6-7 we defined the different strength parameters and visualized the meanings of them. Here in this Chapter we will show the equations which are the basics of the design procedures of a CLT panel in FEM-Design. All of the given checking equations in the following sub-chapters could be relevant in any layers of the CLT panel, therefore the following equations must be checked in every layers to design a given panel.

REMARK: In this chapter the 0 and 90 indices by the normal stress and normal strength parameters indicate the grain and perpendicular to grain direction respectively. Because there is no unified standardization to the notation of the different shear stresses and shear strengths therefore in this chapter by these values the x - y - z indices mean the orthotropy directions of a specific layer.

The design formulas are based on Ref. [22-23],[29-35].

5.8.1 Normal stresses from compression, tension and bending

In this Chapter the design equations will be shown to the checking the normal stresses in one layer in the CLT panel. Thus it means that all of the given equations in Chapter 5.8.1 is relevant in the direction of the grain and perpendicular to the grain of one layer. The meanings of the separation of the normal stresses in the grain or perpendicular to the grain direction is given in Fig. 11.

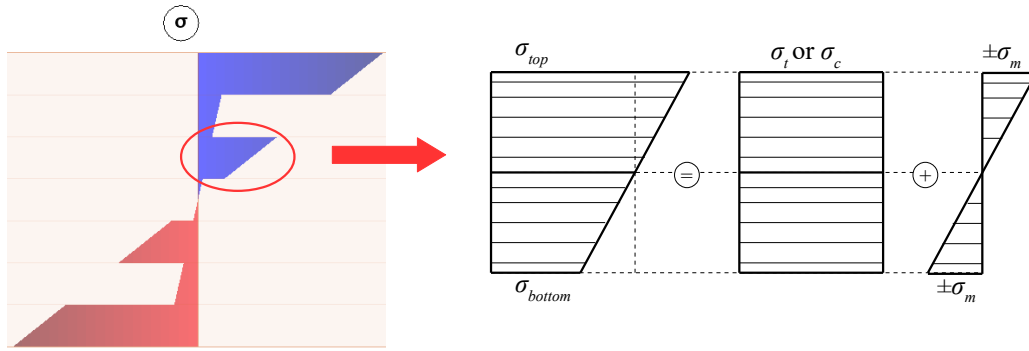


Figure 11. - The meanings of the separation of compressive or tensile and the bending in-plane stresses in one layer in case of strength check

5.8.1.1 Tension and bending parallel to grain direction

If the greater absolute value of the normal stresses at the top or bottom side in the grain direction of one layer is tensile stress then the following equation should be fulfilled.

$$\frac{\sigma_{t,0,d}}{f_{t,0,d}} + \frac{|\sigma_{m,0,d}|}{f_{m,0,d}} \leq 1.0 \quad (\text{Eq. 54})$$

5.8.1.2 Tension and bending perpendicular to grain direction

If the greater absolute value of the normal stresses at the top or bottom side in perpendicular direction of the grain of one layer is tensile stress then the following equation should be fulfilled.

$$\frac{\sigma_{t,90,d}}{f_{t,90,d}} + \frac{|\sigma_{m,90,d}|}{f_{m,90,d}} \leq 1.0 \quad (\text{Eq. 55})$$

5.8.1.3 Compression and bending parallel to grain direction

If the greater absolute value of the normal stresses at the top or bottom side in the grain direction of one layer is compressive stress then the following two equations should be fulfilled.

$$\frac{|\sigma_{c,0,d}|}{f_{c,0,d}} \leq 1.0 \quad (\text{Eq. 56})$$

$$\left(\frac{\sigma_{c,0,d}}{f_{c,0,d}} \right)^2 + \frac{|\sigma_{m,0,d}|}{f_{m,0,d}} \leq 1.0 \quad (\text{Eq. 57})$$

5.8.1.4 Compression and bending perpendicular to grain direction

If the greater absolute value of the normal stresses at the top or bottom side in perpendicular direction of the grain of one layer is compressive stress then the following two equations should be fulfilled.

$$\frac{|\sigma_{c,90,d}|}{f_{c,90,d}} \leq 1.0 \quad (\text{Eq. 58})$$

$$\left(\frac{\sigma_{c,90,d}}{f_{c,90,d}} \right)^2 + \frac{|\sigma_{m,90,d}|}{f_{m,90,d}} \leq 1.0 \quad (\text{Eq. 59})$$

5.8.2 Shear stresses from in-plane shear, torsion and transverse shear force

In this Chapter the design equations will be shown to check the different shear stresses in one layer. The meanings of the design values in the different directional shear stresses is given in Fig. 12. In Fig. 10 we saw the meanings of the shear strength parameters.

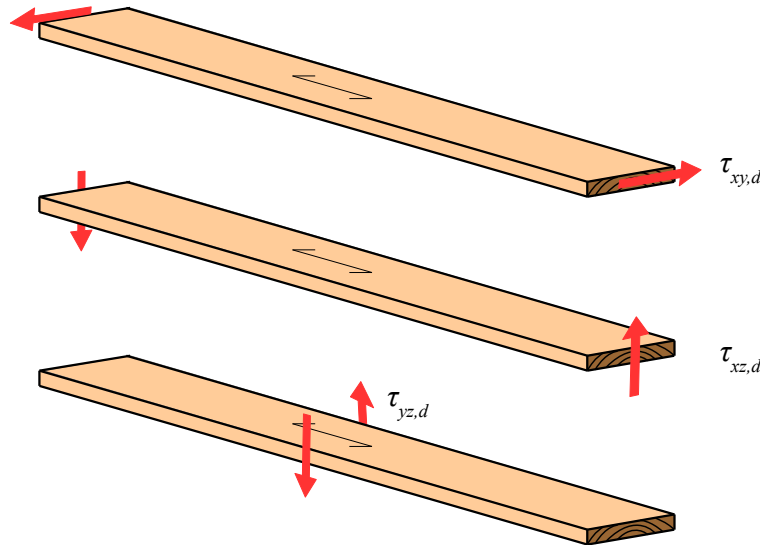


Figure 12 - The interpretation of the design shear stresses in one layer plank

5.8.2.1 Shear stresses from in-plane shear and torsion

The $\tau_{xy,d}$ shear stresses could come from in-plane shear force (n_{xy}) and torsional moments (m_{xy}) as well, see Eq. 17a. The following equation should be fulfilled.

$$\frac{|\tau_{xy,d}|}{f_{xy,d}} \leq 1.0 \quad (\text{Eq. 60})$$

5.8.2.2 Shear stresses from transverse shear force parallel to grain direction

The $\tau_{xz,d}$ transverse shear stresses could come from transverse shear forces, see Eq. 17a. The following equation should be fulfilled.

$$\frac{|\tau_{xz,d}|}{f_{v,d}} \leq 1.0 \quad (\text{Eq. 61})$$

5.8.2.3 Shear stresses from transverse shear force (rolling shear)

The $\tau_{yz,d}$ transverse shear stresses could come from transverse shear forces, see Eq. 17a. This shear stress is the so-called rolling shear. The following equation should be fulfilled.

$$\frac{|\tau_{yz,d}|}{f_{R,d}} \leq 1.0 \quad (\text{Eq. 62})$$

5.8.3 Shear interaction formulas

During the design process depending on the internal force state there can be interactions between different stress types. These interaction formulas can be relevant in any point of one layer, therefor in FEM-Design the interaction check according to these formulas will be performed in several points along the thickness of one layer to get the most unfavourable situation.

5.8.3.1 Summarized shear stresses parallel to grain direction

This checking formula is relevant if there are shear stresses from in-plane effect and transverse shear effect parallel with grains (see Fig. 12). Basically this is the checking of the resultant shear stress parallel with grains. The following equation should be fulfilled.

$$\left(\frac{\tau_{xy,d}}{f_{xy,d}} \right)^2 + \left(\frac{\tau_{xz,d}}{f_{v,d}} \right)^2 \leq 1.0 \quad (\text{Eq. 63})$$

5.8.3.2 Perpendicular tensile normal stresses and rolling shear

This checking formula is relevant if there are rolling shear stress and tensile normal stress perpendicular to the grain direction. The following equation should be fulfilled.

$$\frac{\sigma_{t,90,d}}{f_{t,90,d}} + \frac{|\tau_{yz,d}|}{f_{R,d}} \leq 1.0 \quad (\text{Eq. 64})$$

5.8.3.3 Perpendicular compressive normal stresses and rolling shear

This checking formula is relevant if there are rolling shear stress and compressive normal stress perpendicular to the grain direction. The following equation should be fulfilled.

$$\frac{|\sigma_{c,90,d}|}{f_{c,90,d}} + \frac{|\tau_{yz,d}|}{f_{R,d}} \leq 1.0 \quad (\text{Eq. 65})$$

5.8.4 Shear check at glued contact surface from rolling shear and torsion between layers

This design checking formula only active if the “shear coupling between layers” and “no glue at narrow sides” option is adjusted (see Chapter 5.1) by the application data of the CLT panels. The checking formula will be done in every layers top and bottom side if that side is an intermediate side of the panel (no checking on the top and bottom side of the gross panel). In this Chapter the design formula and the derivation of the formulas are based on Ref. [29][31-35].

$$\frac{|\tau_{tor,d}|}{f_{tor,d}} + \frac{|\tau_{yz,d}^{inplane}| + |\tau_{yz,d}|}{f_{R,d}} \leq 1.0 \quad (\text{Eq. 66})$$

Below you can see the meanings and the calculation method of the members in Eq. 66.

The additional rolling shear stress (from in-plane effect) considers that there is no glue at the narrow sides of the boards (planks). In this case the increment of the normal force in the longitudinal (grain) direction of the adjacent layers should be transferred along the perpendicular direction along the plank width of the examined layer. We calculate this effect with the following formula:

$$\tau_{yz,d}^{inplane} = \frac{\Delta N_y}{a^2} \approx \frac{\frac{\partial n_y}{\partial y}}{N-1} \quad (\text{Eq. 67})$$

where ΔN_y is the normal force increment perpendicular to the grain direction of the examined layer on a^2 area, where a is the width of the plank (one board, see Fig. 13). This additional rolling shear stress approximately equal to the mentioned value in Eq. 67, where $\partial n_y / \partial y$ is the perpendicular specific normal force derivatives in perpendicular direction of the grain and N is the total number of the layers (see Ref. [33-34]).

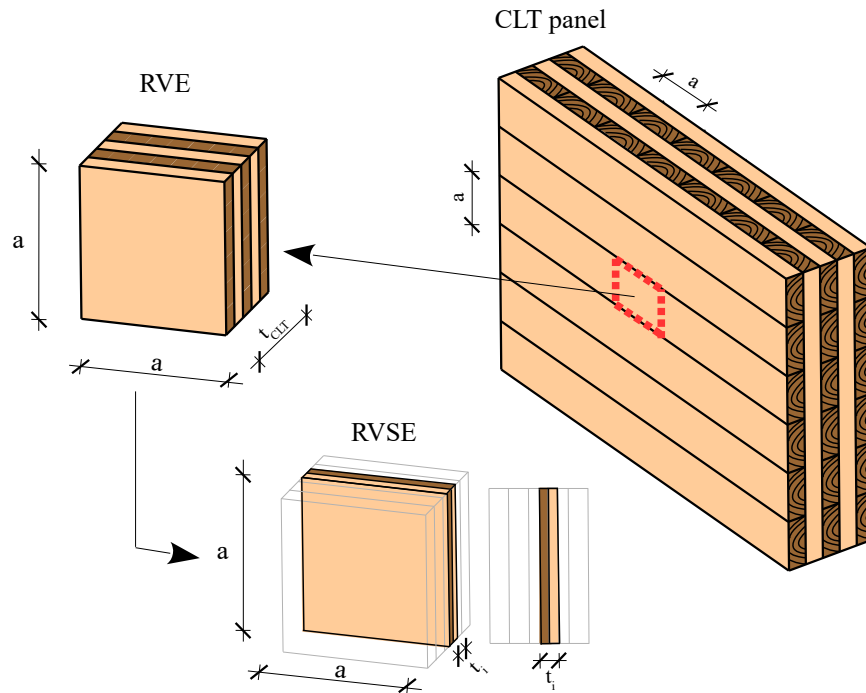


Figure 13 - The meanings of the RVE and RVSE elements on a CLT panel

If there is no glue at the narrow sides of the boards (planks) there will be an additional torsional effect between the adjacent layers (glued surface) which could cause failure.

To consider the additional torsion effect on the glued surfaces between the planks we should introduce the representative volume element (RVE) and the representative volume sub-element (RVSE) of the CLT panel. The RVE is the smallest unit with thickness equal to a CLT element and width and depth equal to the width of a board (plank) plus the half the width of possible gaps between adjacent boards. In the case of CLT with constant layer thicknesses, the RVE is further reduced to an elementary RVSE that represent the smallest unit cell at an intersection between two orthogonal boards with an internal stress state describing the global behaviour of the CLT element (see Fig. 13-14 and Ref. [29][31-35]).

This additional torsional stress is calculated with the following formula:

$$\tau_{tor,d} = \frac{3n_{xy}}{a(N-1)} \quad (\text{Eq. 68})$$

This is comes from a torsional model on a square cross-section where the warping is restrained, according to Ref. [31] and see the meanings of this torsional stress in Fig. 14 right side:

$$\tau_{tor,d} = \frac{M_{tor,d}}{I_p} \frac{a}{2} = 3\tau_{0,d} \frac{t_i}{a} = 3 \frac{n_{xy}}{(N-1)t_i} \frac{t_i}{a} = \frac{3n_{xy}}{a(N-1)} \quad (\text{Eq. 69})$$

Here the polar moment of inertia:

$$I_p = \frac{a^4}{6} \quad (\text{Eq. 70})$$

The calculation of the $M_{tor,d}$ torsional moment (torque) is considering that the shear stresses (nominal shear stress, $\tau_{0,d}$ see Fig. 14 left side) from the n_{xy} in-plane internal force value in reality not transferred along the narrow sides without glue and on the RVSE in reality the shear stresses higher than the calculated shear stresses from a homogenized continuous section. The $\tau_{net,d}$ net shear stress (see Fig. 14 center) is greater than the $\tau_{0,d}$ nominal shear stress.

The resultant of the $\tau_{net,d}$ net shear stress along the two opposite sides of the RVSE is the $M_{tor,d}$ torsional moment:

$$M_{tor,d} = 2\tau_{net,d} a \frac{t_i}{2} \frac{a}{2} = \tau_{net,d} a^2 \frac{t_i}{2} = \tau_{0,d} a^2 t_i \quad (\text{Eq. 71})$$

Where the increased net shear stress ($\tau_{net,d}$) according to the no glue effect at the narrow sides assumed to be:

$$\tau_{net,d} = 2\tau_{0,d} \quad (\text{Eq. 72})$$

And the nominal shear stress ($\tau_{0,d}$) considering constant distribution of shear stresses along the thickness of the CLT panel is the following:

$$\tau_{0,d} = \frac{n_{xy} a}{(N-1) a t_i} = \frac{n_{xy}}{(N-1) t_i} \quad (\text{Eq. 73})$$

here the t_i is the thickness of the RVSE element (see Fig. 13-14), but of course if the layers thicknesses are the same, then this equal to one layer thickness.

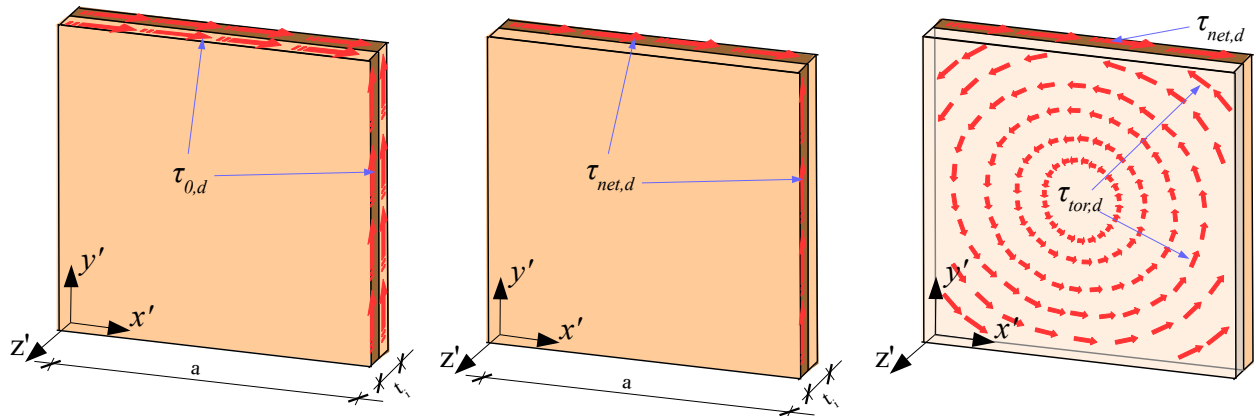


Figure 14 - The meanings of the nominal shear stress on RVSE (left side), the meanings of the net shear stresses without glue at the narrow sides (center), and the meanings of the additional torsional shear stress on the glued surface (right side)

5.8.5 Buckling check

There is no obvious buckling check information related to CLT panels in Eurocode 5. Using the Eurocode methodology the proposed and implemented buckling method in FEM-Design is the following. In EC5 Eq. 74 formula is given to verify a timber structure against buckling based on the effective length method with a reduction factor on the compressive strength.

$$\frac{\sigma_{c,0,d}^{buckling}}{k_c f_{c,0,d}} + \frac{\sigma_{m,0,d}^{buckling}}{f_{m,0,d}} \leq 1.0, \quad (\text{Eq. 74})$$

where above the mentioned values the k_c is a reduction factor on the compressive strength.

Against the separation of bending and compressive stresses by the strength checking layer-by-layer (see Fig. 11) here in Eq. 74 we need to use different separation of the compressive stresses in the most unfavorable layer according to the EC5 methodology related to the timber buckling analysis with Ayrton-Perry formula. In this case when we checking a layer in the grain direction according to Eq. 74 we should consider a compressive stress which arise due to the membrane strains at the mid-plane of the laminated composite (see Eq. 16) and the compressive bending stress comes from that compressive stress which is above this compressive stress from mid-plane strains. In the most simple case the stress separation can be seen in Fig. 15 but in a general case it is detailed later.

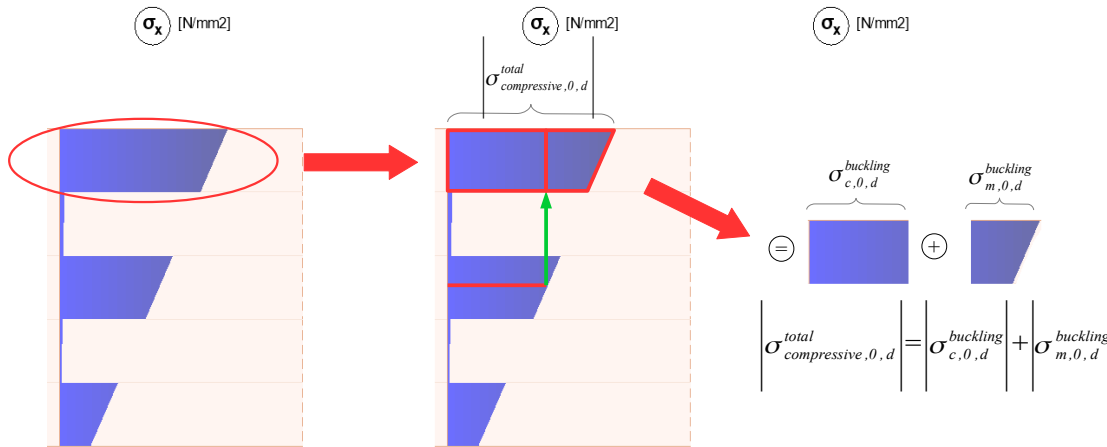


Figure 15 – The compressive stress separation in case of buckling analysis in an outer layer

With this stress separation method the buckling check will be adequate because this fits into the EC5 methodology and because we will define the relative slenderness in a general way as well (see also the verification example later).

By a CLT panel – considering the laminated composite shell theory – this checking formula can be interpreted in every layer and in an arbitrary direction. In FEM-Design the buckling check is calculated with given consideration below. A precondition of this buckling check is that in the specified buckling length direction at the given point the specific normal force should be

negative which means global compression in that direction. If this precondition is not fulfilled it means that the flexural stability failure is not relevant. Furthermore we assume that lateral torisonal buckling can not occur since CLT panel is a surface member.

Furthermore in FEM-Design the k_c reduction factor determined with the method detailed in the sub-chapters below.

5.8.5.1 The generalized relative slenderness

First of all in FEM-Design we provided a calculation method to get general relative slenderness value in a specific direction. The generalized formula of the relative slenderness based on Eurocode:

$$\lambda_{rel} = \sqrt{\frac{Af}{N_{cr}}} \quad , \quad (\text{Eq. 75})$$

where in general A is the cross-sectional area, f is the compressive normal strength and N_{cr} is the elastic critical force considering the effective length. The original EC5 formula to timber buckling analysis comes from this general relative slenderness formula as well.

If the critical elastic force is specific value and the cross-sectional area reduces to a thickness – because now we are talking about shell behaviour – the generalized relative slenderness turns into the following equation:

$$\lambda_{rel} = \sqrt{\frac{\sum_{i=1}^N t_i f_{c,\alpha,k,i}}{n_{cr}}} \quad , \quad (\text{Eq. 76})$$

where t_i is the thickness of the i^{th} layer, $f_{c,\alpha,k,i}$ is the characteristic compressive strength of the i^{th} layer in the direction of the given buckling length (see Fig. 16).

According to EC5 the compressive strength in an arbitrary direction using the strength in the grain direction and perpendicular to grain direction can be formulated with Eq. 77.

$$f_{c,\alpha,k,i} = \frac{f_{c,0,k,i}}{\frac{f_{c,0,k,i}}{f_{c,90,k,i}} \sin^2 \alpha_i + \cos^2 \alpha_i} \quad , \quad (\text{Eq. 77})$$

where above the already mentioned values α_i is the angle between the i^{th} layer grain direction and the given buckling length direction (see Fig. 16).

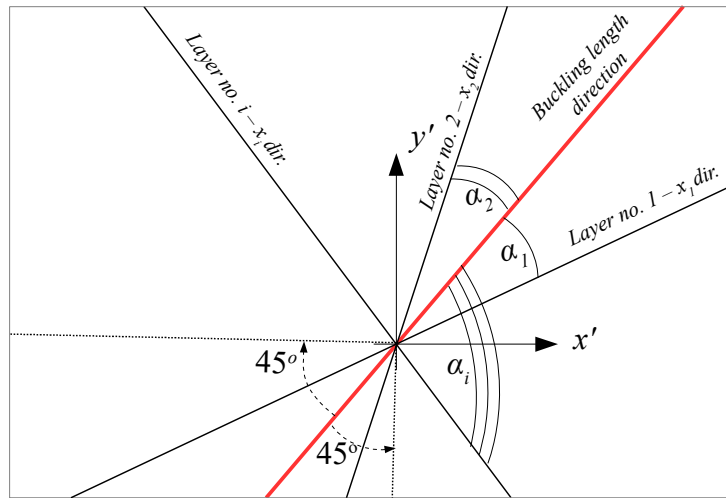


Figure 16 – The α_i directions between the grain directions (x_i) of the layers and the buckling length direction; and the $\pm 45^\circ$ angle range regarding the buckling length direction where the compressive strength reduction occurs

The whole homogenization procedure what was shown in Chapter 3 should be made in the direction of the buckling direction, see Eq. 17-40. It means that the shell local system should be replaced in the transformations with the direction of the buckling length direction and perpendicular to it. In this case with the aim of the homogenization method we can get the relevant bending and shear stiffnesses in the direction of the buckling direction to calculate the elastic critical specific force.

5.8.5.2 The calculation of the elastic critical force with shear deformation

Keep in mind that in the homogenization method all of the elastic parameters should be replaced with its 5% quantile values:

$$\begin{aligned}
 E_{x,05} &= r E_{x,mean} ; \\
 E_{y,05} &= r E_{y,mean} ; \\
 G_{xy,05} &= r G_{xy,mean} ; \\
 G_{xz,05} &= r G_{xz,mean} ; \\
 G_{yz,05} &= r G_{yz,mean} ,
 \end{aligned}
 \tag{Eq. 78}$$

where the r value is usually between 0.67-0.84. It is an input reduction factor in FEM-Design design parameters by buckling calculation because it is not completely clarified in the standard by a CLT panel .

By the calculation of the elastic critical force in the given buckling length direction we should consider the effective buckling length and the shear deformations as well. Thus according to Föppl summation rule the elastic critical force to the given buckling length direction of the CLT panel can be calculated based on the homogenization in the buckling length direction

considering characteristic values of the mentioned elastic parameters with Eq. 79.

$$n_{cr} = \frac{1}{\frac{1}{\left(\frac{D'_{11}\pi^2}{(\beta L)^2}\right)} + \frac{1}{S'_{55}}} \quad , \quad (\text{Eq. 79})$$

where D'_{11} represent the relevant specific bending stiffness (see Eq. 17a) of the panel and S'_{55} is the relevant specific shear stiffness as well in the given buckling direction (see Eq. 17a). The L is the geometric length between the two points where the buckling length direction intersects the boundaries of the shell region (see Fig. 16). The β factor defines the effective buckling length with L in the denominator, $L_{cr} = \beta L$.

5.8.5.3 Calculation of the reduction factor

After the calculation of the relative slenderness the reduction factor formulated with the following well-known equations:

$$k = 0.5(1 + \beta_c(\lambda_{rel} - 0.3) + \lambda_{rel}^2) \quad (\text{Eq. 80})$$

β_c is the straightness parameter by CLT panels. There is no clear instruction in EC5 to this parameter in case of CLT panels, therefore to be on the safe side, in FEM-Design $\beta_c=0.2$ is the default value but it is adjustable (see Fig. 17).

If $\lambda_{rel} \leq 0.3$ no buckling check is necessary, else:

$$k_c = \frac{1}{k + \sqrt{k^2 - \lambda_{rel}^2}} \quad (\text{Eq. 81})$$

This k_c reduction factor in the function of the relative slenderness can be seen in Fig. 17 in different β_c cases and the Euler buckling solution as well.

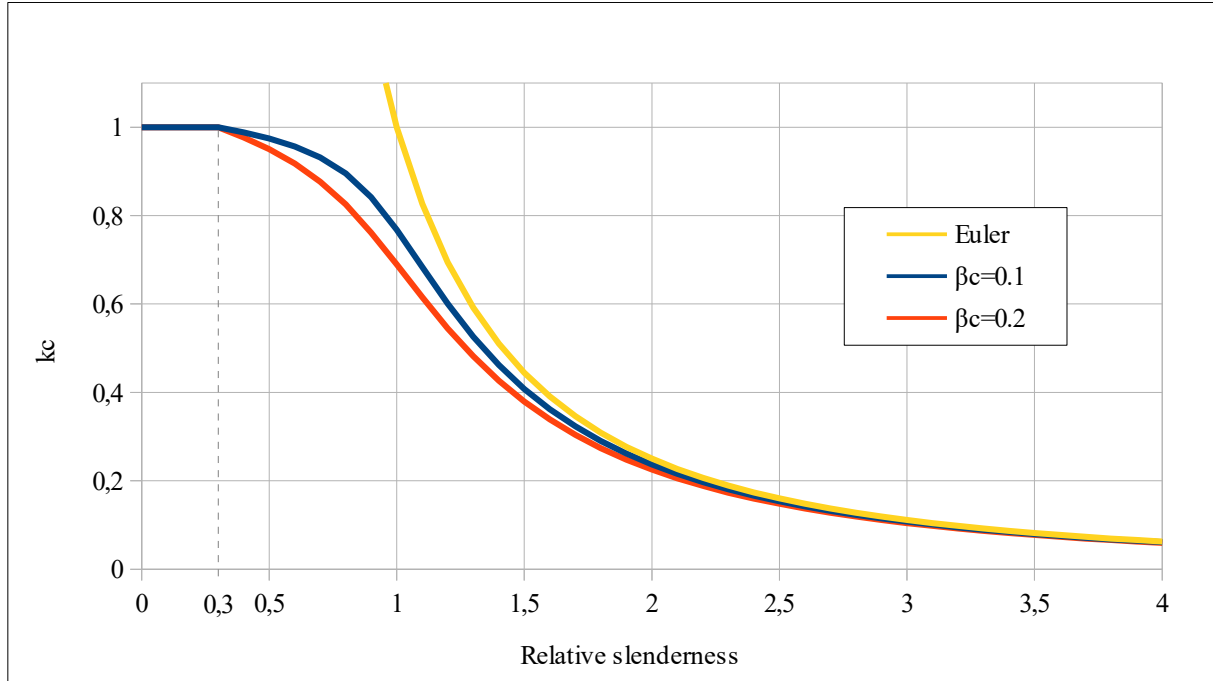


Figure 17 – The k_c reduction factor in the function of relative slenderness

With the aim of this reduction factor which will belong to the given buckling length direction as a parameter of a structural behaviour we will consider this reduction factor in Eq. 74 by those layers which directions are in the $\pm 45^\circ$ angle range regarding the buckling length direction (see Fig. 16).

5.8.5.4 The compressive stress separation by the buckling check in one specific layer

Here we show how we consider in a general direction the compressive stress separation what was mentioned at the beginning of Chapter 5.8.5. Recalling Eq. 74 again:

$$\frac{\left| \sigma_{c,0,d}^{buckling} \right|}{k_c f_{c,0,d}} + \frac{\left| \sigma_{m,0,d}^{buckling} \right|}{f_{m,0,d}} \leq 1.0 \quad (\text{Eq. 74})$$

In a general layer direction which is inside the mentioned $\pm 45^\circ$ angle range (see Fig. 16) first of all we transform the mid-plane strains of the laminated shell from the shell local system into the specific layer direction with the following formula:

$$\begin{bmatrix} \varepsilon_{0x} \\ \varepsilon_{0y} \\ \gamma_{0xy} \end{bmatrix} = \underline{T}_{(3 \times 3)} \begin{bmatrix} \varepsilon_{0x'} \\ \varepsilon_{0y'} \\ \gamma_{0x'y'} \end{bmatrix}, \quad (\text{Eq. 82})$$

where the transformation matrix comes from Eq. 18.

After this step the stress separations what was indicated in Fig. 15 can be made.

The compressive stress in grain direction for buckling analysis from mid-plane strains:

$$\sigma_{c,0,d}^{buckling} = Q_{11} \varepsilon_{0x} + Q_{12} \varepsilon_{0y} \quad , \quad (\text{Eq. 83})$$

where Q_{11} and Q_{12} comes from Eq. 15a considering Table 5 as well.

The bending stress in grain direction for buckling analysis based on the previous equation:

$$\left| \sigma_{m,0,d}^{buckling} \right| = \left| \sigma_{compressive,0,d}^{total} \right| - \left| \sigma_{c,0,d}^{buckling} \right| \quad (\text{Eq. 84})$$

This separation differs from strength check separation (see Fig. 11 and 15) because the methodology of buckling check in EC5 (Eq. 74) is originally comes from the well-know Ayrton-Perry formula (see Ref. [36-37]) and this separation is necessary to get conform results with it.

5.9 Deflection design check in serviceability limit state

In the engineering practice this topic causes misunderstandings because the Eurocode standard and its national annexes are not always consistent by calculation of timber deflections. See Ref. [38-39] about this topic. In Ref. [38] there is an explanation about the contradictions in the EN 1995-1-1 itself and compare with EN 1990.

The method according to EN 1990 and EN 1995-1-1 Chapter 2.2.3(3) is in FEM-Design to avoid the contradictions and use consequent solution to get the final deflections with creep effect.

The **final deflection** of timber structures in serviceability quasi-permanent load combination should be performed with the following equation:

$$w_{fin} = w_{inst} + w_{creep} = \left[\sum_{j \geq 1} w_{inst,G,j} + \sum_{i \geq 1} \psi_{2,i} w_{inst,Q,i} \right] (1 + k_{defSq}) \quad , \quad (\text{Eq. 85})$$

where w_{fin} is the final deflection in SLS quasi-permanent load combination, w_{inst} is the instantaneous deflection, w_{creep} is the additional deflection from creep effect, $w_{inst,G,j}$ is the instantaneous deflection from j^{th} permanent action, $w_{inst,Q,i}$ is the instantaneous deflection from i^{th} variable action, ψ_2 is the factor for quasi-permanent value of a variable action and k_{defSq} is the appropriate deformation factor

REMARK: In FEM-Design if the load combinations compiled in appropriate way by quasi-permanent SLS load combinations then by the CLT panel application data the k_{defSq} (see Chapter

5.5) should be adjusted according to Table 3 or 4 to get appropriate final deflections with accordance with Eq. 85.

EN 1995-1-1 chapter 2.2.3(2) said that the instantaneous deflections should be calculated based on the characteristic load combination without any creep effect.

The **instantaneous deflection** in serviceability characteristic load combination should be performed with the following way:

$$w_{inst} = \sum_{j \geq 1} w_{inst,G,j} + w_{inst,Q,1} + \sum_{i > 1} \psi_{0,i} w_{inst,Q,i} \quad , \quad (\text{Eq. 86})$$

where w_{inst} is the instantaneous deflection, $w_{inst,G,j}$ is the instantaneous deflection from j^{th} permanent action, $w_{inst,Q,i}$ is the instantaneous deflection from i^{th} variable action and ψ_0 is the factor for combination value of a variable action

In FEM-Design if the load combinations compiled in appropriate way by a characteristic SLS load combinations then by the CLT panel application data the k_{defSc} (see Chapter 5.5) should be adjusted to 0 to get the appropriate instantaneous deflections accordance with Eq. 86 because that equation doesn't contain any creep effect, thus $k_{defSc} = 0$ is necessary by the settings.

5.10 Remarks on data of manufacturers and some recommendations

As you can see in the former chapters there are lot of parameters which are adjustable in FEM-Design laminated composite shell (CLT application) modul. The CLT panel library was filled up with data of some manufacturers about different types of panels and layer materials. To perform a relevant calculation it is necessary to use adequate elastic and strength properties as well. According to empirical and practical issues we have made lot of application data and design parameter option by the panel properties to fulfill all choice to follow what the manufacturer provides during the homegization and the design calculation. The CLT panels are not in the recent Eurocode 5 directly, therefore there are several opened questions in the mechanical properties and design properties as well, and we hope this theory book and the indicated references could give some guidance in the applicable data.

If you have a CLT panel manufacturer's brochure you can directly fill up the CLT library with the relevant CLT panel layer properties to get a more adequate calculation. One dominant questionable thing by CLT products is the applied Poisson's ratio of the layer material which is in reality obviously not zero. Another important issue is the glue at the narrow side which has great effect at the final results and load-bearing behaviour of the CLT panel, thus please get the information about it from the manufacturer of the applied CLT panel.

RECOMMENDATION: If the product is glued at narrow side then we recommend to use the no glue at narrow side option (see Chapter 5.1.2) in ULS because the load-bearing capacity can be increased to neglect some irrelevant failure mode, but do not use the no glue at narrow side option in SLS because the deflections can be reduced with this way. The reason of this recommendation is that in reality the behaviour of CLT panel could be non-linear and with this settings we can use all advantages of the laminated composite shell theory.

6 Verification examples

6.1 Calculation of the homogenized shell material stiffness matrix

In the next sub-chapters of this example we will calculate the homogenized stiffness values with different settings using the layer composition what you can see in Fig. 18.

No	Material	Thickness [mm]	Theta [°]	Ex [N/mm ²]	Ey [N/mm ²]	ν _{xy} [-]	G _{xy} [N/mm ²]	G _{xz} [N/mm ²]	G _{yz} [N/mm ²]	Rho [kg/m ³]
1	C24	15.00	0.00	11600	450	0.40	690	690	100	420
2	C16	40.00	90	8000	270	0.40	500	500	50	370
3	C24	35.00	0.00	11600	450	0.40	690	690	100	420

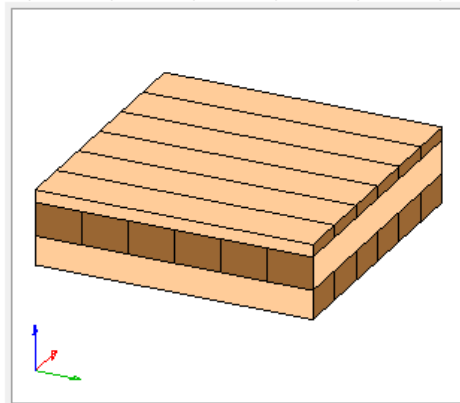


Figure 18 – The adjusted layer composition

In the next calculations (and also by FEM-Design “Display stiffness” button) we will calculate the stiffnesses relate to the mid-surface (center) of the shell layout composition.

The co-ordinates of the edge of the different layers related to the mid-surface:

$$z = \begin{bmatrix} 0.045 \\ 0.030 \\ -0.010 \\ -0.045 \end{bmatrix} \text{ m}$$

If someone adjusts the k_{def} deformation factors by the panel properties in the different limit states then the homogenization method will be the same but before the calculation the Young's moduli and shear moduli will be divided with $1+k_{def}$ and these reduced moduli will be the input values of the homogenization method as it was stated in Chapter 5.5.

6.1.1 Calculation with shear coupling

In this sub-chapter we will show the stiffness calculation in case of shear coupling between the layers when they are working together. In the first Chapter 6.1.1.1 we will show the calculation with the glue at narrow side option, then in Chapter 6.1.1.2 with no glue at narrow side option.

6.1.1.1 Glue at narrow side

First of all we should calculate the material stiffness matrices of the layers interpreted in the grain directions.

Material of layer No. 1 and 3 are the same therefore these matrices are the same:

In-plane part:

$$\begin{bmatrix} Q_{11} & Q_{12} & 0 \\ Q_{12} & Q_{22} & 0 \\ 0 & 0 & Q_{66} \end{bmatrix} = \begin{bmatrix} \frac{E_x}{1-\nu_{xy}^2 \frac{E_y}{E_x}} & \nu_{xy} \frac{E_y}{1-\nu_{xy}^2 \frac{E_y}{E_x}} & 0 \\ \nu_{xy} \frac{E_y}{1-\nu_{xy}^2 \frac{E_y}{E_x}} & \frac{E_y}{1-\nu_{xy}^2 \frac{E_y}{E_x}} & 0 \\ 0 & 0 & G_{xy} \end{bmatrix} =$$

$$= \begin{bmatrix} \frac{11600}{1-0.4^2 \frac{450}{11600}} & 0.4 \frac{450}{1-0.4^2 \frac{450}{11600}} & 0 \\ 0.4 \frac{450}{1-0.4^2 \frac{450}{11600}} & \frac{450}{1-0.4^2 \frac{450}{11600}} & 0 \\ 0 & 0 & 690 \end{bmatrix} = \begin{bmatrix} 11672 & 181.1 & 0 \\ 181.1 & 452.8 & 0 \\ 0 & 0 & 690 \end{bmatrix} \text{ MPa}$$

Transverse part:

$$\begin{bmatrix} Q_{55} & 0 \\ 0 & Q_{44} \end{bmatrix} = \begin{bmatrix} G_{xz} & 0 \\ 0 & G_{yz} \end{bmatrix} = \begin{bmatrix} 690 & 0 \\ 0 & 100 \end{bmatrix} \text{ MPa}$$

Layer No. 2:

In-plane part:

$$\begin{bmatrix} \frac{8000}{1-0.4^2 \frac{270}{8000}} & 0.4 \frac{270}{1-0.4^2 \frac{270}{8000}} & 0 \\ 0.4 \frac{270}{1-0.4^2 \frac{270}{8000}} & \frac{270}{1-0.4^2 \frac{270}{8000}} & 0 \\ 0 & 0 & 500 \end{bmatrix} = \begin{bmatrix} 8043 & 108.6 & 0 \\ 108.6 & 271.5 & 0 \\ 0 & 0 & 500 \end{bmatrix} \text{ MPa}$$

Transverse part:

$$\begin{bmatrix} Q_{55} & 0 \\ 0 & Q_{44} \end{bmatrix} = \begin{bmatrix} 500 & 0 \\ 0 & 50 \end{bmatrix} \text{ MPa}$$

According to Fig. 18 the grain direction of layer No. 1 and 3 are in the local x' direction of the shell (0° orientation). It means that the previously calculated material stiffness will be the one what we need to use during the homogenization:

$$\begin{bmatrix} \bar{Q}_{11} & \bar{Q}_{12} & \bar{Q}_{16} \\ \bar{Q}_{12} & \bar{Q}_{22} & \bar{Q}_{26} \\ \bar{Q}_{16} & \bar{Q}_{26} & \bar{Q}_{66} \end{bmatrix}_{1\&3} = \begin{bmatrix} 11672 & 181.1 & 0 \\ 181.1 & 452.8 & 0 \\ 0 & 0 & 690 \end{bmatrix} \text{MPa}$$

$$\begin{bmatrix} \bar{Q}_{55} & \bar{Q}_{45} \\ \bar{Q}_{45} & \bar{Q}_{44} \end{bmatrix}_{1\&3} = \begin{bmatrix} 690 & 0 \\ 0 & 100 \end{bmatrix} \text{MPa}$$

But by layer No. 2 we can see that the grain direction is perpendicular to the x' local system direction (90° orientation). Thus we should transform the material stiffness into the local x' direction. With the transformation matrix in the theoretical description we will get:

$$\begin{bmatrix} \bar{Q}_{11} & \bar{Q}_{12} & \bar{Q}_{16} \\ \bar{Q}_{12} & \bar{Q}_{22} & \bar{Q}_{26} \\ \bar{Q}_{16} & \bar{Q}_{26} & \bar{Q}_{66} \end{bmatrix}_2 = \begin{bmatrix} 271.5 & 108.6 & 0 \\ 108.6 & 8043 & 0 \\ 0 & 0 & 500 \end{bmatrix} \text{MPa}$$

$$\begin{bmatrix} \bar{Q}_{55} & \bar{Q}_{45} \\ \bar{Q}_{45} & \bar{Q}_{44} \end{bmatrix}_2 = \begin{bmatrix} 50 & 0 \\ 0 & 500 \end{bmatrix} \text{MPa}$$

After these steps we can calculate the ABD and shear part of the stiffness matrix.

The bending part:

$$D_{ij} = \frac{1}{3} \sum_{k=1}^N (\bar{Q}_{ij})_k (z_k^3 - z_{k+1}^3) \quad (i, j = 1, 2, 6)$$

$$D_{11} = \frac{1}{3} [11672(0.045^3 - 0.03^3) + 271.5(0.03^3 - (-0.01^3)) + 11672((-0.01)^3 - (-0.045)^3)] =$$

$$= 0.6027 \frac{\text{MNm}^2}{\text{m}} = 602.7 \text{ kNm}$$

$$D_{12} = \frac{1}{3} [181.1(0.045^3 - 0.03^3) + 108.6(0.03^3 - (-0.01^3)) + 181.1((-0.01)^3 - (-0.045)^3)] =$$

$$= 0.01033 \frac{\text{MNm}^2}{\text{m}} = 10.33 \text{ kNm}$$

$$D_{22} = \frac{1}{3} [452.8(0.045^3 - 0.03^3) + 8043(0.03^3 - (-0.01^3)) + 452.8((-0.01)^3 - (-0.045)^3)] =$$

$$= 0.09835 \frac{\text{MNm}^2}{\text{m}} = 98.35 \text{ kNm}$$

$$D_{66} = \frac{1}{3} [690(0.045^3 - 0.03^3) + 500(0.03^3 - (-0.01^3)) + 690((-0.01)^3 - (-0.045)^3)] =$$

$$= 0.04014 \frac{\text{MNm}^2}{\text{m}} = 40.14 \text{ kNm}$$

In this case because the layers are orthogonal and the directions of orthotropy layer-by-layer coincide with the local system of the shell:

$$D_{16} = D_{26} = 0 \quad .$$

The membrane part:

$$A_{ij} = \sum_{k=1}^N (\bar{Q}_{ij})_k (z_k - z_{k+1}) \quad (i, j = 1, 2, 6)$$

$$\begin{aligned} A_{11} &= 11672(0.045 - 0.03) + 271.5(0.03 - (-0.01)) + 11672((-0.01) - (-0.045)) = \\ &= 594.46 \frac{\text{MN}}{\text{m}} = 594460 \frac{\text{kN}}{\text{m}} \end{aligned}$$

$$\begin{aligned} A_{12} &= 181.1(0.045 - 0.03) + 108.6(0.03 - (-0.01)) + 181.1((-0.01) - (-0.045)) = \\ &= 13.40 \frac{\text{MN}}{\text{m}} = 13400 \frac{\text{kN}}{\text{m}} \end{aligned}$$

$$\begin{aligned} A_{22} &= 452.8(0.045 - 0.03) + 8043(0.03 - (-0.01)) + 452.8((-0.01) - (-0.045)) = \\ &= 344.4 \frac{\text{MN}}{\text{m}} = 344400 \frac{\text{kN}}{\text{m}} \end{aligned}$$

$$\begin{aligned} A_{66} &= 690(0.045 - 0.03) + 500(0.03 - (-0.01)) + 690((-0.01) - (-0.045)) = \\ &= 54.5 \frac{\text{MN}}{\text{m}} = 54500 \frac{\text{kN}}{\text{m}} \end{aligned}$$

In this case because the layers are orthogonal and the directions of orthotropy layer-by-layer coincide with the local system of the shell:

$$A_{16} = A_{26} = 0 \quad .$$

Eccentricity part:

$$B_{ij} = \frac{1}{2} \sum_{k=1}^N (\bar{Q}_{ij})_k (z_k^2 - z_{k+1}^2) \quad (i, j = 1, 2, 6)$$

$$\begin{aligned} B_{11} &= \frac{1}{2} [11672(0.045^2 - 0.03^2) + 271.5(0.03^2 - (-0.01)^2) + 11672((-0.01)^2 - (-0.045)^2)] = \\ &= -4.560 \frac{\text{MNm}}{\text{m}} = -4560 \text{ kN} \end{aligned}$$

$$\begin{aligned} B_{12} &= \frac{1}{2} [181.1(0.045^2 - 0.03^2) + 108.6(0.03^2 - (-0.01)^2) + 181.1((-0.01)^2 - (-0.045)^2)] = \\ &= -0.029 \frac{\text{MNm}}{\text{m}} = -29 \text{ kN} \end{aligned}$$

$$\begin{aligned} B_{22} &= \frac{1}{2} [452.8(0.045^2 - 0.03^2) + 8043(0.03^2 - (-0.01)^2) + 452.8((-0.01)^2 - (-0.045)^2)] = \\ &= 3.036 \frac{\text{MNm}}{\text{m}} = 3036 \text{ kN} \end{aligned}$$

$$B_{66} = \frac{1}{2} [690(0.045^2 - 0.03^2) + 500(0.03^2 - (-0.01)^2) + 690((-0.01)^2 - (-0.045)^2)] =$$

$$= -0.076 \frac{\text{MNm}}{\text{m}} = -76 \text{ kN}$$

In this case because the layers are orthogonal and the directions of orthotropy layer-by-layer coincide with the local system of the shell:

$$B_{16} = B_{26} = 0 \quad .$$

Shear part:

In this case the calculation of transverse shear stiffnesses is much easier than by a general case (see the theory description also about this topic).

$$\text{Here: } \begin{bmatrix} S_{55} & S_{45} \\ S_{45} & S_{44} \end{bmatrix} = \begin{bmatrix} \bar{\bar{S}}_{55} & 0 \\ 0 & \bar{\bar{S}}_{44} \end{bmatrix}$$

With the aim of the following equations first of all we should calculate the shear correction factors in the main stiffness direction (and perpendicular to it) which now coincide with the local system of the shell (see Fig. 18).

The shear correction factors:

$$\rho_{13} = \frac{R_1^2}{d_1 \int_{-\frac{t}{2}}^{\frac{t}{2}} \frac{g_1^2(z)}{\bar{\bar{Q}}_{55}(z)} dz} = 0.1638 \quad ; \quad \rho_{23} = \frac{R_2^2}{d_2 \int_{-\frac{t}{2}}^{\frac{t}{2}} \frac{g_2^2(z)}{\bar{\bar{Q}}_{44}(z)} dz} = 0.8528$$

Based on these the shear stiffnesses:

$$\bar{\bar{S}}_{55} = \rho_{13} \sum_{k=1}^N (\bar{\bar{Q}}_{55})_k (z_k - z_{k+1}) =$$

$$= 0.1638 [690(0.045 - 0.03) + 50(0.03 - (-0.010)) + 690((-0.01) - (-0.045))] = 5979 \frac{\text{kN}}{\text{m}}$$

$$\bar{\bar{S}}_{44} = \rho_{23} \sum_{k=1}^N (\bar{\bar{Q}}_{44})_k (z_k - z_{k+1}) =$$

$$= 0.8528 [100(0.045 - 0.03) + 500(0.03 - (-0.010)) + 100((-0.01) - (-0.045))] = 21320 \frac{\text{kN}}{\text{m}}$$

Thus the final homogenized laminated shell stiffnesses (in kNm, kN and kN/m):

$$\begin{bmatrix} 602.7 & 10.33 & 0 & -4560 & -29 & 0 & 0 & 0 \\ 10.33 & 98.35 & 0 & -29 & 3036 & 0 & 0 & 0 \\ 0 & 0 & 40.14 & 0 & 0 & -76 & 0 & 0 \\ -4560 & -29 & 0 & 594460 & 13400 & 0 & 0 & 0 \\ -29 & 3036 & 0 & 13400 & 344400 & 0 & 0 & 0 \\ 0 & 0 & -76 & 0 & 0 & 54500 & 0 & 0 \\ 0 & 0 & 0 & 0 & 0 & 0 & 5979 & 0 \\ 0 & 0 & 0 & 0 & 0 & 0 & 0 & 21320 \end{bmatrix}$$

Fig. 19 shows the values based on FEM-Design. The values are the same.

Stiffness matrix of timber panel

Calculation Ultimate limit state Close

Flexural stiffness matrix D [kNm]

603	10	0.00
10	98	0.00
0.00	0.00	40

Membrane stiffness matrix A [kN/m]

594481	13400	0.00
13400	344378	0.00
0.00	0.00	54500

Shear stiffness matrix S [kN/m]

5979	0.00
0.00	21319

Eccentricity (coupling) stiffness matrix B [kN]

-4560	-29	0.00
-29	3036	0.00
0.00	0.00	-76

Figure 19 – The relevant stiffness values based on FEM-Design

6.1.1.2 No glue at narrow side

This calculation only differs from Chapter 6.1.1.1 that in the whole homogenization method the Young's moduli of the layers in perpendicular direction to the grains assumed to zero independently from the input data, see Fig. 18.

Material of layer No. 1 and 3 are the same therefore these matrices are the same:

In-plane part:

$$\begin{bmatrix} Q_{11} & Q_{12} & 0 \\ Q_{12} & Q_{22} & 0 \\ 0 & 0 & Q_{66} \end{bmatrix} = \begin{bmatrix} \frac{E_x}{1-\nu_{xy}^2 \frac{E_y}{E_x}} & \nu_{xy} \frac{E_y}{1-\nu_{xy}^2 \frac{E_y}{E_x}} & 0 \\ \nu_{xy} \frac{E_y}{1-\nu_{xy}^2 \frac{E_y}{E_x}} & \frac{E_y}{1-\nu_{xy}^2 \frac{E_y}{E_x}} & 0 \\ 0 & 0 & G_{xy} \end{bmatrix} = \begin{bmatrix} \frac{11600}{1-0.4^2 \frac{0}{11600}} & 0.4 \frac{0}{1-0.4^2 \frac{0}{11600}} & 0 \\ 0.4 \frac{0}{1-0.4^2 \frac{0}{11600}} & \frac{0}{1-0.4^2 \frac{0}{11600}} & 0 \\ 0 & 0 & 690 \end{bmatrix} = \begin{bmatrix} 11600 & 0 & 0 \\ 0 & 0 & 0 \\ 0 & 0 & 690 \end{bmatrix} \text{ MPa}$$

Transverse part:

$$\begin{bmatrix} Q_{55} & 0 \\ 0 & Q_{44} \end{bmatrix} = \begin{bmatrix} G_{xz} & 0 \\ 0 & G_{yz} \end{bmatrix} = \begin{bmatrix} 690 & 0 \\ 0 & 100 \end{bmatrix} \text{ MPa}$$

Layer No. 2:

In-plane part:

$$\begin{bmatrix} \frac{8000}{1-0.4^2 \frac{0}{8000}} & 0.4 \frac{0}{1-0.4^2 \frac{0}{8000}} & 0 \\ 0.4 \frac{0}{1-0.4^2 \frac{0}{8000}} & \frac{0}{1-0.4^2 \frac{0}{8000}} & 0 \\ 0 & 0 & 500 \end{bmatrix} = \begin{bmatrix} 8000 & 0 & 0 \\ 0 & 0 & 0 \\ 0 & 0 & 500 \end{bmatrix} \text{ MPa}$$

Transverse part:

$$\begin{bmatrix} Q_{55} & 0 \\ 0 & Q_{44} \end{bmatrix} = \begin{bmatrix} 500 & 0 \\ 0 & 50 \end{bmatrix} \text{ MPa}$$

According to Fig. 18 the grain direction of layer No. 1 and 3 are in the local x' direction of the

shell (0° orientation). It means that the previously calculated material stiffness will be the one what we need to use during the homogenization.

$$\begin{bmatrix} \bar{Q}_{11} & \bar{Q}_{12} & \bar{Q}_{16} \\ \bar{Q}_{12} & \bar{Q}_{22} & \bar{Q}_{26} \\ \bar{Q}_{16} & \bar{Q}_{26} & \bar{Q}_{66} \end{bmatrix}_{1\&3} = \begin{bmatrix} 11600 & 0 & 0 \\ 0 & 0 & 0 \\ 0 & 0 & 690 \end{bmatrix} \text{MPa}$$

$$\begin{bmatrix} \bar{Q}_{55} & \bar{Q}_{45} \\ \bar{Q}_{45} & \bar{Q}_{44} \end{bmatrix}_{1\&3} = \begin{bmatrix} 690 & 0 \\ 0 & 100 \end{bmatrix} \text{MPa}$$

But by layer No. 2 we can see that the grain direction is perpendicular to the x' local system direction (90° orientation). Thus we should transform the former material stiffness into the local x' direction. With the transformation matrix in the theoretical description we will get:

$$\begin{bmatrix} \bar{Q}_{11} & \bar{Q}_{12} & \bar{Q}_{16} \\ \bar{Q}_{12} & \bar{Q}_{22} & \bar{Q}_{26} \\ \bar{Q}_{16} & \bar{Q}_{26} & \bar{Q}_{66} \end{bmatrix}_2 = \begin{bmatrix} 0 & 0 & 0 \\ 0 & 8000 & 0 \\ 0 & 0 & 500 \end{bmatrix} \text{MPa}$$

$$\begin{bmatrix} \bar{Q}_{55} & \bar{Q}_{45} \\ \bar{Q}_{45} & \bar{Q}_{44} \end{bmatrix}_2 = \begin{bmatrix} 50 & 0 \\ 0 & 500 \end{bmatrix} \text{MPa}$$

After these steps we can calculate the ABD and shear part of the stiffness matrix.

The bending part:

$$D_{ij} = \frac{1}{3} \sum_{k=1}^N (\bar{Q}_{ij})_k (z_k^3 - z_{k+1}^3) \quad (i, j = 1, 2, 6)$$

$$D_{11} = \frac{1}{3} [11600(0.045^3 - 0.03^3) + 0(0.03^3 - (-0.01)^3) + 11600((-0.01)^3 - (-0.045)^3)] =$$

$$= 0.5964 \frac{\text{MNm}^2}{\text{m}} = 596.4 \text{ kNm}$$

$$D_{22} = \frac{1}{3} [0(0.045^3 - 0.03^3) + 8000(0.03^3 - (-0.01)^3) + 0((-0.01)^3 - (-0.045)^3)] =$$

$$= 0.07467 \frac{\text{MNm}^2}{\text{m}} = 74.67 \text{ kNm}$$

$$D_{66} = \frac{1}{3} [690(0.045^3 - 0.03^3) + 500(0.03^3 - (-0.01)^3) + 690((-0.01)^3 - (-0.045)^3)] =$$

$$= 0.04014 \frac{\text{MNm}^2}{\text{m}} = 40.14 \text{ kNm}$$

$$D_{12} = D_{16} = D_{26} = 0 \quad .$$

The membrane part:

$$A_{ij} = \sum_{k=1}^N (\bar{Q}_{ij})_k (z_k - z_{k+1}) \quad (i, j = 1, 2, 6)$$

$$A_{11} = 11600(0.045 - 0.03) + 0(0.03 - (-0.01)) + 11600((-0.01) - (-0.045)) = \\ = 580 \frac{\text{MN}}{\text{m}} = 580000 \frac{\text{kN}}{\text{m}}$$

$$A_{22} = 0(0.045 - 0.03) + 8000(0.03 - (-0.01)) + 0((-0.01) - (-0.045)) = \\ = 320 \frac{\text{MN}}{\text{m}} = 320000 \frac{\text{kN}}{\text{m}}$$

$$A_{66} = 690(0.045 - 0.03) + 500(0.03 - (-0.01)) + 690((-0.01) - (-0.045)) = \\ = 54.5 \frac{\text{MN}}{\text{m}} = 54500 \frac{\text{kN}}{\text{m}}$$

$$A_{12} = A_{16} = A_{26} = 0 \quad .$$

Eccentricity part:

$$B_{ij} = \frac{1}{2} \sum_{k=1}^N (\bar{Q}_{ij})_k (z_k^2 - z_{k+1}^2) \quad (i, j = 1, 2, 6)$$

$$B_{11} = \frac{1}{2} [11600(0.045^2 - 0.03^2) + 0(0.03^2 - (-0.01)^2) + 11600((-0.01)^2 - (-0.045)^2)] = \\ = -4.64 \frac{\text{MNm}}{\text{m}} = -4640 \text{ kN}$$

$$B_{22} = \frac{1}{2} [0(0.045^2 - 0.03^2) + 8000(0.03^2 - (-0.01)^2) + 0((-0.01)^2 - (-0.045)^2)] = \\ = 3.2 \frac{\text{MNm}}{\text{m}} = 3200 \text{ kN}$$

$$B_{66} = \frac{1}{2} [690(0.045^2 - 0.03^2) + 500(0.03^2 - (-0.01)^2) + 690((-0.01)^2 - (-0.045)^2)] = \\ = -0.076 \frac{\text{MNm}}{\text{m}} = -76 \text{ kN}$$

$$B_{12} = B_{16} = B_{26} = 0 \quad .$$

Shear part:

In this case the calculation of the shear correction is much easier than by a general case (see the theory description also about this topic).

$$\text{Here: } \begin{bmatrix} S_{55} & S_{45} \\ S_{45} & S_{44} \end{bmatrix} = \begin{bmatrix} \bar{S}_{55} & 0 \\ 0 & \bar{S}_{44} \end{bmatrix}$$

With the aim of the following equations first of all we should calculate the shear correction factors in the main stiffness direction (and perpendicular to it) which now coincide with the local system of the shell (see Fig. 18).

The shear correction factors:

$$\rho_{13} = \frac{R_1^2}{d_1 \int_{-\frac{t}{2}}^{\frac{t}{2}} \frac{g_1^2(z)}{\bar{Q}_{55}(z)} dz} = 0.1640 \quad ; \quad \rho_{23} = \frac{R_2^2}{d_2 \int_{-\frac{t}{2}}^{\frac{t}{2}} \frac{g_2^2(z)}{\bar{Q}_{44}(z)} dz} = 0.6667$$

Based on these the shear stiffnesses:

$$\begin{aligned} \bar{S}_{55} &= \rho_{13} \sum_{k=1}^N (\bar{Q}_{55})_k (z_k - z_{k+1}) = \\ &= 0.1640 [690(0.045 - 0.03) + 50(0.03 - (-0.010)) + 690((-0.01) - (-0.045))] = 5986 \frac{\text{kN}}{\text{m}} \end{aligned}$$

$$\begin{aligned} \bar{S}_{44} &= \rho_{23} \sum_{k=1}^N (\bar{Q}_{44})_k (z_k - z_{k+1}) = \\ &= 0.6667 [100(0.045 - 0.03) + 500(0.03 - (-0.010)) + 100((-0.01) - (-0.045))] = 16668 \frac{\text{kN}}{\text{m}} \end{aligned}$$

Thus the final homogenized laminated shell stiffnesses (in kNm, kN and kN/m):

$$\begin{bmatrix} 596.4 & 0 & 0 & -4640 & 0 & 0 & 0 & 0 \\ 0 & 74.67 & 0 & 0 & 3200 & 0 & 0 & 0 \\ 0 & 0 & 40.14 & 0 & 0 & -76 & 0 & 0 \\ -4640 & 0 & 0 & 580000 & 0 & 0 & 0 & 0 \\ 0 & 3200 & 0 & 0 & 320000 & 0 & 0 & 0 \\ 0 & 0 & -76 & 0 & 0 & 54500 & 0 & 0 \\ 0 & 0 & 0 & 0 & 0 & 0 & 5986 & 0 \\ 0 & 0 & 0 & 0 & 0 & 0 & 0 & 16668 \end{bmatrix}$$

Fig. 20 shows the values based on FEM-Design. The values are the same.

Stiffness matrix of timber panel ✕

Calculation Ultimate limit state Close

Flexural stiffness matrix D [kNm]

596	0.00	0.00
0.00	75	0.00
0.00	0.00	40

Membrane stiffness matrix A [kN/m]

580000	0.00	0.00
0.00	320000	0.00
0.00	0.00	54500

Shear stiffness matrix S [kN/m]

5986	0.00
0.00	16667

Eccentricity (coupling) stiffness matrix B [kN]

-4640	0.00	0.00
0.00	3200	0.00
0.00	0.00	-76

Figure 20 – The relevant stiffness values based on FEM-Design

6.1.2 Calculation without shear coupling

In this sub-chapter we will show the stiffness calculation in case of without shear coupling between the layers when they are NOT working together. In Chapter 6.1.2.1 we will show the calculation with the glue at narrow side option, then in Chapter 6.1.2.2 with no glue at narrow side option.

6.1.2.1 Glue at narrow side

The material stiffness properties are the same layer-by-layer in the shell local system just like in Chapter 6.1.1.1.

Layer No. 1 and 3:

$$\begin{bmatrix} \bar{Q}_{11} & \bar{Q}_{12} & \bar{Q}_{16} \\ \bar{Q}_{12} & \bar{Q}_{22} & \bar{Q}_{26} \\ \bar{Q}_{16} & \bar{Q}_{26} & \bar{Q}_{66} \end{bmatrix}_{1\&3} = \begin{bmatrix} 11672 & 181.1 & 0 \\ 181.1 & 452.8 & 0 \\ 0 & 0 & 690 \end{bmatrix} \text{MPa}$$

$$\begin{bmatrix} \bar{Q}_{55} & \bar{Q}_{45} \\ \bar{Q}_{45} & \bar{Q}_{44} \end{bmatrix}_{1\&3} = \begin{bmatrix} 690 & 0 \\ 0 & 100 \end{bmatrix} \text{MPa}$$

Layer No. 2:

$$\begin{bmatrix} \bar{Q}_{11} & \bar{Q}_{12} & \bar{Q}_{16} \\ \bar{Q}_{12} & \bar{Q}_{22} & \bar{Q}_{26} \\ \bar{Q}_{16} & \bar{Q}_{26} & \bar{Q}_{66} \end{bmatrix}_2 = \begin{bmatrix} 271.5 & 108.6 & 0 \\ 108.6 & 8043 & 0 \\ 0 & 0 & 500 \end{bmatrix} \text{MPa}$$

$$\begin{bmatrix} \bar{Q}_{55} & \bar{Q}_{45} \\ \bar{Q}_{45} & \bar{Q}_{44} \end{bmatrix}_2 = \begin{bmatrix} 50 & 0 \\ 0 & 500 \end{bmatrix} \text{MPa}$$

Based on these information the ABD and shear part of the stiffness matrix can be calculated.

The bending part:

$$D_{ij} = \sum_{k=1}^N (\bar{Q}_{ij})_k \frac{(z_k - z_{k+1})^3}{12}$$

$$D_{11} = \frac{1}{12} [11672(0.045 - 0.03)^3 + 271.5(0.03 - (-0.01))^3 + 11672((-0.01) - (-0.045))^3] =$$

$$= 0.04643 \frac{\text{MNm}^2}{\text{m}} = 46.43 \text{ kNm}$$

$$D_{12} = \frac{1}{12} [181.1(0.045 - 0.03)^3 + 108.6(0.03 - (-0.01))^3 + 181.1((-0.01) - (-0.045))^3] =$$

$$= 0.001277 \frac{\text{MNm}^2}{\text{m}} = 1.277 \text{ kNm}$$

$$D_{22} = \frac{1}{12} [452.8(0.045-0.03)^3 + 8043(0.03-(-0.01))^3 + 452.8((-0.01)-(-0.045))^3] =$$

$$= 0.04464 \frac{\text{MNm}^2}{\text{m}} = 44.64 \text{ kNm}$$

$$D_{66} = \frac{1}{12} [690(0.045-0.03)^3 + 500(0.03-(-0.01))^3 + 690((-0.01)-(-0.045))^3] =$$

$$= 0.005325 \frac{\text{MNm}^2}{\text{m}} = 5.325 \text{ kNm}$$

In this case because the layers are orthogonal and the directions of orthotropy layer-by-layer coincide with the local system of the shell:

$$D_{16} = D_{26} = 0 \quad .$$

The membrane part:

$$A_{ij} = \sum_{k=1}^N (\bar{Q}_{ij})_k (z_k - z_{k+1}) \quad (i, j = 1, 2, 6)$$

$$A_{11} = 11672(0.045-0.03) + 271.5(0.03-(-0.01)) + 11672((-0.01)-(-0.045)) =$$

$$= 594.46 \frac{\text{MN}}{\text{m}} = 594460 \frac{\text{kN}}{\text{m}}$$

$$A_{12} = 181.1(0.045-0.03) + 108.6(0.03-(-0.01)) + 181.1((-0.01)-(-0.045)) =$$

$$= 13.40 \frac{\text{MN}}{\text{m}} = 13400 \frac{\text{kN}}{\text{m}}$$

$$A_{22} = 452.8(0.045-0.03) + 8043(0.03-(-0.01)) + 452.8((-0.01)-(-0.045)) =$$

$$= 344.4 \frac{\text{MN}}{\text{m}} = 344400 \frac{\text{kN}}{\text{m}}$$

$$A_{66} = 690(0.045-0.03) + 500(0.03-(-0.01)) + 690((-0.01)-(-0.045)) =$$

$$= 54.5 \frac{\text{MN}}{\text{m}} = 54500 \frac{\text{kN}}{\text{m}}$$

In this case because the layers are orthogonal and the directions of orthotropy layer-by-layer coincide with the local system of the shell:

$$A_{16} = A_{26} = 0 \quad .$$

Eccentricity part:

$$B_{ij} = 0 \quad (i, j = 1, 2, 6)$$

Shear part:

In this case the calculation of the shear stiffnesses are similar than the calculation of the shear stiffnesses by a homogeneous isotropic slab:

$$S_{ij} = \frac{5}{6} \sum_{k=1}^N (\bar{Q}_{ij})_k (z_k - z_{k+1}) \quad (i, j = 4, 5)$$

$$S_{55} = \frac{5}{6} [690(0.045 - 0.03) + 50(0.03 - (-0.010)) + 690((-0.01) - (-0.045))] = 30417 \frac{\text{kN}}{\text{m}}$$

$$S_{44} = \frac{5}{6} [100(0.045 - 0.03) + 500(0.03 - (-0.010)) + 100((-0.01) - (-0.045))] = 20833 \frac{\text{kN}}{\text{m}}$$

Thus the final homogenized laminated shell stiffnesses (in kNm and kN/m):

$$\begin{bmatrix} 46.43 & 1.277 & 0 & 0 & 0 & 0 & 0 & 0 \\ 1.277 & 44.64 & 0 & 0 & 0 & 0 & 0 & 0 \\ 0 & 0 & 5.325 & 0 & 0 & 0 & 0 & 0 \\ 0 & 0 & 0 & 594460 & 13400 & 0 & 0 & 0 \\ 0 & 0 & 0 & 13400 & 344400 & 0 & 0 & 0 \\ 0 & 0 & 0 & 0 & 0 & 54500 & 0 & 0 \\ 0 & 0 & 0 & 0 & 0 & 0 & 30417 & 0 \\ 0 & 0 & 0 & 0 & 0 & 0 & 0 & 20833 \end{bmatrix}$$

Fig. 21 shows the values based on FEM-Design. The values are the same.

Stiffness matrix of timber panel

Calculation Ultimate limit state Close

Flexural stiffness matrix D [kNm]

46	1.3	0.00
1.3	45	0.00
0.00	0.00	5.3

Membrane stiffness matrix A [kN/m]

594481	13400	0.00
13400	344378	0.00
0.00	0.00	54500

Shear stiffness matrix S [kN/m]

30417	0.00
0.00	20833

Eccentricity (coupling) stiffness matrix B [kN]

0.00	0.00	0.00
0.00	0.00	0.00
0.00	0.00	0.00

Figure 21 – The relevant stiffness values based on FEM-Design

6.1.2.2 No glue at narrow side

The material stiffness properties are the same layer-by-layer in the shell local system just like in Chapter 6.1.1.2.

Layer No. 1 and 3:

$$\begin{bmatrix} \bar{Q}_{11} & \bar{Q}_{12} & \bar{Q}_{16} \\ \bar{Q}_{12} & \bar{Q}_{22} & \bar{Q}_{26} \\ \bar{Q}_{16} & \bar{Q}_{26} & \bar{Q}_{66} \end{bmatrix}_{1\&3} = \begin{bmatrix} 11600 & 0 & 0 \\ 0 & 0 & 0 \\ 0 & 0 & 690 \end{bmatrix} \text{MPa}$$

$$\begin{bmatrix} \bar{Q}_{55} & \bar{Q}_{45} \\ \bar{Q}_{45} & \bar{Q}_{44} \end{bmatrix}_{1\&3} = \begin{bmatrix} 690 & 0 \\ 0 & 100 \end{bmatrix} \text{MPa}$$

Layer No. 2:

$$\begin{bmatrix} \bar{Q}_{11} & \bar{Q}_{12} & \bar{Q}_{16} \\ \bar{Q}_{12} & \bar{Q}_{22} & \bar{Q}_{26} \\ \bar{Q}_{16} & \bar{Q}_{26} & \bar{Q}_{66} \end{bmatrix}_2 = \begin{bmatrix} 0 & 0 & 0 \\ 0 & 8000 & 0 \\ 0 & 0 & 500 \end{bmatrix} \text{MPa}$$

$$\begin{bmatrix} \bar{Q}_{55} & \bar{Q}_{45} \\ \bar{Q}_{45} & \bar{Q}_{44} \end{bmatrix}_2 = \begin{bmatrix} 50 & 0 \\ 0 & 500 \end{bmatrix} \text{MPa}$$

Based on these information the ABD and shear part of the stiffness matrix can be calculated.

The bending part:

$$D_{ij} = \sum_{k=1}^N (\bar{Q}_{ij})_k \frac{(z_k - z_{k+1})^3}{12}$$

$$\begin{aligned} D_{11} &= \frac{1}{12} [11600(0.045 - 0.03)^3 + 0(0.03 - (-0.01))^3 + 11600((-0.01) - (-0.045))^3] = \\ &= 0.04471 \frac{\text{MNm}^2}{\text{m}} = 44.71 \text{ kNm} \end{aligned}$$

$$\begin{aligned} D_{22} &= \frac{1}{12} [0(0.045 - 0.03)^3 + 8000(0.03 - (-0.01))^3 + 0((-0.01) - (-0.045))^3] = \\ &= 0.04267 \frac{\text{MNm}^2}{\text{m}} = 42.67 \text{ kNm} \end{aligned}$$

$$\begin{aligned} D_{66} &= \frac{1}{12} [690(0.045 - 0.03)^3 + 500(0.03 - (-0.01))^3 + 690((-0.01) - (-0.045))^3] = \\ &= 0.005325 \frac{\text{MNm}^2}{\text{m}} = 5.325 \text{ kNm} \end{aligned}$$

$$D_{12} = D_{16} = D_{26} = 0 \quad .$$

The membrane part:

$$A_{ij} = \sum_{k=1}^N (\bar{Q}_{ij})_k (z_k - z_{k+1}) \quad (i, j = 1, 2, 6)$$

$$A_{11} = 11600(0.045 - 0.03) + 0(0.03 - (-0.01)) + 11600((-0.01) - (-0.045)) = \\ = 580 \frac{\text{MN}}{\text{m}} = 580000 \frac{\text{kN}}{\text{m}}$$

$$A_{22} = 0(0.045 - 0.03) + 8000(0.03 - (-0.01)) + 0((-0.01) - (-0.045)) = \\ = 320 \frac{\text{MN}}{\text{m}} = 320000 \frac{\text{kN}}{\text{m}}$$

$$A_{66} = 690(0.045 - 0.03) + 500(0.03 - (-0.01)) + 690((-0.01) - (-0.045)) = \\ = 54.5 \frac{\text{MN}}{\text{m}} = 54500 \frac{\text{kN}}{\text{m}}$$

$$A_{12} = A_{16} = A_{26} = 0 \quad .$$

Eccentricity part:

$$B_{ij} = 0 \quad (i, j = 1, 2, 6)$$

Shear part:

In this case the calculation of the shear stiffnesses are similar than the calculation of the shear stiffnesses by a homogeneous isotropic slab:

$$S_{ij} = \frac{5}{6} \sum_{k=1}^N (\bar{Q}_{ij})_k (z_k - z_{k+1}) \quad (i, j = 4, 5)$$

$$S_{55} = \frac{5}{6} [690(0.045 - 0.03) + 50(0.03 - (-0.010)) + 690((-0.01) - (-0.045))] = 30417 \frac{\text{kN}}{\text{m}}$$

$$S_{44} = \frac{5}{6} [100(0.045 - 0.03) + 500(0.03 - (-0.010)) + 100((-0.01) - (-0.045))] = 20833 \frac{\text{kN}}{\text{m}}$$

Thus the final homogenized laminated shell stiffnesses (in kNm and kN/m):

$$\begin{bmatrix}
 44.71 & 0 & 0 & 0 & 0 & 0 & 0 & 0 \\
 0 & 42.67 & 0 & 0 & 0 & 0 & 0 & 0 \\
 0 & 0 & 5.325 & 0 & 0 & 0 & 0 & 0 \\
 0 & 0 & 0 & 580000 & 0 & 0 & 0 & 0 \\
 0 & 0 & 0 & 0 & 320000 & 0 & 0 & 0 \\
 0 & 0 & 0 & 0 & 0 & 54500 & 0 & 0 \\
 0 & 0 & 0 & 0 & 0 & 0 & 30417 & 0 \\
 0 & 0 & 0 & 0 & 0 & 0 & 0 & 20833
 \end{bmatrix}$$

Fig. 22 shows the values based on FEM-Design. The values are the same.

Stiffness matrix of timber panel

Calculation Ultimate limit state

Close

Flexural stiffness matrix D [kNm]

45	0.00	0.00
0.00	43	0.00
0.00	0.00	5.3

Membrane stiffness matrix A [kN/m]

580000	0.00	0.00
0.00	320000	0.00
0.00	0.00	54500

Shear stiffness matrix S [kN/m]

30417	0.00
0.00	20833

Eccentricity (coupling) stiffness matrix B [kN]

0.00	0.00	0.00
0.00	0.00	0.00
0.00	0.00	0.00

Figure 22 – The relevant stiffness values based on FEM-Design

Download link to the example file:

[http://download.strusoft.com/FEM-Design/inst190x/models/9.4.2.1 Calculation of the homogenized shell material stiffness matrix.str](http://download.strusoft.com/FEM-Design/inst190x/models/9.4.2.1%20Calculation%20of%20the%20homogenized%20shell%20material%20stiffness%20matrix.str)

6.2 Deflection and stresses of a CLT panel supported on two opposite edges

In this example we analyze a one-way CLT panel with beam-a-like behaviour and material properties to verify the calculation results compared with hand calculation. The geometry (10 m x 2.45 m) and the total distributed load can be seen with the supports in Fig. 23.

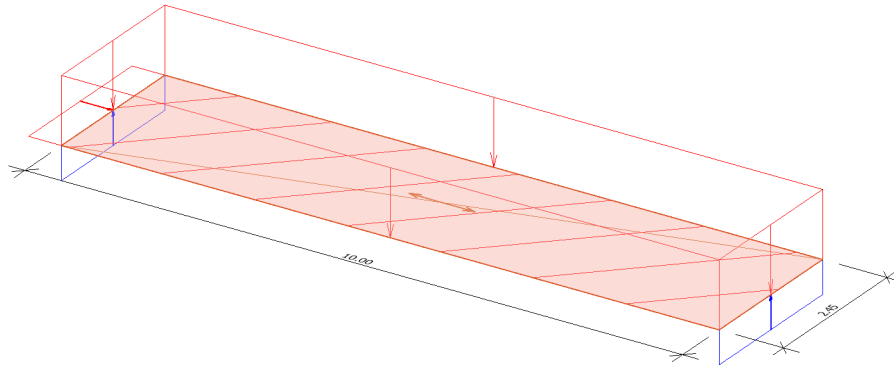


Figure 23 – The one-way CLT slab supported on two opposite edges, the longer direction is x'

The material properties are reduced to consider beam-a-like behaviour (see Fig. 24) and to better comparison between the FEM-Design calculation and hand calculation, but in reality the Poisson's ratio and the E_y modulus by a CLT panel is not equal to zero. The grain direction of the top layer is in the span direction.

Layers (top down order)											
No	Material	Thickness [mm]	Beta [°]	E_x [N/mm ²]	E_y [N/mm ²]	ν_{xy} [-]	G_{xy} [N/mm ²]	G_{xz} [N/mm ²]	G_{yz} [N/mm ²]	Rho [kg/m ³]	
1	C24	30	0.00	11000	0.10	0.00	690	690	69	420	^
2	C24	40	90	11000	0.10	0.00	690	690	69	420	
3	C24	30	0.00	11000	0.10	0.00	690	690	69	420	
4	C24	40	90	11000	0.10	0.00	690	690	69	420	
5	C24	30	0.00	11000	0.10	0.00	690	690	69	420	
6	C24	40	90	11000	0.10	0.00	690	690	69	420	
7	C24	30	0.00	11000	0.10	0.00	690	690	69	420	v

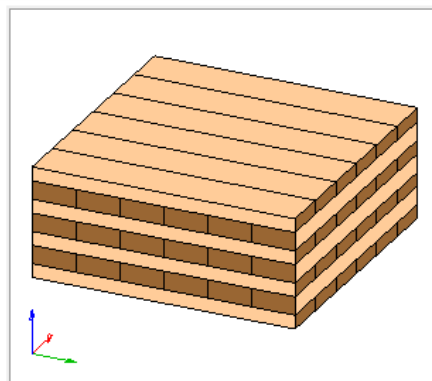


Figure 24 – The layer compositions and the reduced material properties

The specific surface load in ULS:

$$q_U = 1.35 \cdot 0.9888 + 1.5 \cdot 2 = 4.335 \text{ kN/m}^2$$

The maximum specific shear force at the support (calculated as a simply supported beam):

$$V_{max} = q_U \frac{L}{2} = \frac{4.335 \cdot 10}{2} = 21.68 \text{ kN/m}$$

The FEM-Design result according to Fig. 20:

$$V_{max}^{FEM-Design} = 21.67 \text{ kN/m}$$

The maximum specific bending moment at mid-span:

$$M_{max} = q_U \frac{L^2}{8} = 4.335 \frac{10^2}{8} = 54.19 \text{ kNm/m}$$

The FEM-Design result according to Fig. 20:

$$M_{max}^{FEM-Design} = 54.25 \text{ kNm/m}$$

The relevant internal forces from FEM-Design can be seen in Fig. 25.

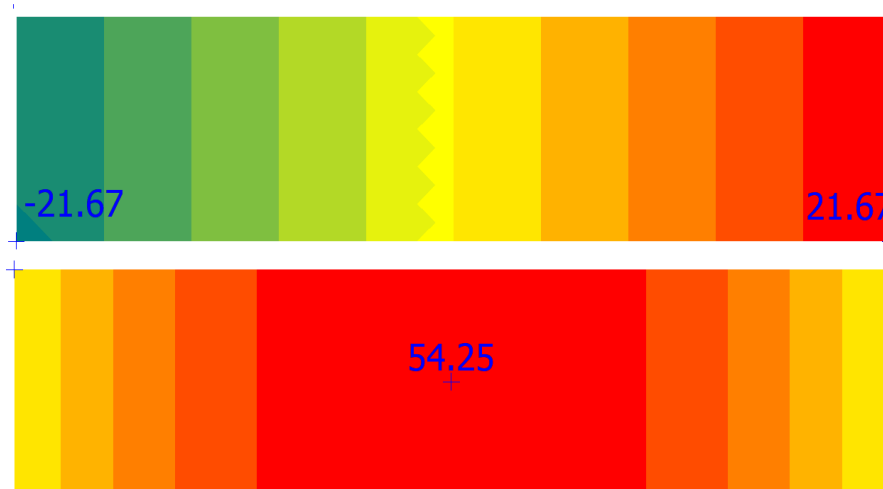


Figure 25 – The specific shear force [$q_{xz'}$, kN/m] and the specific bending moment [$m_{x'}$, kNm/m]

First we would like to calculate the relevant normal stress in the mid-span at the extreme fibers:

The relevant specific inertia (considering the 1st, 3rd, 5th and 7th layer), neglecting the lateral layers (2nd, 4th and 6th):

$$I = 2 \left(\frac{2 \cdot 0.03^3}{12} + 0.03 \cdot 0.105^2 + 0.03 \cdot 0.035^2 \right) = 0.000744 \text{ m}^4/\text{m}$$

The maximum normal stress in grain direction at the extreme fibers:

$$\sigma_{clt,0,d}^{max} = \frac{M_{max}}{I} \frac{t}{2} = \frac{54.19}{0.000744} \frac{0.24}{2} = 8740 \text{ kPa} = 8.74 \text{ MPa}$$

The FEM-Design result according to Fig. 26:

$$\sigma_{max}^{FEM-Design} = 8.75 \text{ MPa}$$

Second we would like to calculate the relevant transverse shear stress at the mid-plane (center of the 4th layer) next to the support:

The specific maximum value of statical moment:

$$S_{max} = 0.03 \cdot 0.105 + 0.03 \cdot 0.035 = 0.0042 \text{ m}^3/\text{m}$$

The maximum rolling shear at the mid-plane next to the support:

$$\tau_{yz,d}^{center} = \tau_{Rolling,d}^{max} = \frac{V_{max} S_{max}}{I b} = \frac{21.68 \cdot 0.0042}{0.000744 \cdot 1} = 122.4 \text{ kPa} = 0.1224 \text{ MPa}$$

The FEM-Design result according to Fig. 26:

$$\tau_{max}^{FEM-Design} = 0.1224 \text{ MPa}$$



Figure 26 – The normal stresses in the span direction at the mid-span and the relevant transverse shear stresses next to the support based on FEM-Design calculation

Third we would like to calculate the deflection in SLS considering creep.

The specific surface load in SLS quasi-permanent combination:

$$q_{sq} = 0.9888 + 0.3 \cdot 2 = 1.589 \text{ kN/m}^2$$

The final deflection at mid-span considering creep and neglecting shear deformation:

$$w_{fin} = \frac{5}{384} \frac{q_{sq} L^4}{EI} (1 + k_{defSq}) = \frac{5}{384} \frac{1.589 \cdot 10^4}{11000000 \cdot 0.000744} (1 + 0.8) = 0.0455 \text{ mm} = 45.5 \text{ mm}$$

The FEM-Design result according to Fig. 27:

$$w_{fin}^{FEM-Design} = 47.00 \text{ mm}$$

The results based on the hand calculation and FEM-Design are identical except the deflection because in FEM-Design the shear deformations are also considered, therefore the maximum deflection at the mid-span is a bit larger compared to the hand calculation.

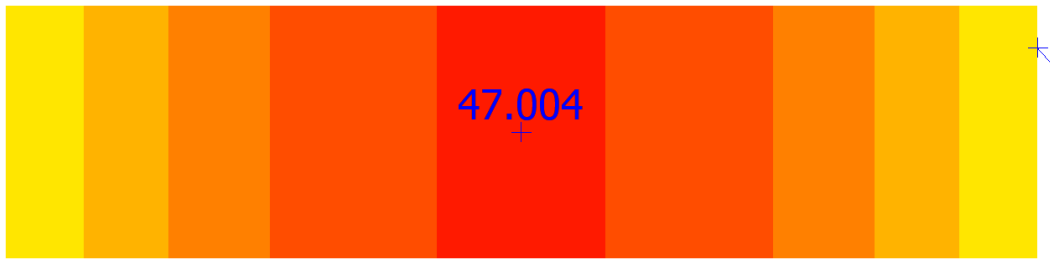


Figure 27 – The deflections in the SLS combination [mm]

Download link to the example file:

[http://download.strusoft.com/FEM-Design/inst190x/models/9.4.2.2 Deflection and stresses of a CLT panel supported on two opposite edges.str](http://download.strusoft.com/FEM-Design/inst190x/models/9.4.2.2%20Deflection%20and%20stresses%20of%20a%20CLT%20panel%20supported%20on%20two%20opposite%20edges.str)

6.3 Deflection and stresses of a CLT simply supported two-way slab

By this verification example we calculated a simply supported two-way CLT slab (7m x 5m) with uniformly distributed load (see Fig. 28).

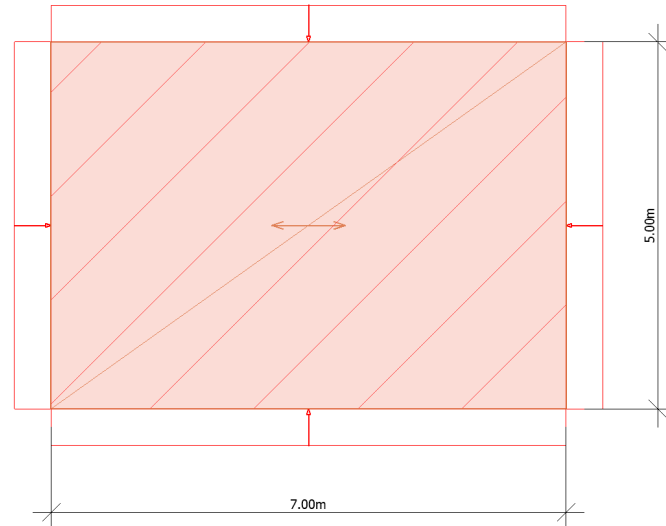


Figure 28 – The geometry of the considered plate with the uniformly distributed load

The layer composition with the mechanical properties can be seen in Fig. 29. The grain direction of the top layer is in the longer direction of the slab (see also Fig. 28). The total thickness is $t = 240$ mm. During the calculation we considered shear coupling between layers and glue at narrow sides.

Layers (top down order)										
No	Material	Thickness [mm]	Beta [°]	Ex [N/mm ²]	Ey [N/mm ²]	ν _{xy} [-]	G _{xy} [N/mm ²]	G _{xz} [N/mm ²]	G _{yz} [N/mm ²]	Rho [kg/m ³]
1	C24	30	0.00	11000	370	0.20	690	690	69	420
2	C24	40	90	11000	370	0.20	690	690	69	420
3	C24	30	0.00	11000	370	0.20	690	690	69	420
4	C24	40	90	11000	370	0.20	690	690	69	420
5	C24	30	0.00	11000	370	0.20	690	690	69	420
6	C24	40	90	11000	370	0.20	690	690	69	420
7	C24	30	0.00	11000	370	0.20	690	690	69	420

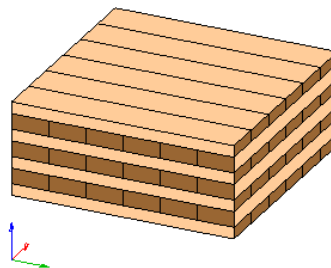


Figure 29 – The layer composition with the thicknesses and material parameters

The considered combination is a ULS combination, thus $k_{defU} = 0$. The design value of the considered value of the uniformly distributed surface load contains the self-weight of the CLT panel and a variable load:

$$q_U = 1.35 \left(\frac{420}{1000} 9.81 \cdot 0.24 \right) + 1.5 \cdot 2 = 4.335 \frac{\text{kN}}{\text{m}^2}$$

We compared different FEM-Design results with ANSYS shell281 multilayer element results.

Fig. 30 shows the applied finite element mesh size, the average element size was 0.36m.

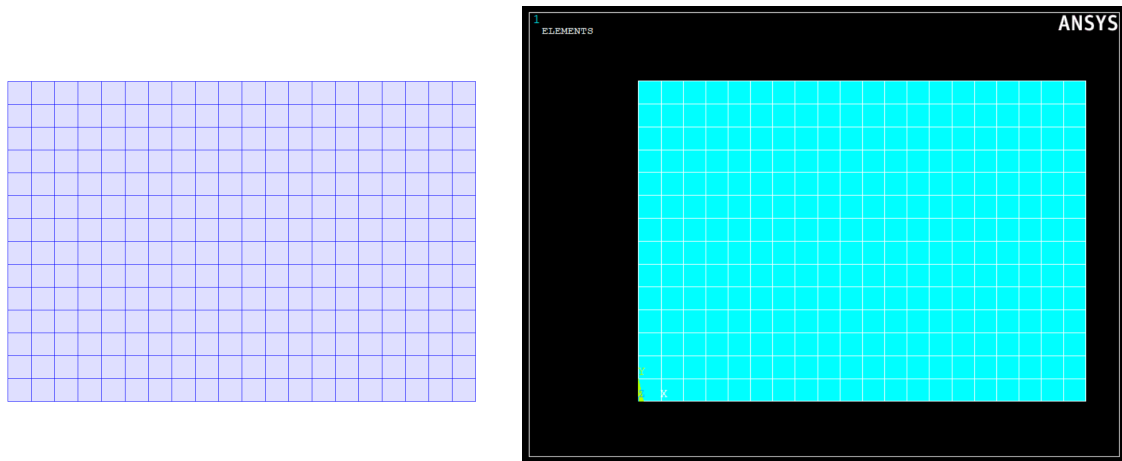


Figure 30 – The finite element mesh of the plate in FEM-Design (left) and in ANSYS (right)

Fig 31. shows the deflection colour palette results. The maximum deflection from the calculations:

$$w_{max}^{FEM-Design} = 5.785 \text{ mm} ; w_{max}^{ANSYS} = 5.786 \text{ mm}$$

Practically the results are the same.

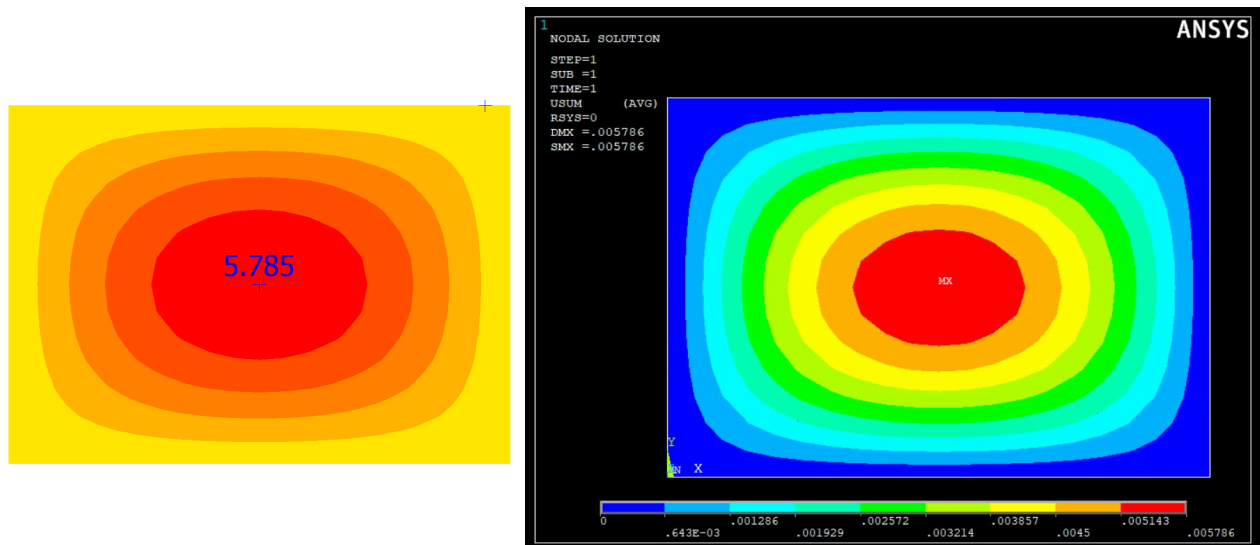


Figure 31 – The deflections of the plate in FEM-Design (left, in [mm]) and in ANSYS (right, in [m])

The normal stress at the bottom of the lowermost layer in the x' direction in shell local system:

$$\sigma_{x'bottom}^{FEM-Design} = 1.302 \text{ MPa} ; \sigma_{x'bottom}^{ANSYS} = 1.303 \text{ MPa}$$

The results are the same, see Fig. 32.

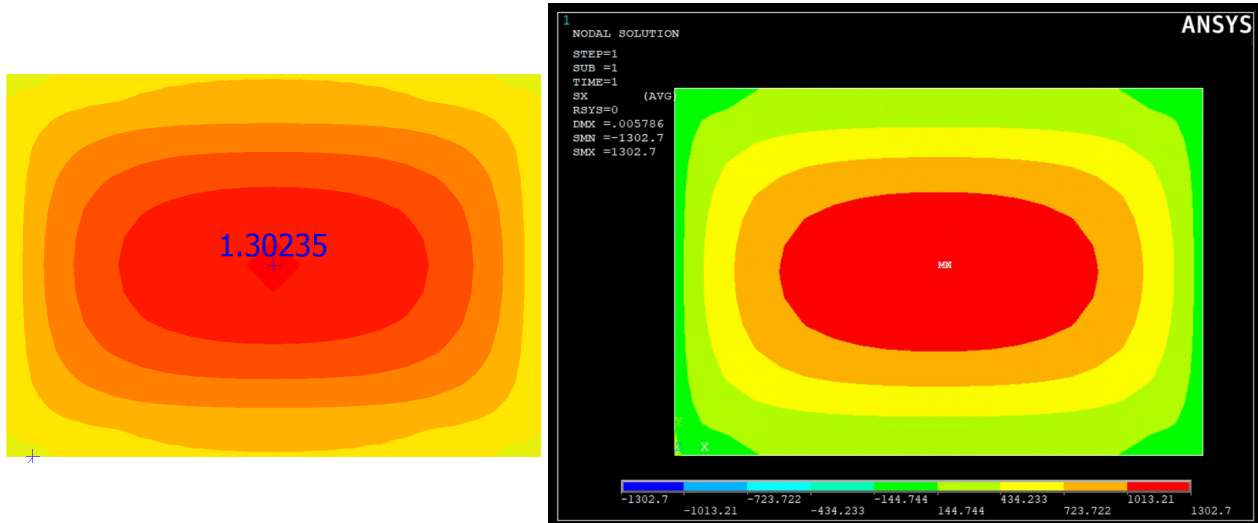


Figure 32 – The $\sigma_{x'}$ stresses at the bottom of the lowermost layer in FEM-Design (left, in [MPa]) and in ANSYS (right, in [kPa])

The normal stress at the bottom of the lowermost layer in the y' direction in shell local system:

$$\sigma_{y'bottom}^{FEM-Design} = 0.09774 \text{ MPa} ; \sigma_{y'bottom}^{ANSYS} = 0.09771 \text{ MPa}$$

The results are the same, see Fig 33.

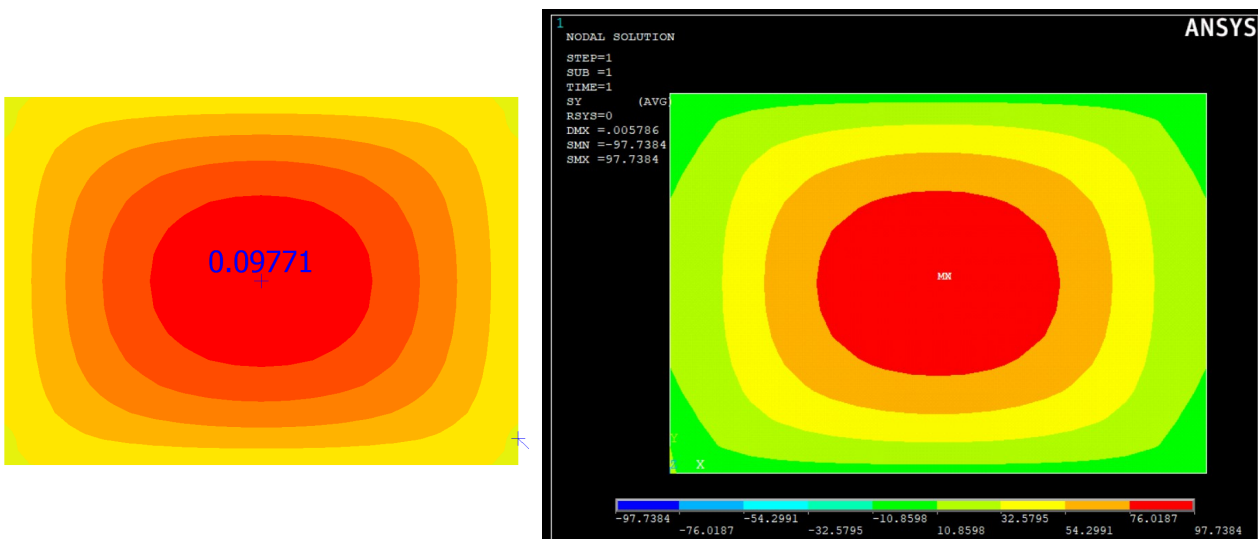


Figure 33 – The $\sigma_{y'}$ stresses at the bottom of the lowermost layer in FEM-Design (left, in [MPa]) and in ANSYS (right, in [kPa])

The in-plane shear stress at the bottom of the lowermost layer in shell local system:

$$\tau_{x'y'bottom}^{FEM-Design} = 0.2380 \text{ MPa} ; \tau_{x'y'bottom}^{ANSYS} = 0.2442 \text{ MPa}$$

The difference between the results is about 2.5%, see Fig. 34.

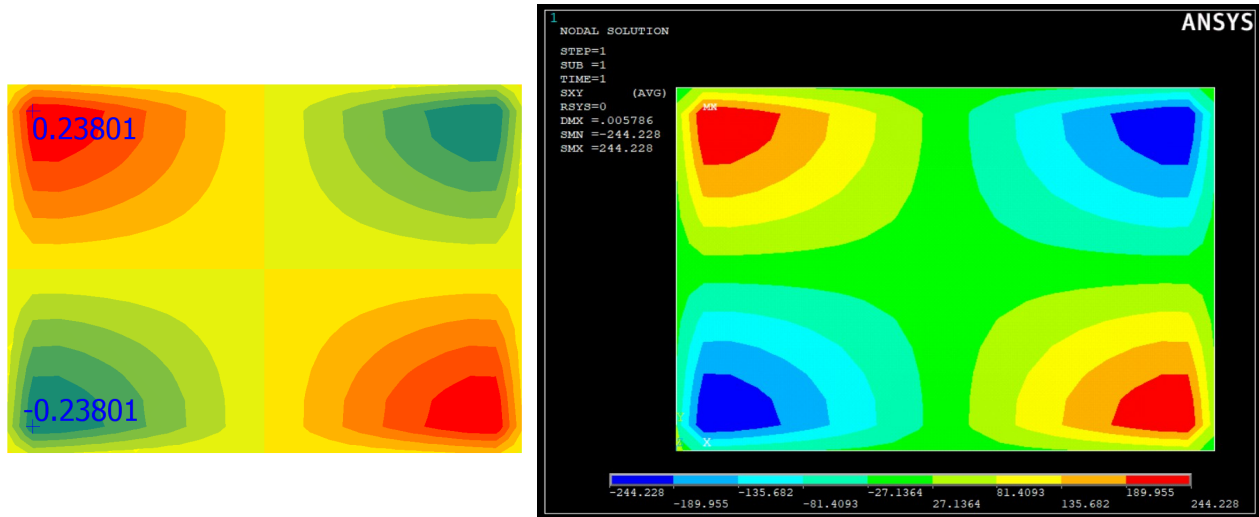


Figure 34 – The τ_{xy} stresses at the bottom of the lowermost layer in FEM-Design (left, in [MPa]) and in ANSYS (right, in [kPa])

The normal stress at the top of the second layer from above in the y' direction in shell local system:

$$\sigma_{y'top}^{FEM-Design} = -1.992 \text{ MPa} ; \sigma_{y'top}^{ANSYS} = -1.993 \text{ MPa}$$

The results are the same, see Fig. 35.

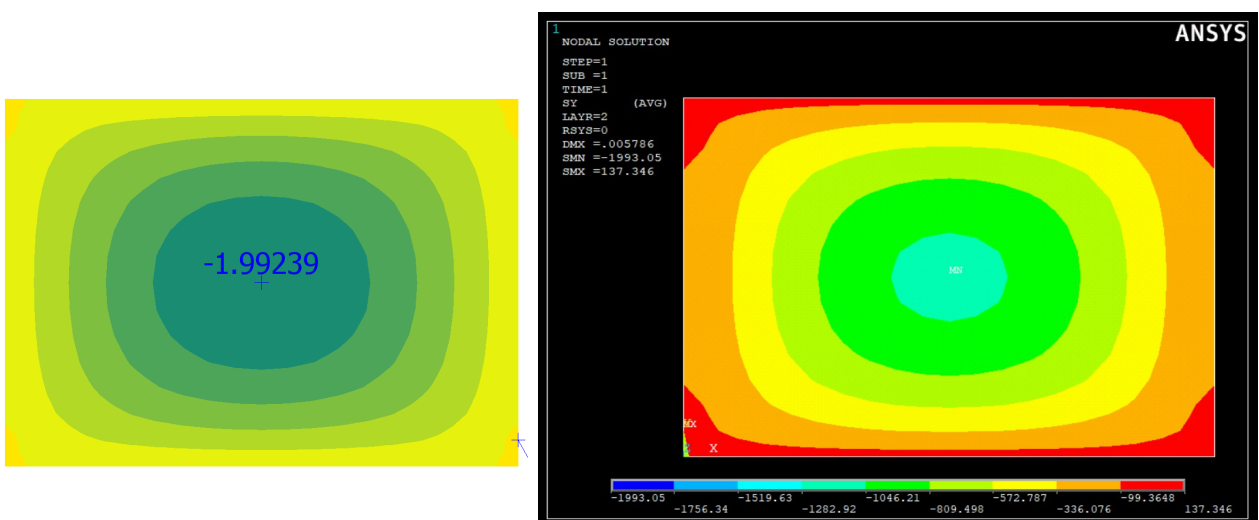


Figure 35 – The $\sigma_{y'}$ stresses at the top of the second layer counted from the top in FEM-Design (left, in [MPa]) and in ANSYS (right, in [kPa])

The transverse shear stresses at the middle of the slab (center of the 4th layer) in $x'z'$ direction in shell local system:

$$\tau_{x'z'middle}^{ANSYS} = 0.05865 \text{ MPa} ; \tau_{x'z'middle}^{ANSYS} = 0.05864 \text{ MPa}$$

The results are the same, see Fig. 36.

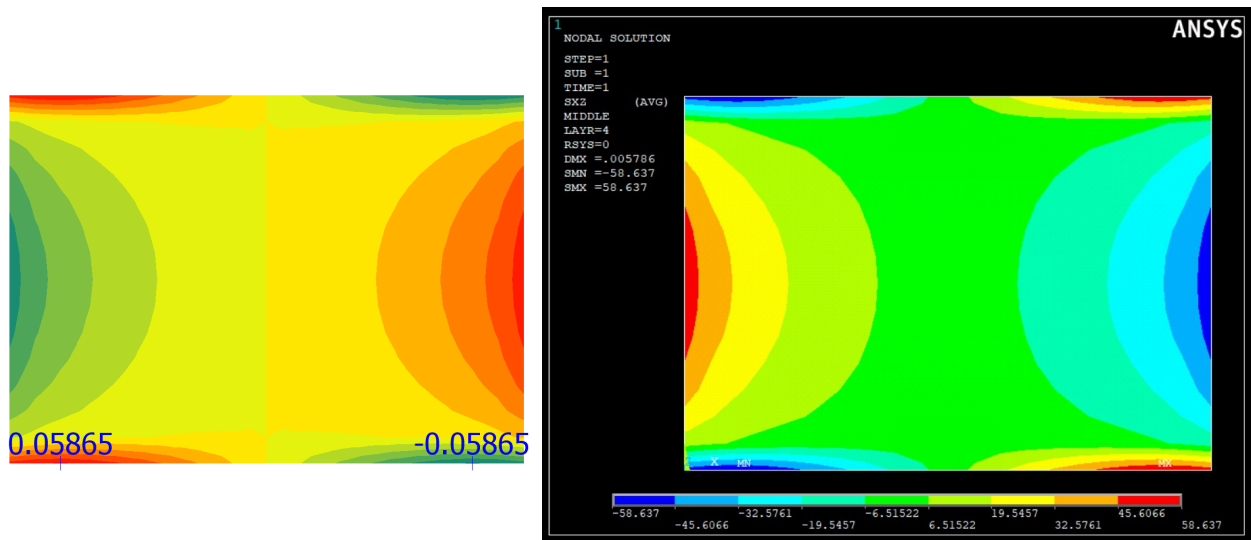


Figure 36 – The $\tau_{x'z'}$ stresses at the middle of the slab (at the center of the 4th layer) in FEM-Design (left, in [MPa]) and in ANSYS (right, in [kPa])

The transverse shear stresses at the middle of the slab (center of the 4th layer) in $y'z'$ direction in shell local system:

$$\tau_{y'z'middle}^{ANSYS} = 0.07181 \text{ MPa} ; \tau_{y'z'middle}^{ANSYS} = 0.07199 \text{ MPa}$$

The difference between the results is about 2.5%, see Fig. 37.

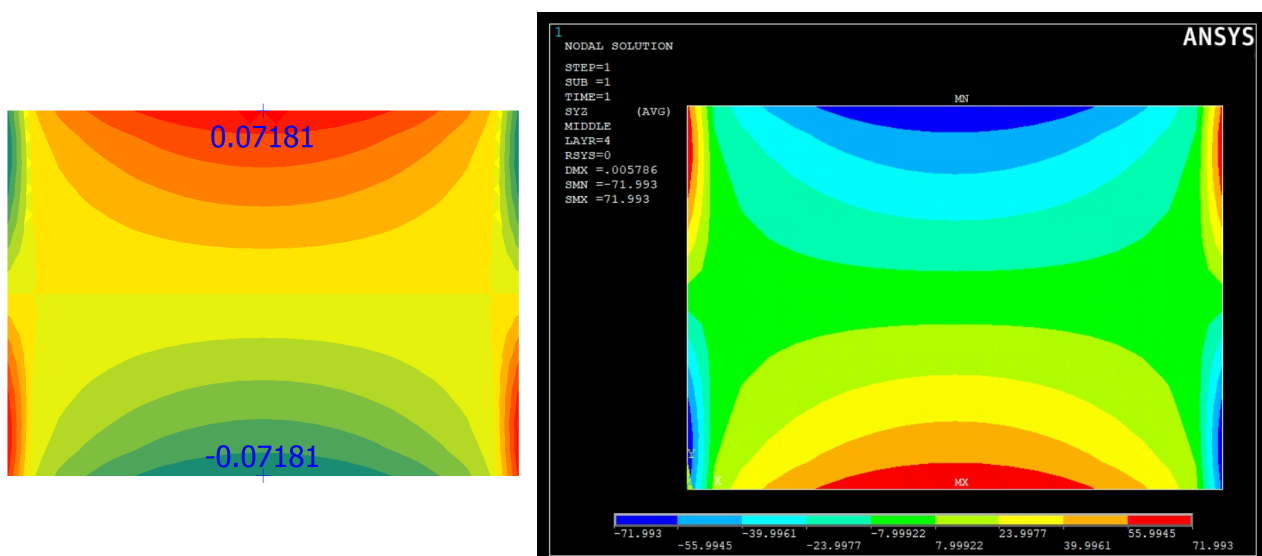


Figure 37 – The $\tau_{y'z'}$ stresses at the middle of the slab (at the center of the 4th layer) in FEM-Design (left, in [MPa]) and in ANSYS (right, in [kPa])

Based on the comparisons of the mentioned results we can say that FEM-Design results considering the laminated composite shell mechanical model by a two-way slab gives adequate results.

Download link to the example file:

[http://download.strusoft.com/FEM-Design/inst190x/models/9.4.2.3 Deflection and stresses of a CLT simply supported two-way slab.str](http://download.strusoft.com/FEM-Design/inst190x/models/9.4.2.3%20Deflection%20and%20stresses%20of%20a%20CLT%20simply%20supported%20two-way%20slab.str)

6.4 In-plane loaded CLT design check to shear failure at glued contact surface

In this example we will verify the FEM-Design design formulas in case of an in-plane loaded CLT panel according to Chapter 5.8.4 and compare the FEM-Design results with analytical/experimental data, see Ref. [40-41].

The calculated static layout can be seen in Fig. 38. The applied force is $F=237$ kN (thus $F/2=118.5$ kN, see Fig. 38. and Ref. [40]). The CLT here is an in-plane loaded panel with the following layer composition and material parameters, see Fig. 33-34. You can see in Fig. 38 that the applied plank (board) width is $a = 150$ mm and the number of the layers $N = 3$. In FEM-Design calculation we use the *No glue at narrow side* option to reach this shear failure formula by the detailed results.

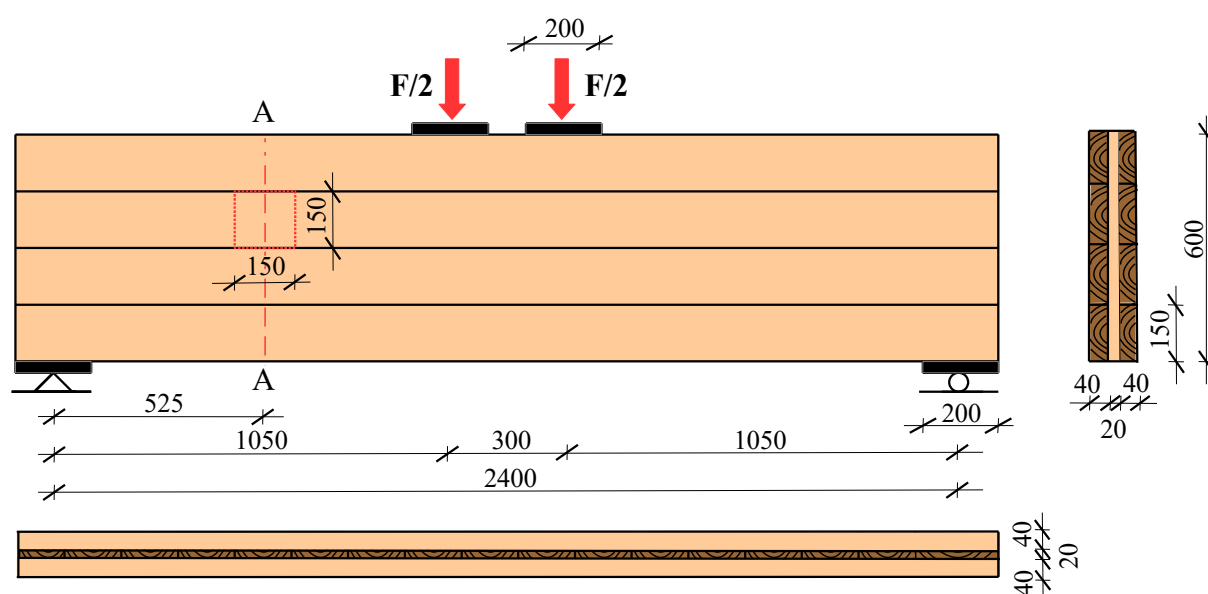


Figure 38 – The geometry, the loads and the analyzed RVE in case of in-plane loaded panel

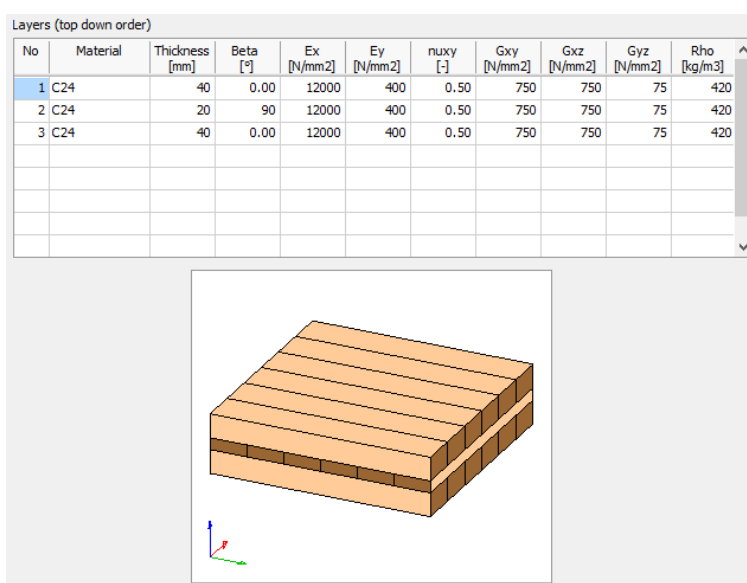
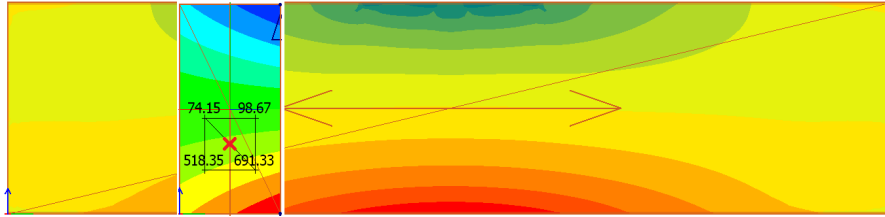


Figure 39 – The layer composition with the thicknesses and the applied material parameters

The additional rolling shear at the glued surface in the middle vertical layer will be the following (see Fig. 42):

$$\tau_{yz,d}^{inplane} = \frac{\Delta N_y}{a^2} \approx \frac{\frac{\partial n_y}{\partial y}}{N-1} = \frac{\left| \frac{(518.3)+(74.15)}{2} - \frac{(691.3)+(98.67)}{2} \right|}{0.15} = 329.2 \text{ kPa} = 0.3292 \text{ MPa}$$



Torsion

Panel: 'TP.1.1', Layer: '2', Side: 'Top', LC: '1', $k_{mod} = 0.60$, PT6

$$\tau_{tor,d} = \frac{3 \cdot n_{xy}}{a \cdot (N-1)} = \frac{3 \cdot 264.65}{150.00 \cdot (3-1)} = 2.65 \text{ N/mm}^2$$

$$\tau_{yz,d,inplane} = \frac{\frac{\partial n_y}{\partial y}}{N-1} = \frac{-98.75}{3-1} = -0.33 \text{ N/mm}^2$$

$$\frac{|\tau_{tor,d}|}{f_{tor,d}} + \frac{|\tau_{yz,d,inplane}| + |\tau_{yz,d}|}{f_{R,d}} = \frac{2.65}{3.50} + \frac{-0.33 + 0.00}{1.50} = 0.98 \leq 1.00 - \text{OK}$$

Figure 42 – Top: The distribution of n_x specific internal forces in the local system of the shell [kN/m]
this specific normal force if perpendicular to the middle layer grain direction
Bottom: The relevant in-plane loaded torsion interaction formula in FEM-Design

According to the mentioned design formula in Chapter 5.8.4 the following interaction should be checked, Fig. 42 also shows this interaction formula based on FEM-Design detailed result:

$$\frac{|\tau_{tor,d}|}{f_{tor,d}} + \frac{|\tau_{yz,d}^{inplane}|}{f_{R,d}} = \frac{2.647}{3.5} + \frac{0.3292}{1.5} = 0.9758 \leq 1.0$$

Based on Ref [40] results and the analytical theory in Ref. [41-42] the reference value of this utilization:

$$\frac{|\tau_{tor,d}|}{f_{tor,d}} + \frac{|\tau_{yz,d}^{inplane}|}{f_{R,d}} = \frac{2.686}{3.5} + \frac{0.25}{1.5} = 0.9341 \leq 1.0$$

The literature data and the FEM-Design results are very close to each other, the difference in the interaction formula is smaller than 5 %.

Download link to the example file:

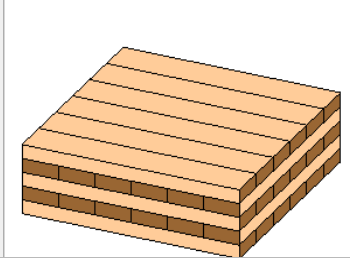
[http://download.strusoft.com/FEM-Design/inst190x/models/9.4.2.4 In-plane loaded CLT design check to shear failure at glued contact surface.str](http://download.strusoft.com/FEM-Design/inst190x/models/9.4.2.4%20In-plane%20loaded%20CLT%20design%20check%20to%20shear%20failure%20at%20glued%20contact%20surface.str)

6.5 Buckling check of a CLT wall

Let's consider the following layer composition in Fig. 43, with the given elastic and strength parameters.

The load-duration class is permanent thus the applied $k_{mod}=0.6$ and $\gamma_M=1.25$.

Layers (top down order)										
No	Material	Thickness [mm]	Beta [°]	Ex [N/mm ²]	Ey [N/mm ²]	nu _{xy} [-]	G _{xy} [N/mm ²]	G _{xz} [N/mm ²]	G _{yz} [N/mm ²]	Rho [kg/m ³]
1	C24	20	0.00	11000	370	0.40	690	690	69	420
2	C24	20	90	11000	370	0.40	690	690	69	420
3	C24	20	0.00	11000	370	0.40	690	690	69	420
4	C24	20	90	11000	370	0.40	690	690	69	420
5	C24	20	0.00	11000	370	0.40	690	690	69	420



No	Material	f _{m0k} [N/mm ²]	f _{m90k} [N/mm ²]	f _{t0k} [N/mm ²]	f _{t90k} [N/mm ²]	f _{c0k} [N/mm ²]	f _{c90k} [N/mm ²]	f _{xyk} [N/mm ²]	f _{yk} [N/mm ²]	f _{Rk} [N/mm ²]	f _{Tork} [N/mm ²]
1	C24	24	24	14	0.50	21	2.5	4.0	4.0	2.0	2.5
2	C24	24	24	14	0.50	21	2.5	4.0	4.0	2.0	2.5
3	C24	24	24	14	0.50	21	2.5	4.0	4.0	2.0	2.5
4	C24	24	24	14	0.50	21	2.5	4.0	4.0	2.0	2.5
5	C24	24	24	14	0.50	21	2.5	4.0	4.0	2.0	2.5

Figure 43 – The layer composition with the thicknesses and the applied material parameters

With this CLT panel we built a wall with L height and 4 m width, applied a constant distributed load on the top edge of the wall and a surface distributed load perpendicular to the panel as you can see in Fig. 44-45. The boundary condition was simply supported. The planks are vertical at the outer layers.

In the first part (case a)) of this verification example we analyzed different height walls ($L = 1, 2, 3, 5$ and 7.5 m) with only theoretically centric load ($F = 543.73$ kN/m; 417 kN/m; 274.84 kN/m; 123 kN/m; and 60 kN/m respectively; $q = 0$) on the top edge. Here the FEM-Design calculation method will be shown firstly with the mentioned buckling calculation method (Chapter 5.8.5, effective length method with reduction factor) in details. After the buckling utilizations what we get from FEM-Design calculation we show a comparison with GMNIA (geometric and material non-linear analysis with imperfections) with the aim of a structural multiphysics program. Nowadays the GMNIA is the most precise engineering method to get the load bearing capacity of a structure with numerical simulation. By the verification we used in this other program solid finite elements to model more realistic structural behaviour with GMNIA.

In the second part (case b)) we show the behaviour in case of $L=3\text{m}$ height with different vertical and horizontal loads ($F = 274.84 \text{ kN/m}$; 252 kN/m ; 234.99 kN/m ; 208.33 kN/m ; 171.53 kN/m ; and 130.5 kN/m ; $q = 0$; 0.84 kN/m^2 ; 1.567 kN/m^2 ; 2.778 kN/m^2 ; 4.574 kN/m^2 ; 6.96 kN/m^2 respectively). First the FEM-Design calculation method will be shown in details. After the buckling utilizations what we get from FEM-Design calculation we show a comparison with GMNIA with the same way what was introduced in case a).

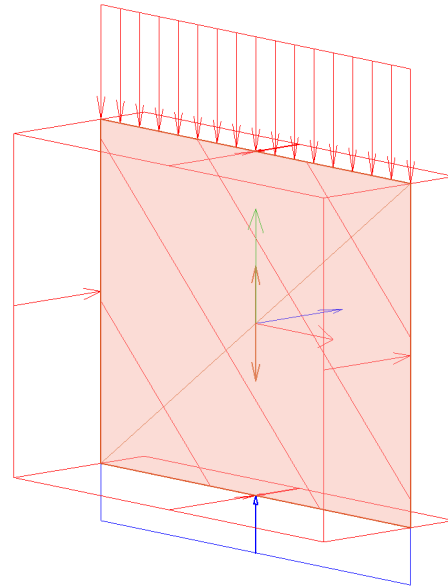


Figure 44 – The CLT wall model in FEM-Design

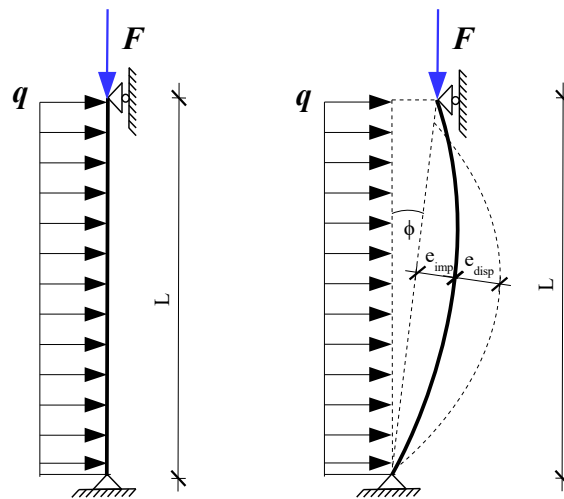


Figure 45 – The simplified static system to the effective length reduction factor method (left) and to the GMNIA (right)

Case a)

In case of centric loading (see Fig. 44-45, $q=0$) the analyzed height and centric loads of the walls:

L [m]	F [kN/m]	q [kN/m ²]
1	543.7	0.0
2	417.0	0.0
3	274.8	0.0
5	123.0	0.0
7.5	60.00	0.0

Based on the layers material elastic properties in Fig. 43 and with the buckling length we would like to calculate the relative slenderness and the reduction factor. The r reduction factor what was mentioned in Chapter 5.8.5 will help us to provide the characteristic values of the elastic properties to get the relative slenderness with the aim of the composite shell homogenization. The adjusted reduction factor on the elastic properties here was: $r = 0.8333$ (which is usually accepted by glue laminated or CLT products).

$$E_{x,05} = r E_{x,mean} = 0.8333 \cdot 11000 = 9170 \text{ MPa} ,$$

$$E_{y,05} = r E_{y,mean} = 0.8333 \cdot 370 = 308 \text{ MPa} ,$$

$$G_{xy,05} = r G_{xy,mean} = 0.8333 \cdot 690 = 575 \text{ MPa} ,$$

$$G_{xz,05} = r G_{xz,mean} = 0.8333 \cdot 690 = 575 \text{ MPa} ,$$

$$G_{yz,05} = r G_{yz,mean} = 0.8333 \cdot 69 = 57.5 \text{ MPa} .$$

From the FEM-Design laminated composite homogenization method in the background with the characteristic elastic modulus values based on Chapter 3.2 we get the following stiffness value to get the elastic critical force of the CLT panel:

$$D'_{11} = 614 \frac{\text{kNm}^2}{\text{m}} \text{ as the relevant specific bending stiffness and}$$

$$S'_{55} = 8943 \text{ kN/m} \text{ as the relevant specific shear stiffness.}$$

Based on these stiffnesses we can get the elastic critical forces which depends on the buckling length of the panel. In the first part of this example we will analyze theoretically centrically loaded panels with different buckling lengths. The β factors are 1.0 because the wall was simply supported but the height of the walls are different. Thus the elastic critical forces are as follows:

$$n_{cr}^{1m} = \frac{1}{\frac{1}{\left(\frac{D'_{11}\pi^2}{(\beta L)^2}\right)} + \frac{1}{S'_{55}}} = \frac{1}{\frac{1}{\left(\frac{614\pi^2}{(1.0 \cdot 1)^2}\right)} + \frac{1}{8943}} = 3612 \frac{\text{kN}}{\text{m}}$$

$$n_{cr}^{2m} = \frac{1}{\frac{1}{\left(\frac{D'_{11}\pi^2}{(\beta L)^2}\right)} + \frac{1}{S'_{55}}} = \frac{1}{\frac{1}{\left(\frac{614\pi^2}{(1.0 \cdot 2)^2}\right)} + \frac{1}{8943}} = 1296 \frac{\text{kN}}{\text{m}}$$

$$n_{cr}^{3m} = \frac{1}{\frac{1}{\left(\frac{D'_{11}\pi^2}{(\beta L)^2}\right)} + \frac{1}{S'_{55}}} = \frac{1}{\frac{1}{\left(\frac{614\pi^2}{(1.0 \cdot 3)^2}\right)} + \frac{1}{8943}} = 626.2 \frac{\text{kN}}{\text{m}}$$

$$n_{cr}^{5m} = \frac{1}{\frac{1}{\left(\frac{D'_{11}\pi^2}{(\beta L)^2}\right)} + \frac{1}{S'_{55}}} = \frac{1}{\frac{1}{\left(\frac{614\pi^2}{(1.0 \cdot 5)^2}\right)} + \frac{1}{8943}} = 236 \frac{\text{kN}}{\text{m}}$$

$$n_{cr}^{7.5m} = \frac{1}{\frac{1}{\left(\frac{D'_{11}\pi^2}{(\beta L)^2}\right)} + \frac{1}{S'_{55}}} = \frac{1}{\frac{1}{\left(\frac{614\pi^2}{(1.0 \cdot 7.5)^2}\right)} + \frac{1}{8943}} = 106.5 \frac{\text{kN}}{\text{m}}$$

Based on these elastic critical force values the relative slenderness could be calculated with the aim of the given data:

The thickness of the different layers:

$$t_1 = t_2 = t_3 = t_4 = t_5 = 20 \text{ mm} = 0.020 \text{ m}$$

The characteristic compression strength in the grain and perpendicular to grain direction:

$$f_{c,0,k,1} = f_{c,0,k,2} = f_{c,0,k,3} = 21000 \text{ kPa}$$

$$f_{c,90,k,2} = f_{c,90,k,4} = 2500 \text{ kPa}$$

The generalized relative slenderness:

$$\lambda_{rel} = \sqrt{\frac{\sum_{i=1}^N t_i f_{c,\alpha,k,i}}{n_{cr}}},$$

according to this equation the relative slenderness for the different height walls are as follows.

$$\lambda_{rel}^{1m} = \sqrt{\frac{\sum_{i=1}^N t_i f_{c, \alpha, k, i}}{n_{cr}^{1m}}} = \sqrt{\frac{3 \cdot 0.02 \cdot 21000 + 2 \cdot 0.02 \cdot 2500}{3612}} = 0.6136$$

Similarly with the other lengths:

$$\lambda_{rel}^{2m} = 1.024 \quad ; \quad \lambda_{rel}^{3m} = 1.474 \quad ; \quad \lambda_{rel}^{5m} = 2.401 \quad ; \quad \lambda_{rel}^{7.5m} = 3.574$$

According to the used Ayrton-Perry formula in EC5 the reduction factor calculation:

$$k = 0.5(1 + \beta_c(\lambda_{rel} - 0.3) + \lambda_{rel}^2)$$

$$k_c = \frac{1}{k + \sqrt{k^2 - \lambda_{rel}^2}}$$

In these examples we used here $\beta_c = 0.1$ straightness factor, but it is adjustable in FEM-Design.

The reduction factors are as follows according to the previous equations and data:

$$k_c^{1m} = 0.9534 \quad ; \quad k_c^{2m} = 0.7483 \quad ; \quad k_c^{3m} = 0.4210 \quad ; \quad k_c^{5m} = 0.1662 \quad ; \quad k_c^{7.5m} = 0.07617$$

The table below summarizes the calculated values by the different cases.

$\beta_c = 0.1$				
L [m]	n_{cr} [kN/m]	λ_{rel} [-]	k [-]	k_c [-]
1	3612	0.6136	0.7039	0.9534
2	1296	1.024	1.060	0.7483
3	626.2	1.474	1.645	0.4210
5	236.0	2.401	3.487	0.1662
7.5	106.5	3.574	7.050	0.07617

To calculate the buckling utilizations it is necessary to define the design values of the compressive and bending strengths. The design values of the compressive and bending strength of the layers:

$$f_{c,0,d} = k_{mod} \frac{f_{c,0,k}}{\gamma_M} = 0.6 \frac{21}{1.25} = 10.08 \text{ MPa}$$

$$f_{m,0,d} = k_{mod} \frac{f_{m,0,k}}{\gamma_M} = 0.6 \frac{24}{1.25} = 11.52 \text{ MPa}$$



Figure 46 – The relevant normal stress distribution in the five different height walls with the given centric loads

Fig. 46. shows the relevant stress results layer-by-layer from FEM-Design in the CLT panels with the given heights and loads.

With the calculated reduction factors the buckling utilization of the different height walls with the different centric loads (based on Fig. 46) in the grain directions of the relevant layers:

$$Util^{1m} = \frac{|\sigma_{c,0,d}^{buckling}|}{k_c f_{c,0,d}} + \frac{|\sigma_{m,0,d}^{buckling}|}{f_{m,0,d}} = \frac{|-8.866|}{0.9534 \cdot 10.08} + \frac{0}{11.52} = 0.9226$$

$$Util^{2m} = \frac{|\sigma_{c,0,d}^{buckling}|}{k_c f_{c,0,d}} + \frac{|\sigma_{m,0,d}^{buckling}|}{f_{m,0,d}} = \frac{|-6.799|}{0.7483 \cdot 10.08} + \frac{0}{11.52} = 0.9014$$

$$Util^{3m} = \frac{|\sigma_{c,0,d}^{buckling}|}{k_c f_{c,0,d}} + \frac{|\sigma_{m,0,d}^{buckling}|}{f_{m,0,d}} = \frac{|-4.481|}{0.4210 \cdot 10.08} + \frac{0}{11.52} = 1.056$$

$$Util^{5m} = \frac{|\sigma_{c,0,d}^{buckling}|}{k_c f_{c,0,d}} + \frac{|\sigma_{m,0,d}^{buckling}|}{f_{m,0,d}} = \frac{|-2.006|}{0.1662 \cdot 10.08} + \frac{0}{11.52} = 1.197$$

$$Util^{7.5m} = \frac{|\sigma_{c,0,d}^{buckling}|}{k_c f_{c,0,d}} + \frac{|\sigma_{m,0,d}^{buckling}|}{f_{m,0,d}} = \frac{|-0.9783|}{0.07617 \cdot 10.08} + \frac{0}{11.52} = 1.274$$

After we have these utilization values we have made GMNIA analysis with an other software to make a comparison between the proposed practically usable effective length reduction factor method what was implemented in FEM-Design and one of the most precise numerical simulation method.

In the GMNIA the used finite elements were solid elements and the material model was orthotropic with the given nonlinear stress-strain models in Fig. 47 layer-by-layer.

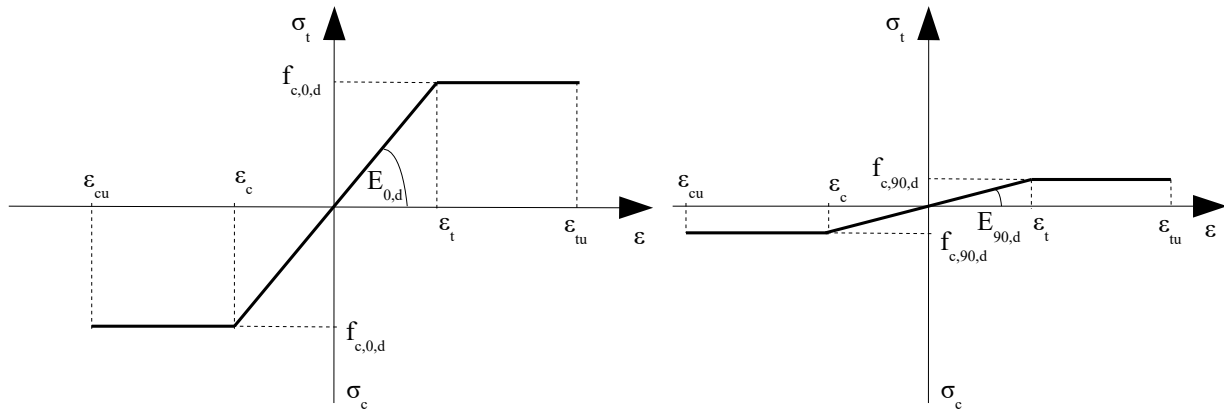


Figure 47 – The considered non-linear stress-strain model by GMNIA

In the GMNIA the adjusted elastic moduli were the following according to Ref. [41]:

$$E_{0,d} = 0.8 \frac{E_{x,05}}{\gamma_M} = 0.8 \frac{0.84 \cdot 11000}{1.25} = 5914 \text{ MPa}$$

$$E_{90,d} = 0.8 \frac{E_{y,05}}{\gamma_M} = 0.8 \frac{0.84 \cdot 370}{1.25} = 198.9 \text{ MPa}$$

$$G_{xy,d} = 0.8 \frac{G_{xy,05}}{\gamma_M} = 0.8 \frac{0.84 \cdot 690}{1.25} = 370.9 \text{ MPa}$$

$$G_{xz,d} = 0.8 \frac{G_{xz,05}}{\gamma_M} = 0.8 \frac{0.84 \cdot 690}{1.25} = 370.9 \text{ MPa}$$

$$G_{yz,d} = 0.8 \frac{G_{yz,05}}{\gamma_M} = 0.8 \frac{0.84 \cdot 69}{1.25} = 37.09 \text{ MPa}$$

The plastic limit values can be seen in Fig. 47, despite of the behaviour is symmetric in tension and compression the calculation is adequate because the analyzed cases are mainly under compression and on the tensioned side the values were not above the tension plastic limit at the failure load of GMNIA. It is important to note because it is very well-known that the timber material shows brittle fracture under pure tension, see Ref. [41].

By GMNIA another important question is the right consideration of the imperfections.

First of all a global initial sway was considered, see Fig. 45 right side. The initial sway according to the Eurocode was:

$$\phi = \alpha_h \frac{1}{200} ; \text{ where } \alpha_h = \frac{2}{\sqrt{L}} \text{ but } 2/3 \leq \alpha_h \leq 1.0 \text{ where } L \text{ is the wall height.}$$

Secondly it is necessary to consider an initial bow imperfection with its design value. This value is very important because it should contain not only the geometrical bow imperfection of the member but also other imperfections such as the material and load (eccentricity). According to the EC5 and Ref. [46-47] an adequate design value of the initial bow imperfection is:

$$e_{imp} = \frac{L}{300} , \text{ where } L \text{ is the wall height.}$$

With these given values we performed the GMNIA with an independent software based on solid finite elements.

The given centric specific loads in case a) were the load-bearing capacity of the different height walls according to the GMNIA. Fig. 48 shows the back-calculated reduction factor values based on GMNIA.

Based on the fact that the reduction factor curves in Eurocode comes from stochastic and empiric calculation we can say that the results of the proposed FEM-Design buckling check method are very close to the GMNIA. The results are closer to each other if we consider that the practically relevant relative slenderness is up to around 2.0 here.

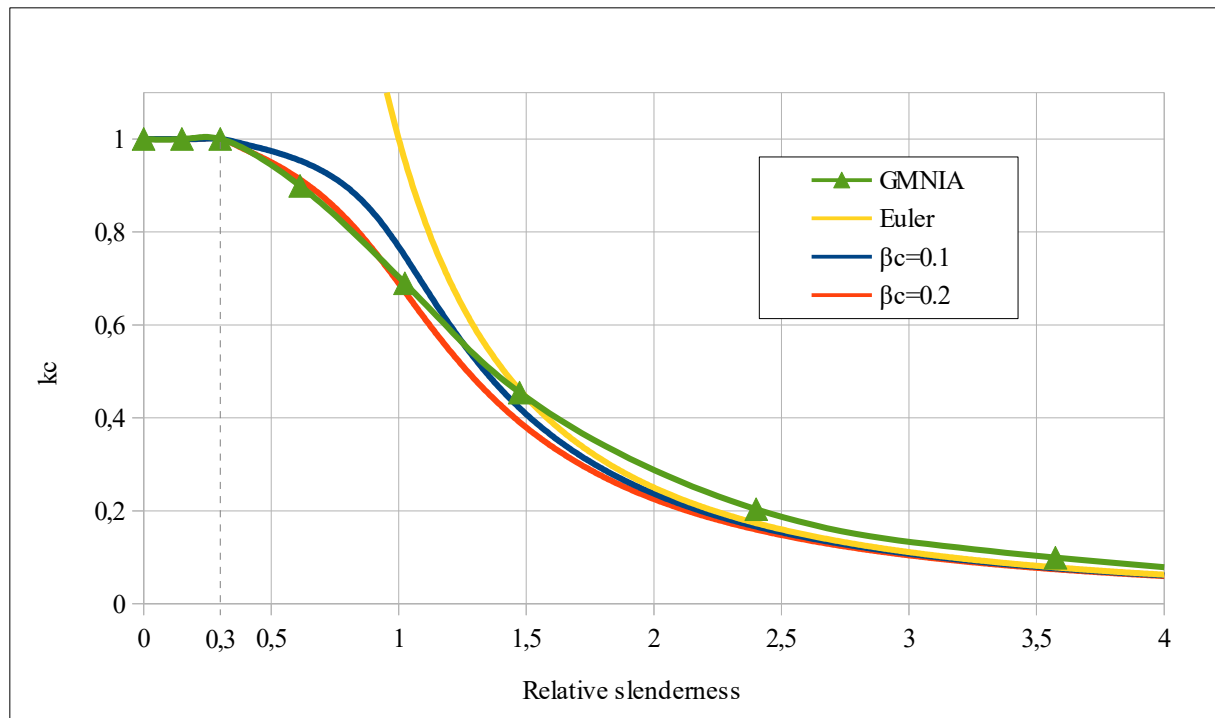


Figure 48 – The results of GMNIA in centric compression case compared to the proposed FEM-Design method

Fig. 49 shows the load-displacement curves from GMNIA. It is worth noting that by the first two short wall height (1 and 2 m) the load-displacement curves are almost straight, which means that the failure is close to the strength failure as expected. By the $L = 3$ m according to the results the failure is a mixture between the stability and strength failure. By the last two cases (5 and 7.5 m) the failure mode is stability failure which is obvious from Fig. 49.

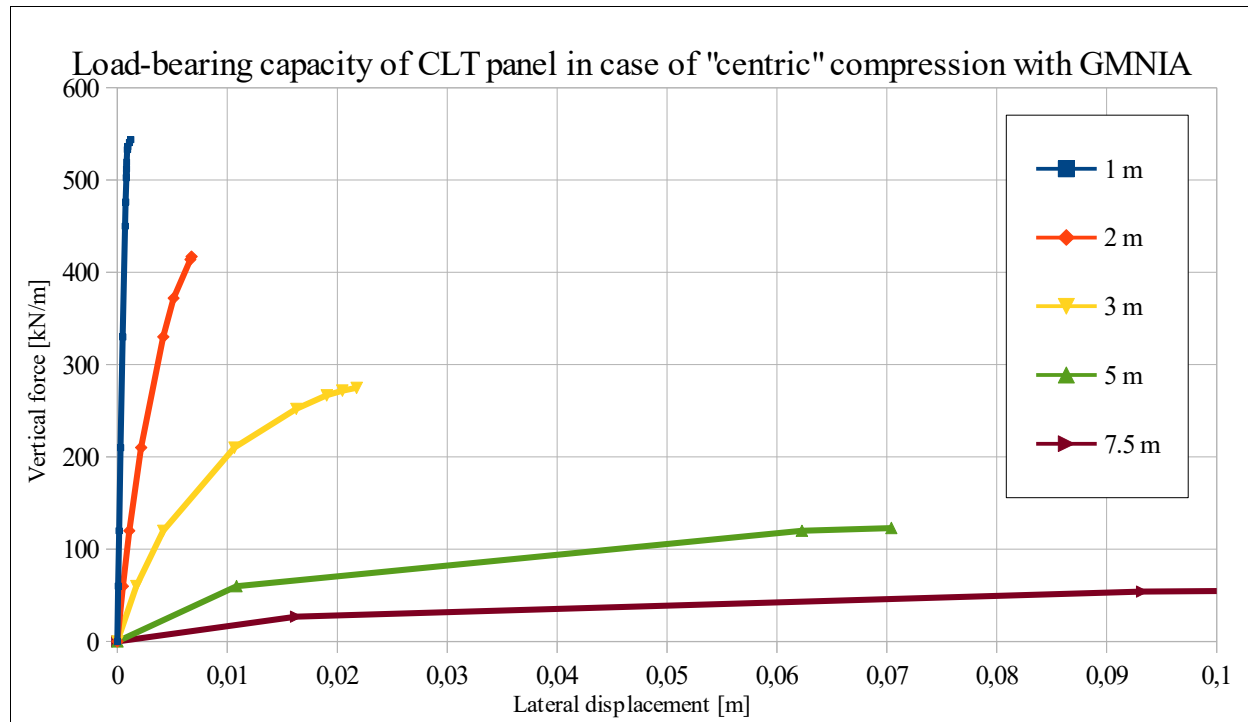


Figure 49 – The results of GMNIA – The applied vertical force versus the lateral displacement of the mid-section of the wall

Case b)

In this case the height of the wall was constant, but we increased the lateral loads on the wall as well.

The analyzed cases can be seen in the table below where we indicated the applied height of the wall and furthermore the applied vertical and later loads (see Fig. 44-45).

L [m]	F [kN/m]	q [kN/m ²]
3	274.8	0.0
3	252.0	0.840
3	235.0	1.567
3	208.3	2.778
3	171.5	4.574
3	130.5	6.960

Fig. 50 shows the relevant stress distribution in the walls under the different load conditions at the mid-section of the walls.

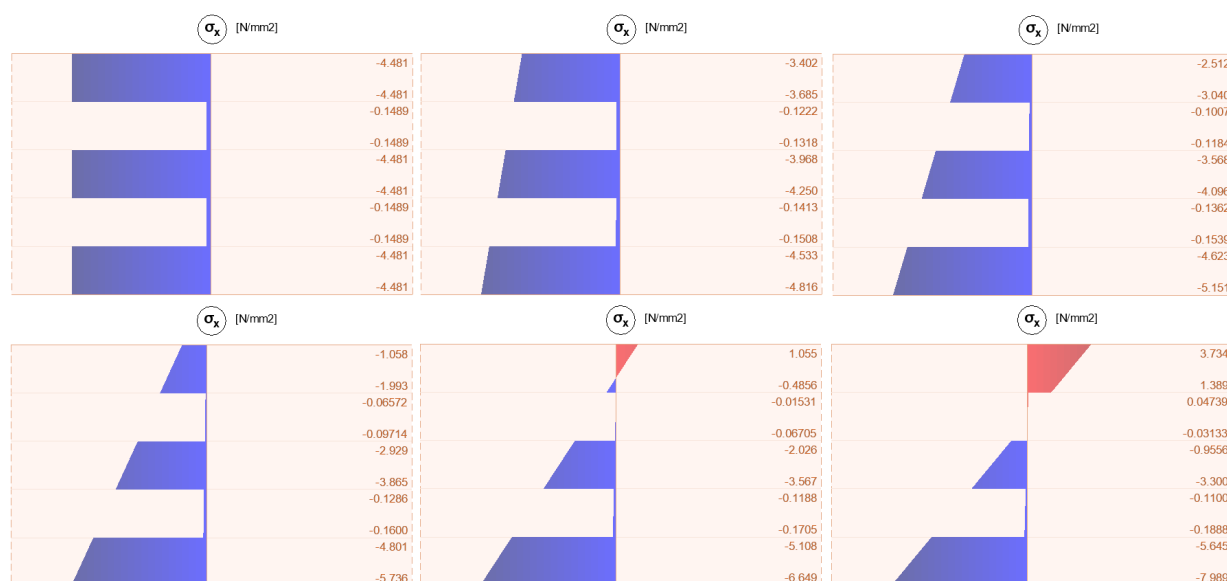


Figure 50 – The relevant normal stress distribution in the six different cases with the given centric and lateral loads

In case a) we calculated based on the proposed FEM-Design method the reduction factor to the 3 m height wall, thus we used that value by these calculations as well. The buckling utilizations of the walls with the different vertical and lateral loads by the six different load situations are as follows based on Fig. 45 and the mentioned stress separation in Chapter 5.8.5.4:

$$Util^1 = \frac{|\sigma_{c,0,d}^{buckling}|}{k_c f_{c,0,d}} + \frac{|\sigma_{m,0,d}^{buckling}|}{f_{m,0,d}} = \frac{|-4.481|}{0.4210 \cdot 10.08} + \frac{0}{11.52} = 1.056$$

$$Util^2 = \frac{|\sigma_{c,0,d}^{buckling}|}{k_c f_{c,0,d}} + \frac{|\sigma_{m,0,d}^{buckling}|}{f_{m,0,d}} = \frac{|-4.109|}{0.4210 \cdot 10.08} + \frac{0.707}{11.52} = 1.030$$

$$Util^3 = \frac{|\sigma_{c,0,d}^{buckling}|}{k_c f_{c,0,d}} + \frac{|\sigma_{m,0,d}^{buckling}|}{f_{m,0,d}} = \frac{|-3.832|}{0.4210 \cdot 10.08} + \frac{1.319}{11.52} = 1.017$$

$$Util^4 = \frac{|\sigma_{c,0,d}^{buckling}|}{k_c f_{c,0,d}} + \frac{|\sigma_{m,0,d}^{buckling}|}{f_{m,0,d}} = \frac{|-3.397|}{0.4210 \cdot 10.08} + \frac{2.339}{11.52} = 1.004$$

$$Util^5 = \frac{|\sigma_{c,0,d}^{buckling}|}{k_c f_{c,0,d}} + \frac{|\sigma_{m,0,d}^{buckling}|}{f_{m,0,d}} = \frac{|-2.797|}{0.4210 \cdot 10.08} + \frac{3.853}{11.52} = 0.9936$$

$$Util^6 = \frac{|\sigma_{c,0,d}^{buckling}|}{k_c f_{c,0,d}} + \frac{|\sigma_{m,0,d}^{buckling}|}{f_{m,0,d}} = \frac{|-2.128|}{0.4210 \cdot 10.08} + \frac{5.861}{11.52} = 1.010$$

To verify these utilizations we performed GMNIA with the same input parameters what were used in case a) but we modified the loads. The given load situations in case b) were the load-bearing capacities of the analyzed walls based on GMNIA. Fig. 51 shows the load-displacement curves of the analyzed walls. Do not forget that by these vertical loads there were simultaneously increasing lateral loads as well on the walls during the calculation.

According to these information we can say that the utilizations of FEM-Design proposed calculation are very close to GMNIA results. We can conclude that FEM-Design provides an adequate stability calculation method in its new CLT modul design calculation.

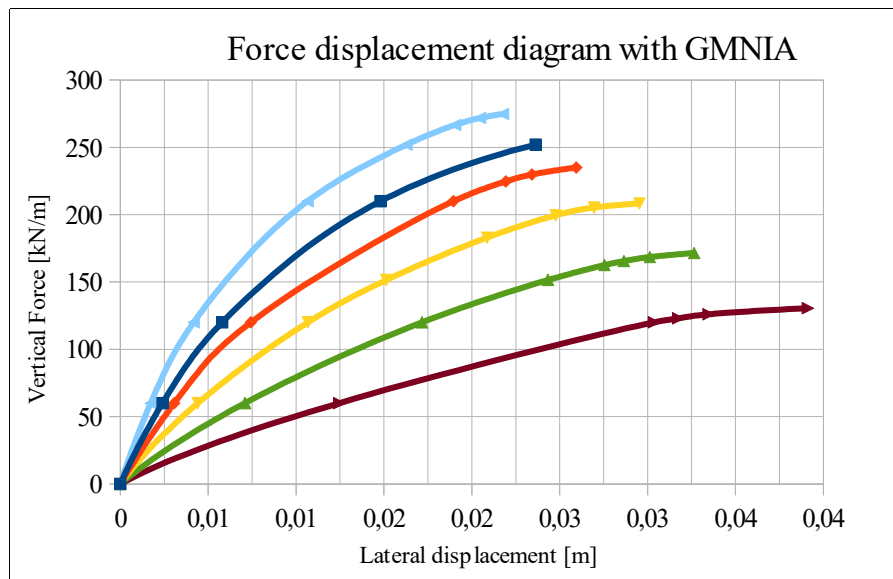


Figure 51 – The results of GMNIA – The applied vertical force versus the lateral displacement of the mid-section of the wall

Download link to the example file:

Case a):

<http://download.strusoft.com/FEM-Design/inst190x/models/9.4.2.5 Buckling check of a CLT wall case a.str>

Case b):

<http://download.strusoft.com/FEM-Design/inst190x/models/9.4.2.5 Buckling check of a CLT wall case b.str>

References

- [1] Reddy JN., An evaluation of equivalent-single-layer and layerwise theories of composite laminates, *Composite Structures*, Vol. 25., 21-25., 1993.
- [2] Kulikov GM., Plotnikova SV., Equivalent single-layer and layerwise shell theories and rigid-body motions-Part II: computational aspect, Vol. 12. *Mechanics of Advanced Materials and Structures*, 331-340., 2005.
- [3] Kollár L. P., Springer G. S., *Mechanics of Composite Structure*, Cambridge Press, 2003.
- [4] Yeongbin K., Lee PS., Bathe KJ., The MITC4+ shell element and its performance, *Computers and Structures*, Vol. 169., 57-68., 2016.
- [5] Lee PS., Bathe KJ., Development of MITC isotropic triangular shell finite elements, *Computers and Structures*, Vol. 82, 945-962., 2004.
- [6] Mindlin R.D., Influence of rotary inertia and shear on flexural motions of isotropic, elastic plates, *Journal of Applied Mechanics*, Vol. 18., 31-38., 1951.
- [7] Voigt W., *Lehrbuch der kristallphysik*. Teubner, Leipzig, 1910.
- [8] Auricchio F., Sacco E., A Mixed-Enhanced Finite-Element for the Analysis of Laminated Composite Plates, *International Journal for Numerical Methods in Engineering*, Vol. 44., 1481-1504., 1999.
- [9] Vlachoutsis S., Shear Correction Factors for Plates and Shells, *International Journal for Numerical Methods in Engineering*, Vol. 33., 1537-1552., 1992.
- [10] Laitinen M., Lahtinen H., Sjölin S.-G., Transverse Shear Correction Factors for Laminates in Cylindrical Bending, *Communications in Numerical Methods in Engineering*, Vol. 11., 41-47., 1995
- [11] Stürzenbecher R., Hofstetter K., Eberhardsteiner J., Cross laminated timber: A multi-layer, shear compliant plate and its mechanical behavior, 11th World Conference on Timber Engineering 2010, WCTE 2010, 2010.
- [12] CLT Handbook, Cross-Laminated Timber, U.S. Edition, FPIInnovations and Binational Softwood Lumber Council, 2013.
- [13] Möhler K.: Über das Tragverhalten von Biegeträgern und Druckstäben mit zusammengesetzten Querschnitten und nachgiebigen Verbindungsmittel. Habilitationsschrift, Technische Hochschule Karlsruhe, 1956.
- [14] Blass H., Fellmoser P.: Design of solid wood panels with cross layers. In: 8th World Conference on Timber Engineering, Lahti, 1001-1006., 2004.
- [15] Kozaric L.M., Prokic A., Berevic M., Purcar M.V., Design methods for cross laminated timber elements used as beams, 5th International Conference, Contemporary achievements in civil engineering 21., Subotica, Serbia, April 2017.
- [16] Kreuzinger H., Platten, scheiben und schalen - ein berechnungsmodell für gängige statikprogramme, in: *Bauen mit Holz*, Vol. 1, Bruderverlag, Karlsruhe, 34-39., 1999.
- [17] Schickhofer G., Thiel A.: *BSPHandbuch: Holzmassivbauweise in Brettsperholz*, International Holzbau-Forum 10, Technische Universität Graz, 2009.

- [18] Thiel A., Schickhofer G., A software tool for designing cross laminated timber elements: 1D-plate design, World Conference on Timber Engineering, 2010.
- [19] Czaderski C., Steiger R., Howald M., Olia S., Gülzow A., Niemz P., Versuche und Berechnungen an allseitig gelagerten 3-schichtigen Brettsperrholzplatten, Vol. 65. Holz Roh Werkst, 383-402., 2007
- [20] Stürzenbecher R., De Borst K., Hofstetter K., Eberhardsteiner J., Composites Science and Technology, Structural design of Cross Laminated Timber (CLT) by advanced plate theories, Vol. 70(9), 1368-1379., 2010.
- [21] Pagano N., Exact solutions for rectangular bidirectional composites and sandwich plates, Journal of Composite Materials, Vol. 4., 20-24., 1970.
- [22] DIN EN 1995-1-1
- [23] Eurocode 1995-1-1 Design of timber structure
- [24] Jacob M., Harrington J. Robinson B., The structural use of timber – Handbook for Eurocode 5: Part 1-1., COFORD, Department of Agriculture, Food and the Marine, Dublin, 2018.
- [25] Jöbstl R.A., Schickhofer, Comparative examination of creep of GLT and CLT slabs in bending, Working comission CIB-W18 – Timber Structure, Vol. 40., 1-15., 2007.
- [26] Karacabeyli E., Douglas B., CLT Handbook - Cross laminated timber, US edition, Library and Archives Canada Cataloguing in Publication, 2013.
- [27] Wallner-Novak M., Koppelhuber J., Pock K., Cross-laminated timber structural design, basic design and engineering principles according to Eurocode, proHolz, Austria, 2014.
- [28] Wood handbook, Wood as an engineering material, Gen. Tech. Rep. FPL–GTR–113. Madison, WI: U.S. Department of Agriculture, Forest Service, Forest Products Laboratory. 1999.
- [29] Jelec M., Rajcic V., Varevac D., Cross-laminated timber (CLT) – a state of art report, Gradevinar, Vol. 70, 75-95., 2018.
- [30] DIN 1052
- [31] Bogensperger T., Moosbrugger T., Silly G., Verification of CLT-plates under loads in plane, WCTE – World conference on timber engineering, 2010.
- [32] Bernhard H., Ein Beitrag zur Bestimmung der Scheibenschubfestigkeit von Brettsperrholz, Institut für Holzbau und Holztechnologie, Technische Universität Graz, 2011.
- [33] Blass H.J., Flaig M., Stabförmige Bauteile aus Brettsperrholz, KIT Scientific Publishing, Karlsruher Berichte zum Ingenieurholzbau, 2012.
- [34] Flaig M., Biegetrager aus Brettsperrholz bei Beanspruchung in Plattenebene, KIT Scientific Publishing, Karlsruher Berichte zum Ingenieurholzbau, 2013.
- [35] Jelec M., Rajcic V., Strukar K., Structural analysis of in-plane loaded CLT beams, Scientific paper, <https://doi.org/10.13167/2017.14.3>, 20-30., 2017.
- [36] Theiler M., Frangi A., Steiger R., Strain-based calculation model for centrally and eccentrically loaded timber columns, Engineering Structures, Vol. 56., 1103-1116., 2013.
- [37] Olivier P., Strength and Stability of Cross-Laminated-Timber Walls at Short and Long

Term, Matériaux composites et construction. Université Paris-Est, 2017.

[38] Fink G., Honfi D., Kohler J., Dietsch P., Basis of Design Principles for Timber Structures, A state-of-the-art report by COST Action FP1402 / WG 1, 2018.

[39] Ingenieur Holzbau.de, Glulam-Bulletin, December, 2017.

[40] Jelec M., Danielsson H., Rajcic V., Serrano E., Experimental and numerical investigation of cross-laminated timber elements at in-plane beam loading conditions, Construction and Building Materials, Vol. 206., 329-346., 2019.

[41] Danielsson H., Jelec M., Serrano E. Rajcic V., Cross laminated timber at in-plane beam loading – Comparison model predictions and FE-analyses, Engineering Structures, Vol. 179., 246-254., 2019

[42] Jelec M., Danielsson H., Rajcic V., Serrano E., Cross laminated timber at in-plane beam loading – New analytical model predictions and relation to EC5, Conference Paper, August 2018, Inter/51-12-5.

Notes